



ADIPOSE TISSUE AND THE KNEE

**Role of inflammation on joint
degeneration and cartilage repair**

Wu Wei

ADIPOSE TISSUE AND THE KNEE

**Role of inflammation on joint
degeneration and cartilage repair**

Wu Wei

The printing of this thesis was financially supported by:

- Department of Orthopedics, Erasmus MC University Medical Center, Rotterdam
- Nederlandse Orthopaedische Vereniging (NOV), 's Hertogenbosch
- Anna Fonds, Leiden
- Centrum Orthopedie Rotterdam b.v., Rotterdam
- Livit Orthopedie, Amsterdam
- Chipsoft b.v. Amsterdam

Cover design: Niek Dekker, Amsterdam, niekdekker.com

Layout and printed by: Optima Grafische Communicatie, Rotterdam, the Netherlands

ISBN: 978-94-6361-004-9

Copyright Wu Wei, Rotterdam, The Netherlands, 2017.

No part of this thesis may be reproduced, stored or transmitted in any form or by any means without prior permission of the author.

De digitale versie van dit proefschrift is te vinden in de YourThesis app en kan worden gelezen op tablet of smartphone. De app kan worden gedownload in de App store en de Google Play store, of middels het scannen van onderstaande QR-code



ADIPOSE TISSUE AND THE KNEE
Role of inflammation on joint degeneration
and cartilage repair

Vetweefsel en de knie
Rol van ontsteking op gewrichtsdegeneratie
en kraakbeenherstel

Proefschrift

ter verkrijging van de graad van doctor aan de
Erasmus Universiteit Rotterdam
op gezag van de
rector magnificus

Prof.dr. H.A.P. Pols

en volgens besluit van het College voor Promoties.
De openbare verdediging zal plaatsvinden op

vrijdag 20 oktober 2017 om 13:30 uur

door

Wu Wei
geboren te Hubei, China

Erasmus University Rotterdam



PROMOTIECOMMISSIE

Promotoren: Prof. dr. G.J.V.M. van Osch
Prof. dr. J.A.N. Verhaar

Overige leden: Prof. dr. J.M.W. Hazes
Prof. dr. S.K. Bulstra
Dr. P.J. Emans

Copromotor: Dr. Y.M. Bastiaansen-Jenniskens

Voor mijn ouders

致我的父母

CONTENTS

Chapter 1	General introduction, aims and outline of the thesis	11
-----------	--	----

Part I Local effects of adipose tissue

Chapter 2	The size of infrapatellar fat pad adipocytes is not influenced by obesity	27
Chapter 3	Stimulation of fibrotic processes by the infrapatellar fat pad in cultured synoviocytes from patients with osteoarthritis: a possible role for prostaglandin $F_{2\alpha}$	37
Chapter 4	The infrapatellar fat pad from diseased joints inhibits chondrogenesis of mesenchymal stem cells	59
Chapter 5	Anti-chondrogenic and pro-catabolic effect of infrapatellar fat pad and its residing macrophages can be modulated by triamcinolone acetonide	79

Part II Systemic effects of adipose tissue

Chapter 6	Statins and fibrates do not affect development of spontaneous cartilage damage in STR/Ort mice	99
Chapter 7	High fat diet accelerates cartilage repair in DBA/1 mice	119

Epilogue

Chapter 8	Summary and general discussion	137
	Addendum figures	153
	Nederlandse samenvatting	155
	中文简介	159
	PhD portfolio	161
	List of publications	165
	About the author	169
	Dankwoord	171



CHAPTER 1

General introduction, aims and outline of the thesis

GENERAL INTRODUCTION

The normal knee

The knee joint is one of the complex and heavily loaded joints of the human body. It is a bicondylar synovial joint which is formed by articulations between the tibia, femur and patella. The knee joint allows flexion, extension and some degrees of internal and external rotations. Tendons connect the bones to the muscles and together with the ligaments create stability to the joint. The articulating ends of the bones are covered by articular cartilage and the fibrocartilaginous menisci lie between the tibia and the femur.

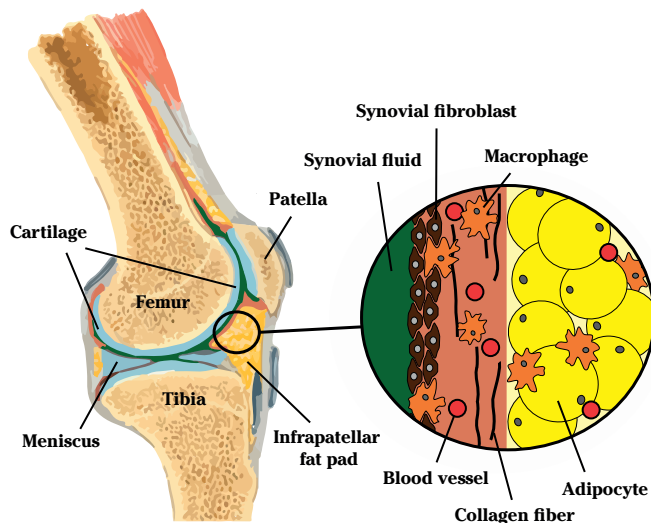


Figure 1 The normal knee

The knee joint is formed by articulations between the tibia, femur and patella. The infrapatellar fat pad is located inside the joint capsule but outside the synovial membrane. The synovial membrane is richly vascularized. It consists of a layer of fibroblasts and macrophages followed by a layer of connective tissue. The infrapatellar fat pad consists mainly of adipocytes.

Articular cartilage allows smooth gliding movements and acts as a shock absorber. It is a specialized tissue that is avascular and aneural and only harbors a small number of cells. These cells are called chondrocytes and they produce and maintain the articular cartilage extracellular matrix (ECM). The articular cartilage ECM consists mainly of collagen type 2 fibers and proteoglycans. The negatively charged glycosaminoglycans (GAG) side chains on the proteoglycans attract water. These GAGs attract water in such extent that 65%-80% of the cartilage consists of water. Due to its avascular nature, the articular cartilage receives its nutrients

from the synovial fluid or from the subchondral bone underneath the cartilage through diffusion¹.

The synovium fluid is encapsulated by the synovial membrane, which is also an integral part of the joint. The synovial membrane is a richly vascularized connective tissue that is responsible for the production of synovial fluid and for filtering of debris out of the synovial fluid. The membrane is mainly composed of two cell types: macrophages and synovial fibroblasts².

Macrophages are a type of cells that can phagocytize for example cellular debris, foreign material and microbes. Macrophages play an important role in inflammation and wound healing. In reaction to stimuli from their microenvironment these macrophages can become activated into a spectrum of different types. Roughly, macrophages can be categorized into pro-inflammatory (often referred to as M1) macrophages and anti-inflammatory/wound healing (often referred to as M2) macrophages³.

Synovial fibroblasts are cells that can synthesize ECM such as collagen type 1, but also hyaluronic acid and lubricin for the synovial fluid. During inflammation, these synovial fibroblasts can also be triggered to secrete inflammatory and catabolic factors. Outside the synovial membrane but inside the joint capsule several fat depots are localized of which the infrapatellar fat pad (IPFP) is the largest. The IPFP is also called Hoffa's fat pad, named after dr. Albert Hoffa who first described it in 1904⁴. The IPFP fills the anterior knee compartment and its posterior surface is covered with synovial membrane. The IPFP provides mechanical cushioning and facilitates the distribution of synovial fluids. The IPFP is richly vascularized and innervated. Furthermore, it contains many immune cells such as macrophages and stem cells^{5,6}. These immune cells could play a role in the pathogenesis of knee osteoarthritis (OA) and the stem cells could be used for tissue engineering purposes.

The diseased knee

The knee joint is vulnerable to trauma and the development of OA. According to the United States Bone and Joint Initiative, the socio economic burden of joint diseases in 2014 was very high with more than 50% of people aged 18 years and older in the US reporting a musculoskeletal condition and all costs associated with musculoskeletal condition was about 5.7% of the gross domestic product⁷. OA is the most common degenerative joint disorder and affects 1.1 million in the Netherlands⁸. Knee OA is a disease of the whole joint and is more than 'wear and tear'

of the cartilage alone. The symptoms of knee OA are pain, reduced movement and disability. There are several risk factors for the development of knee OA, which include age, sex, obesity and previous joint injury. Structurally, there is cartilage damage, subchondral bone sclerosis, osteophytes formation and synovial inflammation and fibrosis⁹. Some of the structural changes in OA are associated with the degree of symptoms. It has been shown that inflammation of the IPFP is associated to knee pain and that synovial fibrosis with reduced joint movement. Currently, there is no cure for OA. There are only treatments against the symptoms of knee OA, including replacement by arthroplasty in end-stage knee OA⁹.

It is generally assumed that articular cartilage damage if left untreated, eventually could lead to OA. Articular cartilage normally does not heal spontaneously or only partially due to its avascular and aneural nature. Furthermore, it harbors only a relatively small number of chondrocytes that could potentially produce matrix. In the case of cartilage damage, these chondrocytes react by producing proteolytic enzymes at the site of injury that destroy the ECM and thereby worsening the damage¹⁰.

Cartilage repair

Treatment strategies

Successful treatment of these cartilage defects remains a challenging clinical problem because none of the current regeneration options are able to completely restore the original structural and biomechanical properties of the cartilage. In the knee, surgical treatment options are marrow stimulation techniques, such as microfracture, for small symptomatic cartilage lesions and autologous chondrocyte implantation (ACI) and mosaicplasty for larger lesions¹⁰.

The microfracture procedure, first introduced by Steadman¹¹, is a simple and low cost method to stimulate the body's own repair response. In the original technique, during knee arthroscopy, the cartilage defect is debrided down till the subchondral bone layer and small holes are 'fractured' into the subchondral bone^{11,12}. This in turn creates a 'bleeding' from the underlying bone marrow and thus stimulation of a repair response by bioactive factors and mesenchymal stem cells (MSC) from the underlying bone marrow¹³. This procedure can potentially be enhanced by adding growth factors or scaffolds, or by changing the technique of creating the holes or the size, number and depth of the holes¹⁴⁻¹⁶. The microfracture treatment is generally used for single defects smaller than 2.5 cm² and leads to clinical improvement in function and pain¹⁶⁻¹⁸, but not to hyaline cartilage repair.

Instead, a fibrocartilaginous tissue fills the defect, which is of inferior biomechanical properties^{13;19;20}.

The ACI procedure uses laboratory expanded autologous articular chondrocytes harvested from healthy part of the joint to fill up the defect²¹. These implanted articular chondrocytes can potentially repair the defect by laying down a new hyaline cartilage ECM. It is also possible to enhance the repair process by adding a (bio)scaffold^{22;23}. The ACI procedure is generally used for cartilage defects greater than 4 cm² or multiple defects and the long term results are good²⁴. Compared to microfracture, the ACI procedure is expensive and requires two surgeries. Furthermore, there is much discussion on the superiority of this technique compared to the cheaper marrow stimulation techniques such as microfracture^{17; 25; 26}.

Besides microfracture and ACI procedure, an osteochondral transplantation can be performed. In this procedure, also called mosaicplasty, autologous osteochondral grafts from healthy, less demanding parts of the joint are transplanted. Allogeneous graft can also be used. No evidence is yet available about the superiority of this procedure versus microfracture and patients are left with a new defect at the donor site that causes donor site morbidity^{25;27}.

Next to these interventions, current research is also focused on transplantation of specific engineered MSC-based constructs. In these strategies, a novel graft is engineered in-vitro using MSCs, scaffolds and growth factors¹⁰. These strategies could potentially reduce donor site morbidity and lead to implantation of a hyaline cartilage implant²⁸. However, these are only experimental treatments and currently no randomized controlled trial has been published yet on these strategies.

Effect of inflammation

Cartilage repair results can be influenced by several factors. Twenty four hours after joint trauma, there is a peak in pro-inflammatory cytokines in the knee, including tumor necrosis factor alpha (TNF- α), interleukin-1 beta (IL-1 β), as well as matrix metalloproteinase(MMP)-1 and MMP-13²⁹⁻³². It has been shown that these pro-inflammatory cytokines can inhibit chondrogenesis and therefore potentially inhibit successful hyaline cartilage repair³³⁻³⁵.

Although the level of these pro-inflammatory cytokines drops over time, the level of inflammatory cytokines in injured knees is still higher than in non-injured knees one year after injury³⁶. Any cartilage repair procedure in the knee therefore takes place in an environment with some degree of inflammation. Inflammation is not

always detrimental to successful wound healing, because some degree of inflammation is necessary to initiate and maintain any healing response³⁷. Controlling the amount of inflammation and reducing the amount of pro-inflammatory anti-chondrogenic cytokines in the knee is therefore important.

Obesity and adipose tissue inflammation

Obesity is another factor that could influence cartilage repair results in the knee. Obesity is defined by a body mass index (BMI) above 30. Studies have suggested that a higher BMI could adversely affect the clinical outcome of microfracture^{18; 38} and ACI³⁹ in the knee and patients with a BMI above 30 are now generally excluded from treatment⁴⁰.

Obesity is a well-known risk factor for the development of OA⁴¹. A typical structural change in obesity is the increase in adipose tissue size. Excessive dietary intake of lipids and carbohydrates leads to adipocyte hypertrophy, death and subsequently influx of inflammatory cells into the adipose tissue. This in turn leads to increased inflammatory cytokine secretion by the adipose tissue and systemic inflammation. These inflammatory changes leads to systemic metabolic changes such as hyperglycemia, hyperinsulinemia and dyslipidemia⁴²⁻⁴⁴. Combined with obesity, these changes are called metabolic syndrome and are all risk factors for the development of OA⁴¹. Besides increasing the risk of developing OA, obesity also could exaggerates post-traumatic arthritis^{45;46} and decrease skin wound repair⁴⁶.

Most of the adipose tissue in the body is located subcutaneously. There are also adipose tissue located intra-articularly. In the knee joint, the IPFP is the biggest. The IPFP is however not the same as subcutaneous adipose tissue. On MRI, total IPFP volume is not associated to BMI^{47;48} and IPFP adipocyte size in mice is not influenced by high fat feeding⁴⁹. The IPFP does play an role in joint homeostasis. MRI studies have shown that a larger IPFP is even associated with less OA^{47;50-52}. Previously we have shown that the secretion of pro-inflammatory cytokines by the IPFP can be increased by an inflammatory stimulus⁵³ and that the IPFP secretes factors that could influence the cartilage in degenerative joint disease⁵⁴. Other authors report that the IPFP contains many inflammatory cells and that it is a source of inflammatory factors^{55;56}.

AIMS AND OUTLINE OF THE THESIS

Adipose tissue becomes inflamed in obesity and secretes factors that affect the knee joint. These factors originate from adipose tissue located outside the knee joint and thus influence the knee through systemically secreted factors. There is however also the intra-articularly located IPFP that can directly locally affect the knee joint. Therefore, the main aim of this thesis is to investigate the effect of inflammation in adipose tissue on degenerative joint disease and cartilage repair.

More specifically, we investigate:

1. whether adipose tissue in and outside the knee influences degenerative joint disease and cartilage repair in the knee
2. what the role is of adipose tissue resident macrophages in degenerative joint disease and cartilage in the knee
3. whether we can modulate adipose tissue and macrophages with medication to reduce degenerative joint disease and to improve cartilage repair.

Adipocyte size in subcutaneous and visceral adipose tissue is increased in obesity. This increase in adipocyte size is associated with adipose tissue inflammation. However, there is no information yet available about whether obesity influences the adipocytes in the IPFP in humans. In **Chapter 2** we investigate whether the adipocytes in the IPFP are increased in obese patients. The posterior aspect of the IPFP is covered by synovial membrane and the synovial membrane is heavily influenced by factors secreted by the IPFP. Synovial fibrosis is common in knee OA and causes joint stiffness. In **Chapter 3** we determine whether IPFP secretes factors that influence fibrotic processes in synovial fibroblasts. Previously, we have shown that the IPFP secretes factors that influence cartilage. In **Chapter 4** we examine whether the IPFP secretes factors that also influence MSC-based cartilage repair. Furthermore, in **Chapter 4** we describe the role of macrophages residing in the IPFP on MSC-based cartilage repair. To improve the joint environment for cartilage repair, in **Chapter 5** we focus on the effect of different anti-inflammatory medication on the IPFP and macrophages in the IPFP.

The IPFP is an intra-articular adipose depot and most adipose tissue are located extra-articular. Subcutaneous and visceral adipose tissue depots are located outside the joint and obesity leads to changes in these depots. This results in systemic metabolic and inflammatory changes that could influence degenerative joint disease and cartilage repair. These systemic effects are complex and therefore in-vivo studies are more suitable. In **Chapter 6** we test whether commonly used lipid modifying medications can prevent degenerative joint disease and cartilage dam-

age in a mouse model of spontaneous cartilage damage with metabolic syndrome. However, when cartilage damage does occur in obese patients a cartilage repair treatment might be needed. Currently, there are no studies available examining the structural cartilage repair outcome in obese patients or explaining how obesity influences cartilage repair. In **Chapter 7** we investigate whether a high fat diet can influence cartilage repair in a mouse model of cartilage repair. In this way, I hope to find new treatments to improve the joint environment to reduce cartilage damage and improve cartilage repair. Finally, in **Chapter 8** I will summarize and discuss our most important findings. I will end with my perspective on future research.

REFERENCES

1. Sophia Fox AJ, Bedi A, Rodeo SA. 2009. The basic science of articular cartilage: structure, composition, and function. *Sports Health* 1:461-468.
2. Smith MD. 2011. The normal synovium. *Open Rheumatol J* 5:100-106.
3. Murray PJ, Allen JE, Biswas SK, et al. 2014. Macrophage activation and polarization: nomenclature and experimental guidelines. *Immunity* 41:14-20.
4. Hoffa A. 1904. Influence of adipose tissue with regard to the pathology of the knee joint. *JAMA*:795–796.
5. Clockaerts S, Bastiaansen-Jenniskens YM, Runhaar J, et al. 2010. The infrapatellar fat pad should be considered as an active osteoarthritic joint tissue: a narrative review. *Osteoarthritis Cartilage* 18:876-882.
6. Dragoo JL, Johnson C, McConnell J. 2012. Evaluation and treatment of disorders of the infrapatellar fat pad. *Sports Med* 42:51-67.
7. USBJ. 2014. United States Bone and Joint Initiative: The Burden of Musculoskeletal Diseases in the United States
8. Chorus AMDFS. 2011. Nationale Peiling van het Bewegingsapparaat 2010.
9. Lane NE, Brandt K, Hawker G, et al. 2011. OARSI-FDA initiative: defining the disease state of osteoarthritis. *Osteoarthritis Cartilage* 19:478-482.
10. Hunziker EB, Lippuner K, Keel MJ, et al. 2015. An educational review of cartilage repair: precepts & practice—myths & misconceptions—progress & prospects. *Osteoarthritis Cartilage* 23:334-350.
11. Steadman JR, Miller BS, Karas SG, et al. 2003. The microfracture technique in the treatment of full-thickness chondral lesions of the knee in National Football League players. *J Knee Surg* 16:83-86.
12. Mithoefer K, McAdams T, Williams RJ, et al. 2009. Clinical efficacy of the microfracture technique for articular cartilage repair in the knee: an evidence-based systematic analysis. *Am J Sports Med* 37:2053-2063.
13. Shapiro F, Koide S, Glimcher MJ. 1993. Cell origin and differentiation in the repair of full-thickness defects of articular cartilage. *J Bone Joint Surg Am* 75:532-553.
14. Gomoll AH. 2012. Microfracture and augments. *J Knee Surg* 25:9-15.
15. Orth P, Duffner J, Zurakowski D, et al. 2016. Small-Diameter Awls Improve Articular Cartilage Repair After Microfracture Treatment in a Translational Animal Model. *Am J Sports Med* 44:209-219.
16. Fischer S, Kisser A. 2016. Single-step scaffold-based cartilage repair in the knee: A systematic review. *J Orthop* 13:246-253.
17. Erggelet C, Vavken P. 2016. Microfracture for the treatment of cartilage defects in the knee joint - A golden standard? *J Clin Orthop Trauma* 7:145-152.
18. Mithoefer K, Williams RJ, 3rd, Warren RF, et al. 2005. The microfracture technique for the treatment of articular cartilage lesions in the knee. A prospective cohort study. *J Bone Joint Surg Am* 87:1911-1920.
19. Frisbie DD, Oxford JT, Southwood L, et al. 2003. Early events in cartilage repair after subchondral bone microfracture. *Clin Orthop Relat Res*:215-227.
20. Kaul G, Cucchiari M, Remberger K, et al. 2012. Failed cartilage repair for early osteoarthritis defects: a biochemical, histological and immunohistochemical analysis of the repair tissue after treatment with marrow-stimulation techniques. *Knee Surg Sports Traumatol Arthrosc* 20:2315-2324.
21. Brittberg M. 2008. Autologous chondrocyte implantation—technique and long-term follow-up. *Injury* 39 Suppl 1:S40-49.

22. Benders KE, Boot W, Cokelaere SM, et al. 2014. Multipotent Stromal Cells Outperform Chondrocytes on Cartilage-Derived Matrix Scaffolds. *Cartilage* 5:221-230.
23. Brittberg M. 2010. Cell carriers as the next generation of cell therapy for cartilage repair: a review of the matrix-induced autologous chondrocyte implantation procedure. *Am J Sports Med* 38:1259-1271.
24. Pareek A, Carey JL, Reardon PJ, et al. 2016. Long-Term Outcomes after Autologous Chondrocyte Implantation: A Systematic Review at Mean Follow-Up of 11.4 Years. *Cartilage* 7:298-308.
25. Gracitelli GC, Moraes VY, Franciozi CE, et al. 2016. Surgical interventions (microfracture, drilling, mosaicplasty, and allograft transplantation) for treating isolated cartilage defects of the knee in adults. *Cochrane Database Syst Rev* 9:CD010675.
26. Knutsen G, Drogset JO, Engebretsen L, et al. 2016. A Randomized Multicenter Trial Comparing Autologous Chondrocyte Implantation with Microfracture: Long-Term Follow-up at 14 to 15 Years. *J Bone Joint Surg Am* 98:1332-1339.
27. Andrade R, Vasta S, Pereira R, et al. 2016. Knee donor-site morbidity after mosaicplasty - a systematic review. *J Exp Orthop* 3:31.
28. Anz AW, Bapat A, Murrell WD. 2016. Concepts in regenerative medicine: Past, present, and future in articular cartilage treatment. *J Clin Orthop Trauma* 7:137-144.
29. Bigoni M, Sacerdote P, Turati M, et al. 2013. Acute and late changes in intraarticular cytokine levels following anterior cruciate ligament injury. *J Orthop Res* 31:315-321.
30. Catterall JB, Stabler TV, Flannery CR, et al. 2010. Changes in serum and synovial fluid biomarkers after acute injury (NCT00332254). *Arthritis Res Ther* 12:R229.
31. Irie K, Uchiyama E, Iwaso H. 2003. Intraarticular inflammatory cytokines in acute anterior cruciate ligament injured knee. *Knee* 10:93-96.
32. Sward P, Frobell R, Englund M, et al. 2012. Cartilage and bone markers and inflammatory cytokines are increased in synovial fluid in the acute phase of knee injury (hemarthrosis)—a cross-sectional analysis. *Osteoarthritis Cartilage* 20:1302-1308.
33. Heldens GT, Blaney Davidson EN, Vitters EL, et al. 2012. Catabolic factors and osteoarthritis-conditioned medium inhibit chondrogenesis of human mesenchymal stem cells. *Tissue Eng Part A* 18:45-54.
34. Wehling N, Palmer GD, Pilapil C, et al. 2009. Interleukin-1beta and tumor necrosis factor alpha inhibit chondrogenesis by human mesenchymal stem cells through NF-kappaB-dependent pathways. *Arthritis Rheum* 60:801-812.
35. Yang KG, Saris DB, Verbout AJ, et al. 2006. The effect of synovial fluid from injured knee joints on in vitro chondrogenesis. *Tissue Eng* 12:2957-2964.
36. Lieberthal J, Sambamurthy N, Scanzello CR. 2015. Inflammation in joint injury and post-traumatic osteoarthritis. *Osteoarthritis Cartilage* 23:1825-1834.
37. Koh TJ, DiPietro LA. 2011. Inflammation and wound healing: the role of the macrophage. *Expert Rev Mol Med* 13:e23.
38. Negrin L, Kutscha-Lissberg F, Gartlehner G, et al. 2012. Clinical outcome after microfracture of the knee: a meta-analysis of before/after-data of controlled studies. *Int Orthop* 36:43-50.
39. Jaiswal PK, Bentley G, Carrington RW, et al. 2012. The adverse effect of elevated body mass index on outcome after autologous chondrocyte implantation. *J Bone Joint Surg Br* 94:1377-1381.
40. Gomoll AH, Farr J, Gillogly SD, et al. 2010. Surgical management of articular cartilage defects of the knee. *J Bone Joint Surg Am* 92:2470-2490.
41. Berenbaum F, Griffin TM, Liu-Bryan R. 2017. Review: Metabolic Regulation of Inflammation in Osteoarthritis. *Arthritis Rheumatol* 69:9-21.

42. Apovian CM, Bigornia S, Mott M, et al. 2008. Adipose macrophage infiltration is associated with insulin resistance and vascular endothelial dysfunction in obese subjects. *Arterioscler Thromb Vasc Biol* 28:1654-1659.
43. Grant RW, Dixit VD. 2015. Adipose tissue as an immunological organ. *Obesity (Silver Spring)* 23:512-518.
44. Ouchi N, Parker JL, Lugus JJ, et al. 2011. Adipokines in inflammation and metabolic disease. *Nat Rev Immunol* 11:85-97.
45. Louer CR, Furman BD, Huebner JL, et al. 2012. Diet-induced obesity significantly increases the severity of posttraumatic arthritis in mice. *Arthritis Rheum* 64:3220-3230.
46. Wu CL, Jain D, McNeill JN, et al. 2015. Dietary fatty acid content regulates wound repair and the pathogenesis of osteoarthritis following joint injury. *Ann Rheum Dis* 74:2076-2083.
47. Cai J, Xu J, Wang K, et al. 2015. Association Between Infrapatellar Fat Pad Volume and Knee Structural Changes in Patients with Knee Osteoarthritis. *J Rheumatol* 42:1878-1884.
48. Chuckpaiwong B, Charles HC, Kraus VB, et al. 2010. Age-associated increases in the size of the infrapatellar fat pad in knee osteoarthritis as measured by 3T MRI. *J Orthop Res* 28:1149-1154.
49. Barboza E, Hudson J, Chang WP, et al. 2017. Pro-fibrotic infrapatellar fat pad remodeling without M1-macrophage polarization precedes knee osteoarthritis in diet-induced obese mice. *Arthritis Rheumatol*.
50. Duran S, Aksahin E, Kocadal O, et al. 2015. Effects of body mass index, infrapatellar fat pad volume and age on patellar cartilage defect. *Acta Orthop Belg* 81:41-46.
51. Han W, Cai S, Liu Z, et al. 2014. Infrapatellar fat pad in the knee: is local fat good or bad for knee osteoarthritis? *Arthritis Res Ther* 16:R145.
52. Pan F, Han W, Wang X, et al. 2015. A longitudinal study of the association between infrapatellar fat pad maximal area and changes in knee symptoms and structure in older adults. *Ann Rheum Dis* 74:1818-1824.
53. Clockaerts S, Bastiaansen-Jenniskens YM, Feijt C, et al. 2012. Cytokine production by infrapatellar fat pad can be stimulated by interleukin 1beta and inhibited by peroxisome proliferator activated receptor alpha agonist. *Ann Rheum Dis* 71:1012-1018.
54. Bastiaansen-Jenniskens YM, Clockaerts S, Feijt C, et al. 2012. Infrapatellar fat pad of patients with end-stage osteoarthritis inhibits catabolic mediators in cartilage. *Ann Rheum Dis* 71:288-294.
55. Klein-Wieringa IR, de Lange-Brokaar BJ, Yusuf E, et al. 2016. Inflammatory Cells in Patients with Endstage Knee Osteoarthritis: A Comparison between the Synovium and the Infrapatellar Fat Pad. *J Rheumatol* 43:771-778.
56. Klein-Wieringa IR, Kloppenburg M, Bastiaansen-Jenniskens YM, et al. 2011. The infrapatellar fat pad of patients with osteoarthritis has an inflammatory phenotype. *Ann Rheum Dis* 70:851-857.

PART I

Local effects of adipose tissue



CHAPTER 2

The size of infrapatellar fat pad adipocytes is not influenced by obesity

John Garcia

Wu Wei

Jos Runhaar

Karina Wright

Gerjo J.V.M. van Osch

Yvonne M. Bastiaansen-Jenniskens

The data presented in this chapter is accepted as part of the manuscript "Lack of high BMI-related features in adipocytes and inflammatory cells in the infrapatellar fat pad" by A.J. De Jong et al in Arthritis Research & Therapy

ABSTRACT

Adipocyte hypertrophy and the resulting adipose tissue inflammation are key features of obesity. However, it is still unclear whether obesity causes the adipocytes in the infrapatellar fat pad (IPFP) to contribute to joint inflammation. The aim of this study was to determine the effect of obesity on the size of IPFP adipocytes. IPFP was obtained from end-stage osteoarthritis patients with a mean body mass index (BMI) of 29.7 kg/m² (range 21.5–48.47 kg/m²). Subcutaneous fat was obtained from 12 end-stage osteoarthritis donors with a mean BMI of 33.0 kg/m² (range 24.2–48.5 kg/m²). Fat tissues were cryosectioned and stained with haematoxylin and eosin. The cross-sectional area of adipocytes was determined using image analysis software. No relationship between adipocyte size and BMI was observed in IPFP adipocytes ($r=-0.06$, $p=0.82$), whereas subcutaneous adipocyte size positively correlates with donor BMI ($r=0.63$, $p=0.028$). For non-obese donors, size of IPFP adipocytes was not significantly different to subcutaneous adipocytes ($p>0.99$). Subcutaneous adipocytes from obese donors were significantly larger than the IPFP adipocytes from other obese donors ($p=0.03$). Our results demonstrate that obesity does not affect the size of adipocytes in the IPFP, which suggests that inflammation of the IPFP is not influenced by obesity associated adipocyte hypertrophy.

INTRODUCTION

A high body mass index as a result of expansion of adipose tissue is a well-known risk factor in the development of knee osteoarthritis (OA)¹. During expansion, adipocytes in adipose tissue become hypertrophic. Large adipocytes have been shown to produce substantially more pro-inflammatory cytokines and adipokines than smaller adipocytes². This increased secretion of pro-inflammatory molecules such as IL-6 and tumor necrosis factor alpha (TNF- α) promotes the recruitment of macrophages and their differentiation into a pro-inflammatory phenotype. This leads to low-grade systemic inflammation and metabolic changes, both of which have been associated with OA¹. Besides mechanical overloading, obesity related inflammation and metabolic changes have also been associated with OA¹.

The infrapatellar fat pad (IPFP) is an adipose tissue located intracapsular yet extra-synovial. IPFP is a potential source of inflammatory factors in the knee joint³. Due to its intra-articular location and because adipose tissues generally become inflamed in obesity, it has been long thought that the IPFP could play a major role in obesity related joint inflammation. Unlike subcutaneous adipose tissue, MRI studies have suggested that total IPFP volume is not associated to body mass index (BMI)⁴. However, these MRI studies did not investigate the susceptibility of the IPFP to obesity related events that lead to inflammation, such as adipocyte hypertrophy. The aim of this study was to investigate whether increased adipocyte size, which contributes to adipose tissue inflammation, is associated with BMI in the IPFP.

METHODS

Tissue sample preparation

Eighteen IPFPs were obtained from end stage OA patients with a mean body mass index (BMI) of 29.7 kg/m² (range 21.5–48.47 kg/m²) undergoing total knee arthroplasty. Subcutaneous adipose tissue was obtained from twelve end stage OA donors with a mean BMI of 33.0 kg/m² (range 24.2–48.5 kg/m²) undergoing total hip or knee replacement. Consent was given in accordance with the guidelines of the Federation of Biomedical Scientific Societies (<http://www.federa.org>) after approval by the local ethical committee (MEC 2008-181 and MEC 2012-267). Donors were subdivided into obese (BMI ≥ 30) and non-obese (BMI < 30) for each of the adipose tissues (a total of 4 groups). Tissue samples were cryosectioned and

stained with haematoxylin and eosin (H&E) and imaged using an Olympus SC30 camera (Olympus, Zoeterwoude, Netherlands).

Measurement of adipocyte size

The cross-sectional area of the imaged adipocytes was calculated using Fiji Is Just ImageJ software with the additional Adiposoft plugin. Three separate sections, with a minimum of 25 adipocytes in each section were measured per donor. The Adiposoft application was calibrated to identify cells with a diameter between 30-130 μm . A measuring scale of 0.33 μm /pixel was also used by the application to determine the cross-sectional area (size) of each adipocyte identified in the images. A manual inspection of output data was performed to confirm the consistency of the measurements (Figure 1).

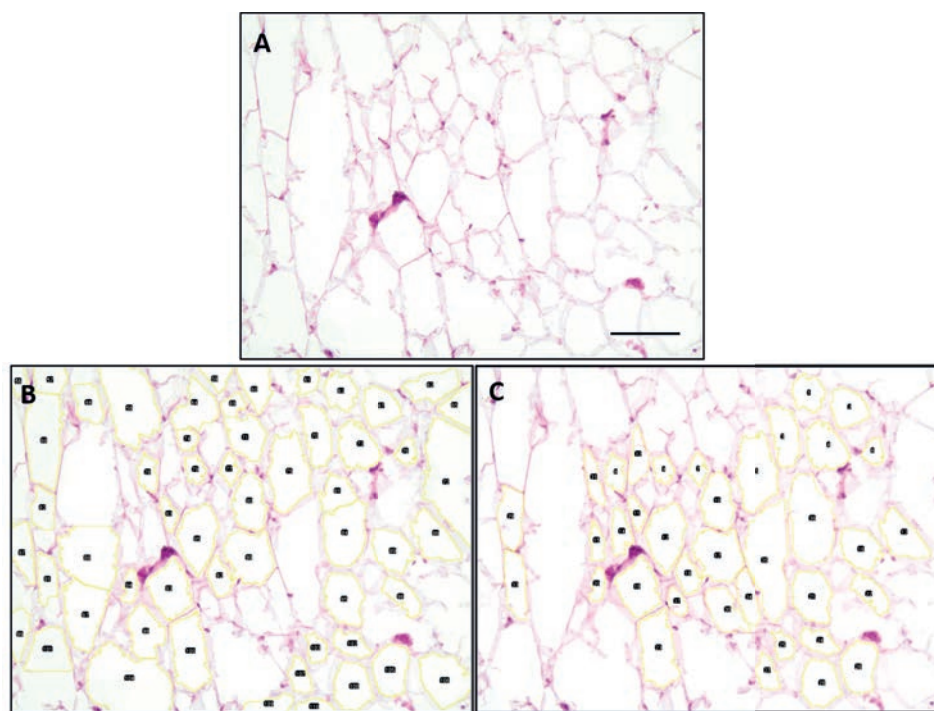


Figure 1 Identification of adipocytes using the Adiposoft plugin for Fiji.

A) Haematoxylin and eosin staining of adipose tissue imaged at 100x magnification. B) Image processed in Adiposoft, C) Corrected image after manual inspection of processed imaged. The yellow contours (B and C) represent the cross-sectional area of an adipocyte. Scale bar = 100 μm .

Statistical analysis

The Shapiro-Wilk test was conducted to assess the distribution of the adipocyte sizes for each donor. The size of adipocytes from individual donors was not nor-

mally distributed. Spearman's rho was determined to relate BMI to adipocyte size in IPFP and subcutaneous adipose tissue. The Kruskal-Wallis test with multiple comparisons was used to compare the median size of adipocytes from IPFP and subcutaneous fat from both non-obese and obese donors. Statistical significance was considered for p -values <0.05 .

RESULTS

A microscopic observation of the adipose tissues showed no distinct difference between adipocytes in terms of general morphology and distribution across donor groups, however relatively larger adipocytes were noticeable in subcutaneous fat of obese donors compared to other donor groups (Figure 2). The size of adipocytes in subcutaneous adipose tissue was correlated to donor BMI ($r=0.63$, $p=0.028$), which was not the case in the IPFP ($r=-0.06$, $p=0.82$) (Figure 3A, B). For non-obese donors (BMI < 30), IPFP adipocyte size ($1765 \mu\text{m}^2 \pm 163.5$) was not significantly different to subcutaneous adipocyte size ($2157 \mu\text{m}^2 \pm 835.6$, $p > 0.99$). However the size of adipocytes from the IPFP of obese ($1732 \mu\text{m}^2 \pm 292.4$) and non-obese donors ($1765 \mu\text{m}^2 \pm 163.5$) were significantly smaller than subcutaneous adipocytes from obese donors ($3195 \mu\text{m}^2 \pm 833.9$, $p=0.03$ and $p=0.04$ respectively) (Figure 3C).

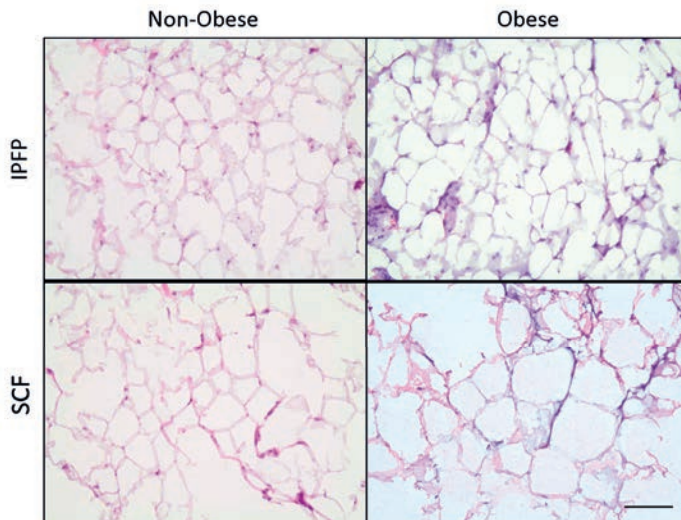


Figure 2 Representative images of H&E stained cryosections of adipose tissue from the IPFP and subcutaneous fat (SCF) of non-obese and obese donors.

IPFP: infrapatellar fat pad, SCF: subcutaneous fat. Scale bar = $100\mu\text{m}$.

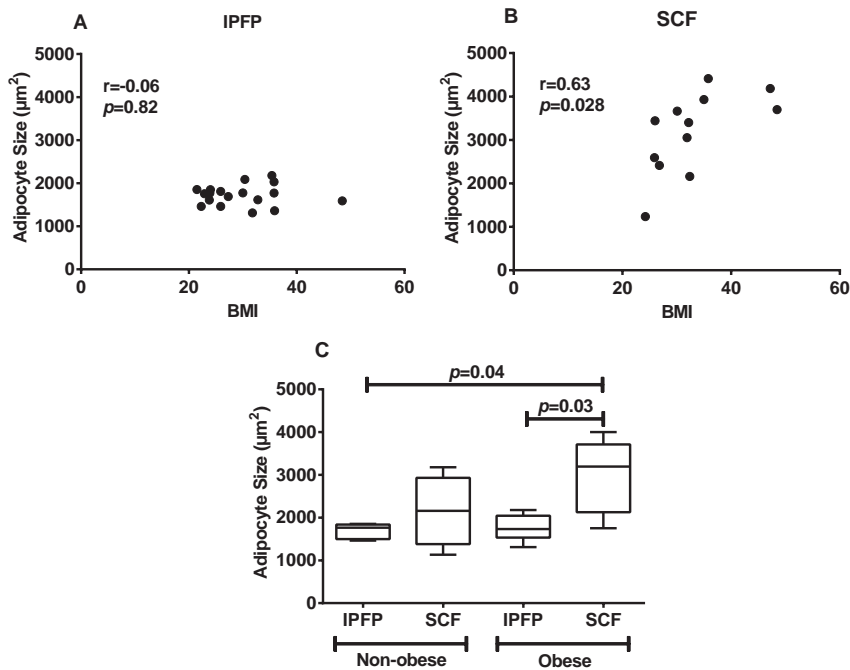


Figure 3 Obesity does not affect IPFP adipocyte size.

Spearman's test for correlation between donor BMI and adipocyte size in the A) infrapatellar fat pad (IPFP) and B) subcutaneous fat (SCF). Each dot represents an individual donor. C) Comparison of size of adipocytes between IPFP and SCF in obese and non-obese donor. Values are mean \pm SD

DISCUSSION

The obesity-related alterations that occur in adipose tissues, such as increased adipocyte size⁵, are not well characterised in the IPFP. In the current study, we have shown that unlike subcutaneous adipose tissue adipocytes, the size of IPFP adipocytes was not associated with BMI.

Our observations in human tissues provide evidence that the IPFP adipocytes do not undergo the metabolic alterations that often engenders cellular hypertrophy⁶, and confirms a previous investigation that showed the absence of hypertrophic adipocytes in the IPFP of obese mice.⁷ Subcutaneous adipose tissue is considered as both an energy storage and an endocrine organ that is susceptible to inflammatory macrophage infiltration during obesity. The IPFP is a potential contributor to local joint inflammation via the production of adipokines and cytokines³ that exacerbate joint degeneration. It has been shown that inflammation of the IPFP is

associated with knee pain and disability in obese OA patients.⁸ Since the adipocytes of the IPFP itself are not altered, at least not in size as a result of obesity, it could be inferred that the IPFP derived adipocytes do not possess the same pro-inflammatory phenotype as subcutaneous adipocytes. Hence, our findings could highlight novel functional differences between the IPFP and subcutaneous adipose tissue in obesity. Perhaps the inflammatory role of the IPFP in the pathogenesis of obesity related OA is separate to that of subcutaneous fat. The cellular, genetic or molecular mechanisms that causes this difference in sensitivity to obesity in the IPFP and other adipose tissues is not fully understood and warrants further investigation.

It is noteworthy however, that recent MRI based studies have associated large IPFP with a reduced number of a bone marrow lesions, low walking pain and higher total cartilage volume in OA patients.⁹ Furthermore, conditioned media of IPFP adipocytes from obese OA patients was found to have no effect on the secretion of TNF- α in lipopolysaccharide stimulated macrophages *in vitro*, but interestingly inhibited the production of IL-12p40 in these stimulated macrophages.¹⁰ We have also shown that there were no differences between the amount of secreted factors in conditioned media of IPFP from obese and non-obese OA donors¹¹, and that conditioned media from OA IPFP explants have a chondroprotective effect on cartilage.¹² In a rat model for ageing, only synovial thickness as one of the many OA features was correlated with IPFP adipocyte size and this correlation was independent of age. The secretion of the pro-inflammatory cytokine TNF- α from IPFP was associated with age, but no association between IPFP adipocyte size and cytokines release was reported¹³. The progressive age-dependant downregulation of genes related to anti-inflammatory macrophages in IPFP explants from these rats suggests that a shift towards a pro-inflammatory phenotype is likely to be mediated by immune cells rather than adipocytes. Taking this together, it is clear that further investigations are required to clarify whether and how obesity influences the IPFP, and if so, what the implications are for OA.

The use of unmatched IPFP and subcutaneous fat is a limitation to this study. Assessing a bigger sample size with matched IPFP and subcutaneous fat would further confirm the differences in adipocyte size in the two tissues within a particular donor. A recent study reported considerably larger adipocyte sizes for both IPFP ($3708 \pm 976 \mu\text{m}^2$) and subcutaneous fat ($6082 \pm 628 \mu\text{m}^2$) compared to our results¹⁴. This could be attributed to the difference in methods used to measure cell size. Analysis of the secretory profiles of individual adipocytes would also provide valuable insight concerning the inflammatory status of the IPFP in

obese and non-obese patients. Interestingly, our previous experiments revealed that the secretory profile of IPFP explants and the presence of macrophages in the IPFP are not influenced by donor BMI.^{3,11} This provides supporting evidence for our hypothesis that perhaps an increased BMI does not have significant influence on the adipocytes in the IPFP. Furthermore, we did not have samples from non-OA IPFP donors. We therefore cannot exclude the possibility that the OA could already have influenced the adipocyte size in our donors. The IPFP can also become fibrotic which could possibly limit the enlargement of adipocytes.

In conclusion, to our knowledge, this is the first evidence that IPFP adipocytes do not become hypertrophic with obesity. A difference in the physiological roles of the IPFP and subcutaneous fat could possibly account for the difference in susceptibility of their adipocytes to hypertrophy. The data presented here adds to the growing body of literature investigating the physiological function of the IPFP and its role in the development OA.

REFERENCES

1. Thijssen E, van Caam A, van der Kraan PM. Obesity and osteoarthritis, more than just wear and tear: pivotal roles for inflamed adipose tissue and dyslipidaemia in obesity-induced osteoarthritis. *Rheumatology (Oxford)*. 2015;54(4):588-600. doi:10.1093/rheumatology/keu464.
2. Skurk T, Alberti-huber C, Herder C, Hauner H. Relationship between Adipocyte Size and Adipokine Expression and Secretion. *J Clin Endocrinol Metab*. 2007;92(3):1023-1033. doi:10.1210/jc.2006-1055.
3. Clockaerts S, Bastiaansen-Jenniskens YM, Runhaar J, Van Osch GJVM, Van Offel JF, Verhaar JAN, et al. The infrapatellar fat pad should be considered as an active osteoarthritic joint tissue: a narrative review. *Osteoarthritis Cartilage*. 2010;18(7):876-882. doi:10.1016/j.joca.2010.03.014.
4. Teichtahl A, Wulidasari E, Brady S, Wang Y, Wluka A, Ding C, et al. A large infrapatellar fat pad protects against knee pain and lateral tibial cartilage volume loss. *Arthritis Res Ther*. 2015;17:318. doi:10.1016/j.joca.2015.02.517.
5. Hirsch J, Batchelor B. Adipose tissue cellularity in human obesity. *Clin Endocrinol Metab*. 1976;5(2):299-311. doi:10.1016/S0300-595X(76)80023-0.
6. De Ferranti S, Mozaffarian D. The perfect storm: Obesity, adipocyte dysfunction, and metabolic consequences. *Clin Chem*. 2008;54(6):945-955. doi:10.1373/clinchem.2007.100156.
7. Chang W, DeMoe J, Kent C, Kovats S, Garteiser P, Doblas S, et al. Infrapatellar fat pad hypertrophy without inflammation in a diet-induced mouse model of obesity and osteoarthritis. *Osteoarthritis Cartil*. 2011;19:66. doi:10.1016/S1063-4584(11)60157-X.
8. Ballegaard C, Riis RGC, Bliddal H, Christensen R, Henriksen M, Bartels EM, et al. Knee pain and inflammation in the infrapatellar fat pad estimated by conventional and dynamic contrast-enhanced magnetic resonance imaging in obese patients with osteoarthritis: A cross-sectional study. *Osteoarthritis Cartil*. 2014;22(7):933-940. doi:10.1016/j.joca.2014.04.018.
9. Han W, Cai S, Liu Z, Jin X, Wang X, Antony B, et al. Infrapatellar fat pad in the knee: is local fat good or bad for knee osteoarthritis? *Arthritis Res Ther*. 2014;16(4):R145. doi:10.1186/ar4607.
10. Klein-Wieringa IR, Andersen SN, Kwekkeboom JC, Giera M, de Lange-Brokaar BJE, van Osch GJVM, et al. Adipocytes modulate the phenotype of human macrophages through secreted lipids. *J Immunol*. 2013;191(3):1356-1363. doi:10.4049/jimmunol.1203074.
11. Clockaerts S, Bastiaansen-Jenniskens YM, Feijt C, De Clerck L, Verhaar JAN, Zuurmond A-M, et al. Cytokine production by infrapatellar fat pad can be stimulated by interleukin 1 β and inhibited by peroxisome proliferator activated receptor α agonist. *Ann Rheum Dis*. 2012;71(6):1012-1018. doi:10.1136/annrheumdis-2011-200688.
12. Bastiaansen-Jenniskens YM, Clockaerts S, Feijt C, Zuurmond A-M, Stojanovic-Susulic V, Bridts C, et al. Infrapatellar fat pad of patients with end-stage osteoarthritis inhibits catabolic mediators in cartilage. *Ann Rheum Dis*. 2012;71:288-294. doi:10.1136/ard.2011.153858.
13. Fu Y, Huebner JL, Kraus VB, Griffin TM. Effect of Aging on Adipose Tissue Inflammation in the Knee Joints of F344BN Rats. *Journals Gerontol Ser A Biol Sci Med Sci*. 2015;00(00):1-11. doi:10.1093/gerona/glv151.
14. Macchi V, Porzionato A, Sarasin G, Petrelli L, Guidolin D, Rossato M, et al. The Infrapatellar Adipose Body: A Histotopographic Study. *Cells Tissues Organs*. 2016. doi:10.1159/000442876.



CHAPTER 3

Stimulation of fibrotic processes by the infrapatellar fat pad in cultured synoviocytes from patients with osteoarthritis: a possible role for prostaglandin F_{2α}

Yvonne M Bastiaansen-Jenniskens

Wu Wei

Carola Feijt

Jan H Waarsing

Jan AN Verhaar

Anne-Marie Zuurmond

Roeland Hanemaaijer

Reinout Stoop

Gerjo JvM van Osch

ABSTRACT

Objective

Stiffening of the joint is a feature of knee osteoarthritis (OA) that can be caused by fibrosis of the synovium. The infrapatellar fat pad (IPFP) present in the knee joint produces immune-modulatory and angiogenic factors. The goal of the present study was to investigate whether the IPFP can influence fibrotic processes in synovial fibroblasts, and to determine the role of transforming growth factor β (TGF β) and prostaglandin $F_{2\alpha}$ (PGF $_{2\alpha}$) in these processes.

Methods

Batches of fat-conditioned medium (FCM) were made by culturing pieces of IPFP obtained from the knees of 13 patients with OA. Human OA fibroblast-like synoviocytes (FLS) (from passage 3) were cultured in FCM with or without inhibitors of TGF β / activin receptor-like kinase 5 or PGF $_{2\alpha}$ for 4 days. The FLS were analyzed for production of collagen and expression of the gene for procollagen-lysine,2-oxoglutarate 5-dioxygenase 2 (PLOD2; encoding lysyl hydroxylase 2b, an enzyme involved in collagen crosslinking) as well as the genes encoding α -smooth muscle-actin and type I collagen $\alpha 1$ chain. In parallel, proliferation and migration of the synoviocytes were analyzed.

Results

Collagen production and PLOD2 gene expression by the FLS were increased 1.8-fold ($p < 0.05$) and 6.0-fold ($p < 0.01$), respectively, in the presence of FCM, relative to control cultures without FCM. Moreover, the migration and proliferation of synoviocytes were stimulated by FCM. Collagen production was positively associated with PGF $_{2\alpha}$ levels in the FCM ($r = 0.89$, $p < 0.05$), and inhibition of PGF $_{2\alpha}$ levels reduced the extent of FCM-induced collagen production and PLOD2 expression. Inhibition of TGF β signaling had no effect on the pro-fibrotic changes.

Conclusion

These results indicate that the IPFP can contribute to the development of synovial fibrosis in the knee joint by increasing collagen production, PLOD2 expression, cell proliferation, and cell migration. In addition, whereas the findings showed that TGF β is not involved, the more recently discovered pro-fibrotic factor PGF $_{2\alpha}$ appears to be partially involved in the regulation of pro-fibrotic changes.

INTRODUCTION

Osteoarthritis (OA) is a multifactorial disease of the articular joints, with an incidence that is higher in women, obese subjects, and older individuals^{1,2}. The role of the synovium in OA pathology is becoming more evident. In conjunction with cartilage damage and bone alterations, the pathologic features of inflammation, hyperplasia, and extensive fibrosis are also often observed in the synovium of OA joints³⁻⁵.

Fibrosis can be seen as an abnormal healing process that is characterized by excessive deposition of extracellular matrix proteins, in particular collagen, which, in turn, results in alteration of the structure of the tissue and, finally, even loss of function of this tissue. Fibrotic processes are a response to a variety of insults, such as infection, trauma, autoimmunity, or inflammation, resulting in an inflammatory reaction with rapid recruitment of monocytes from the circulation or macrophages resident in the tissue. These cells are important sources of fibrotic cytokines, such as transforming growth factor β (TGF β) and platelet-derived growth factor, that, in turn, recruit fibroblasts to the site of injury and stimulate them to proliferate⁶.

Fibroblasts can also differentiate toward myofibroblasts. Myofibroblasts, which are characterized by the presence of α -smooth muscle actin, are present during normal tissue repair, but when the wound is closed, they disappear from the site. In the case of fibrosis, myofibroblasts persist in the damaged tissue⁷⁻⁹. An additional hallmark of fibrosis is the increased level of hydroxyallysine collagen crosslinks, which is regulated by lysyl hydroxylase 2b (LH2b), an enzyme encoded by the gene for procollagen-lysine, 2-oxoglutarate 5-dioxygenase 2 (PLOD2)¹⁰. These hydroxyallysine collagen crosslinks are found in fibrotic tissues and are associated with irreversible accumulation of collagen¹¹. Recently, it was demonstrated that PLOD2 expression and the presence of LH2b are up-regulated in the fibrotic synovium of mice with OA¹².

TGF β is a potent inducer of PLOD2 expression and LH2b activity^{12,13}, making TGF β a very potent fibrotic growth factor involved in all of the processes seen in fibrosis. In addition to TGF β , prostaglandin $F_{2\alpha}$ (PGF $_{2\alpha}$) was recently discovered as a cytokine that facilitates pulmonary fibrosis independent of TGF β . Mice lacking the PGF $_{2\alpha}$ receptor did not develop pulmonary fibrosis in response to bleomycin, and cells stimulated with PGF $_{2\alpha}$ produced more collagen^{14,15}.

In addition to cartilage, menisci, ligaments, and synovium, the knee joint contains fat pads. One of the largest of the fat pads is the infrapatellar fat pad (IPFP). The main role of the IPFP is to facilitate distribution of synovial fluid and distribute mechanical forces through the knee joint. Several adipokines and cytokines, such as tumor necrosis factor α , interleukin-6 (IL-6), IL-10, leptin, and vascular endothelial growth factor, are known to be produced by the IPFP¹⁶⁻²⁰. The IPFP is located in close proximity to the synovial layers and cartilage surfaces, making the IPFP able to influence inflammatory processes in the knee²¹. Many secreted proteins are derived from the non-adipocyte fraction of adipose tissue (macrophages, T cells, and B cells)^{18;22}, and it is suggested that most of the cytokines produced by the adipose tissue are macrophage-derived^{23;24}.

Since synovial fibrosis is often seen in end-stage OA, the goal of the present study was to investigate whether the IPFP and its secreted factors influence fibrotic processes in synovial fibroblasts, and to determine the role of 2 potent fibrotic inducers, TGF β and PGF_{2 α} , in the relationship between the IPFP and synovial fibrosis.

MATERIALS AND METHODS

Preparation and analysis of fat-conditioned medium

Samples of IPFP were derived from anonymized leftover knee tissue material obtained from patients with OA who had undergone total knee arthroplasty. The IPFP samples were used to produce FCM. The patients implicitly consented to the use of these tissues for scientific research, in accordance with the guidelines of the Federation of Biomedical Scientific Societies (<http://www.federa.org>), with approval from the local ethics committee in Rotterdam, The Netherlands (approval no. MEC 2008-181). The mean age of the donors was 67.9 years (range 54–81 years) and the mean body mass index (BMI) of the donors was 30.52 kg/m² (range 19.6–44.5 kg/m²). The inner parts of the fat pads, where no synovium is present, were cut into small pieces of ± 10 mg and cultured in suspension for 24 hours in a concentration of 50 mg tissue/ml in Dulbecco's modified Eagle's medium (DMEM) with Glutamax (Gibco BRL), containing insulin, transferrin, selenic acid, and albumin (ITS+) (dilution 1:100; BD Biosciences) as well as 50 μ g/ml gentamicin and 1.5 μ g/ml Fungizone (both from Gibco BRL). As a control medium, we used identically composed culture medium that did not contain pieces of IPFP, cultured in parallel. After 24 hours, the medium was harvested, centrifuged at 300g for 8 minutes to remove (immune) cells, and frozen at -80°C in aliquots of 1.5 ml, resulting in 29

different batches of FCM. This incubation time was chosen arbitrarily, since each mediator has its own optimum regarding release kinetics^{22,25-27}.

Isolation and culture of fibroblast like synoviocytes (FLS)

Samples of human synovium were also obtained as anonymized leftover material from patients with OA who had undergone total knee arthroplasty (approval no. MEC 2004-322). On the basis of its specific structure, the synovium could be distinguished and removed from the adjacent tissue. The synovium samples were then digested in Pronase (2 mg/ml; Sigma) for 2 hours and in collagenase B (1.5 mg/ml; Roche Diagnostics) overnight. Digested cells were plated out as 3,500 cells per cm² and expanded in Iscove's modified Dulbecco's medium with 10% fetal calf serum (FCS), 50 µg/ml gentamicin, and 1.5 µg/ml Fungizone (all from Gibco BRL). Cells from passage 3 were allowed to adhere at a density of 50,000 cells per cm² in DMEM with Glutamax, 10% FCS, and antibiotics (all from Gibco BRL). After overnight attachment, the culture medium was removed and the cells were washed carefully 3 times with saline. FCM was mixed 1:1 with fresh DMEM with Glutamax, supplemented with 50 µg/ml gentamicin, 1.5 µg/ml Fungizone, and ITS+ (dilution 1:100), and applied to the attached FLS. Thereafter, the FLS were cultured for 4 days. The mean age of the FLS donors was 67 years (range 60–81 years) and the mean BMI was 32.4 kg/m² (range 24.2–42.5 kg/m²).

To investigate the involvement of TGFβ1 or PGF_{2α}, 1 µM SB505124 (Sigma), an inhibitor of TGFβ1 signaling, or 10 µM AL8810 (Cayman Chemical), an inhibitor of PGF_{2α} signaling, was added 1 hour prior to adding the FCM; as positive control for the inhibition, 1 ng/ml TGFβ1 or 1 µM PGF_{2α} was added. Concentrations and timing were based on those previously described in a study by Oga et al¹⁴.

Analysis of collagen deposition

Collagen was determined using the Quickzyme soluble collagen assay according to the manufacturer's guidelines (QuickZyme Biosciences, Leiden, the Netherlands). Briefly, culture medium was removed and the cell/matrix fraction was solubilized by overnight incubation in 0.5M acetic acid at 4°C. The assay is based on binding of collagen with Sirius Red.

Analysis of gene expression

After culture, monolayers of synoviocytes were suspended in 350µl RLT buffer (Qiagen, Venlo, the Netherlands) supplemented with 1% β-mercaptoethanol. RNA was extracted and complementary DNA was analyzed for gene expression using previously described methods²⁸. The primer sequences for the genes were as follows: for the GAPDH reference gene, forward GTCAACGGATTGTCGATT-

GGG, reverse TGCCATGGGTGGAATCATATTGG, and probe FAM-CGCCCAATAC-GACCAAATCCGTTGAC-TAMRA; for the type I collagen α 1 chain gene (COL1A1), forward CAGCCGCTTCACCTACAGC, reverse TTTTGTATTCAATCACTGTCTTGCC, and probe FAM-CCGGTGTGACTCGTGCAGCCATC-TAMRA; for PLOD2, forward CCCTCCGATCAGAGATGATT and reverse AATGTTTCCGGAGTAGGGGAGTCTTTTT; and for the gene encoding α -smooth muscle actin (ASMA), forward CGTTGCCCCCT-GAAGAGCAT and reverse CCGCCTGGATAGCCACATACA. Primers for the type III collagen gene (COL3) were purchased from Qiagen Assays-on-Demand (QT00058233). For analysis of GAPDH and COL1A1, TaqMan 2x Universal Polymerase Chain Reaction (PCR) Master Mix (Applied Biosystems) was used in the reaction. For analysis of PLOD2 and ASMA, quantitative PCR Master Mix Plus SYBR Green I (Eurogentec) was used in the reaction. In determining the optimal housekeeping gene, we compared GAPDH, 18S RNA, 2-microglobulin, and hypoxanthine guanine phosphoribosyltransferase, and observed that GAPDH was the most stable housekeeping gene in our experiments.

Migration assay

To investigate the migration of the synoviocytes in response to soluble factors, a scratch wound assay was performed. Synoviocytes from passage 3 were seeded at 100,000 cells per cm^2 in 12-well plates and allowed to adhere overnight in DMEM containing 10% FCS. A 10- μl pipette tip was used to make a scratch in the confluent monolayer of the synoviocytes, after marking the scratch location on the bottom of the well. When applicable, SB505124 or AL8810 was added 1 hour prior to making the scratch. Cell debris was removed by washing with saline, and the cell culture was continued in DMEM–1% ITS+ mixed with FCM (1:1) with or without SB505124 or AL8810.

Photographic images were obtained directly after scratching and at 14, 16, and 19 hours after scratching. These time points were chosen on the basis of pilot experiments showing that, from 14 hours onward, migration of the synoviocytes is best visualized (results not shown) without interference from proliferation of the cells. Closure was measured using TScratch software (Computational Science & Engineering Laboratory). The extent of migration is presented as the percentage of closure after wounding.

Proliferation assay

To analyze proliferation, synoviocytes from passage 3 were seeded at a density of 10,000 cells per cm^2 in 12-well plates and allowed to adhere overnight in DMEM containing 10% FCS. To arrest cells in the S1 phase (which was necessary in order

to reduce variation), cells were cultured in DMEM containing 0.1% FCS for 24 hours after adherence. Following 24 hours of starvation, the culture was continued in DMEM–1% ITS+ mixed with FCM (1:1) with or without the addition of SB505124 or AL8810. When applicable, SB505124 or AL8810 was added 1 hour prior to adding the FCM. Samples for DNA measurement were obtained after 1, 2, 3, and 4 days by suspending the monolayer in phosphate buffered saline with 0.1% Triton. The amount of DNA in each sample was determined using ethidium bromide, with calf thymus DNA (Sigma) as standard.

Enzyme-linked immunosorbent assay (ELISA) for TGFβ1

To determine the activity of TGFβ1 in the FCM, a human TGFβ1 Quantikine ELISA kit (R&D Systems) was used according to the manufacturer's guidelines. To activate latent TGFβ1 to the immunoreactive form, acid activation with 1N HCl and neutralization with 1.2N NaOH/0.5M HEPES was performed.

PGF_{2α} measurements using mass spectrometry

To determine the levels of PGF_{2α} in the FCM samples that remained (n=7), samples were analyzed with liquid chromatography tandem mass spectrometry (LC-MS/MS) as described previously²⁹. Briefly, to prepare the samples for measurement, FCM samples, with deuterated PGF_{2α}-d4 (Cayman Chemical) added as internal standard, were extracted with LC-MS-grade methanol (Riedel-de-Haën). The methanol extract was loaded on an HLB SPE column (Oasis), after which the samples were reconstituted in 100 µl ethanol containing CUDA (Cayman Chemical) as a second internal standard, and immediately used for LC-MS/MS analysis on an Acquity C18 BEH Ultra Performance liquid chromatography column coupled to a Xevo TQ-S mass spectrometer (Waters). Cone voltage and collision energy were optimized for each compound individually. Parent and product mass/charge (m/z) values of PGF_{2α} were 353.1 and 193.0. Parent and product m/z values of PGF_{2α}-d4 were 357.1 and 313.4. Parent and product m/z values of CUDA were 339.1 and 214.1. Identification and quantification of peak values were performed using MassLynx software version 4.1.

Statistical analysis

Experiments examining the effect of FCM were performed with samples from 3 different FLS donors and 13 different FCM batches representing 13 different IPFP donors. Experiments examining the effect of inhibition of TGFβ1 or PGF_{2α} together with FCM stimulation were performed with samples from 2 different FLS donors and 8 different FCM batches representing 8 different IPFP donors. All experiments were performed with triplicate samples per condition, which was taken into ac-

count in the statistical analysis. A mixed linear model, followed by a Bonferroni post hoc test, was used to analyze gene expression, collagen deposition, and cell migration. A univariate general linear model was used to analyze the results from the proliferation assays. Since not every FCM batch was tested on FLS from every donor, we allowed for this in the statistical analysis by adding a subject variable indicating the FLS donor. Spearman's rho correlations were determined to examine associations between TGF β 1 or PGF $_{2\alpha}$ levels and other parameters. Data were analyzed with IBM SPSS statistical software (version 20.0).

RESULTS

Induction of fibrotic processes with medium conditioned

by IPFP

In culture conditions with 8 of the 13 FCM batches (derived from 13 different OA IPFP donors), collagen production by FLS was increased 1.8-fold after 4 days of culture, from a mean 1.9 μ g/monolayer in control conditions without FCM to a mean 3.4 μ g/monolayer in cultures with FCM (Figure 1A [all 13 included in the figure]). In addition, gene expression of the enzyme involved in the formation of pyridinolinebased collagen crosslinks, PLOD2, was increased 6.0-fold in the presence of FCM. Surprisingly, COL1A1 expression on day 4 was 2.5-fold lower than

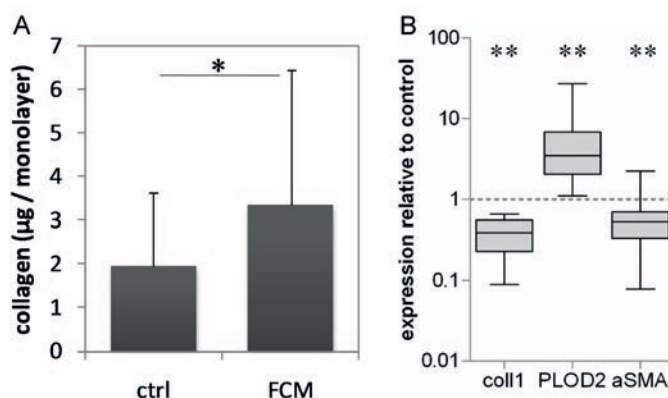


Figure 1 The effect of fat conditioned medium (FCM) on A) total collagen production by FLSs in monolayer after 4 days of culture and B) gene expression after 4 days of culture relative to the control without FCM (set at 1) of genes describing a fibrotic process: *Coll* (coll1, α 1 chain), procollagen-lysine, 2- oxoglutarate 5-dioxygenase 2 (*Plod2*) and α smooth muscle actin (*Asma*). A total of 13 different FCM batches was tested on FLS of three different donors. Bars represent the mean \pm standard deviation. Box-whisker plots indicate the 75th and 25th percentile with the median (boxes) and the maximum and the minimum (whiskers). *indicates $p < 0.05$, **indicates $p < 0.01$.

that in control conditions without FCM, and ASMA expression was 1.7-fold lower (Figure 1B). COL3 expression was unaltered by the addition of FCM (results not shown). The observed increase in collagen production but decrease in COL1A1 expression might be explained by the hypothesis that altered processing of the collagen would lead to more efficient translation, but would not alter expression of COL3. Also, the collagen deposition represents accumulation in the total culture for 4 days, whereas the collagen gene expression is the specific expression at the moment of harvest.

Since TGF β 1 is known to be a potent inducer of collagen deposition and of COL1A1, PLOD2, and ASMA expression, we also included, as a positive control a culture condition in which TGF β 1 was added in all of the experiments. Indeed, irrespective of which FLS donor was used, TGF β 1 induced the same fibrotic processes as seen in FLS cultures with FCM (results not shown).

To investigate whether the BMI of the IPFP donor influenced the effect of FCM on FLSs, we performed a *post hoc* subgroup analysis comparing the FCM batches made from IPFPs of donors who had a BMI lower than 30 kg/m² (n=5) with FCM batches made from IPFPs of donors who had a BMI equal to or higher than 30 kg/m² (n=8). No differences in collagen deposition or expression of COL1A1, PLOD2, or ASMA were observed between the 2 BMI subgroups. Both groups still showed significant differences in gene expression when compared with the control condition without FCM (Figure 2).

To determine the effects on FLS migration, we performed a scratch wound assay (typical examples right after scratching and 19 hours after scratching are shown in Figures 3A and B). Migration of FLS ($p=0.005$) and proliferation of FLS ($p=0.002$) were stimulated in the presence of FCM (Figures 3C and D).

Association of FCM effects with the presence of TGF β 1 or PGF_{2 α}

TGF β 1 and PGF_{2 α} are both known as potent pro-fibrotic mediators and candidates to be involved in the processes seen in the FLS in response to FCM. The mean TGF β 1 content of the FCM was 37.3 pg/ml, ranging from 0.1 pg/ml to 74.9 pg/ml. The mean PGF_{2 α} content in the FCM was 6,204 pg/ml, ranging from 560 pg/ml to 29,718 pg/ml. The level of PGF_{2 α} was positively correlated with the extent of collagen deposition by the FLS (Figure 4A) and negatively associated with COL1A1 expression (Figure 4B).

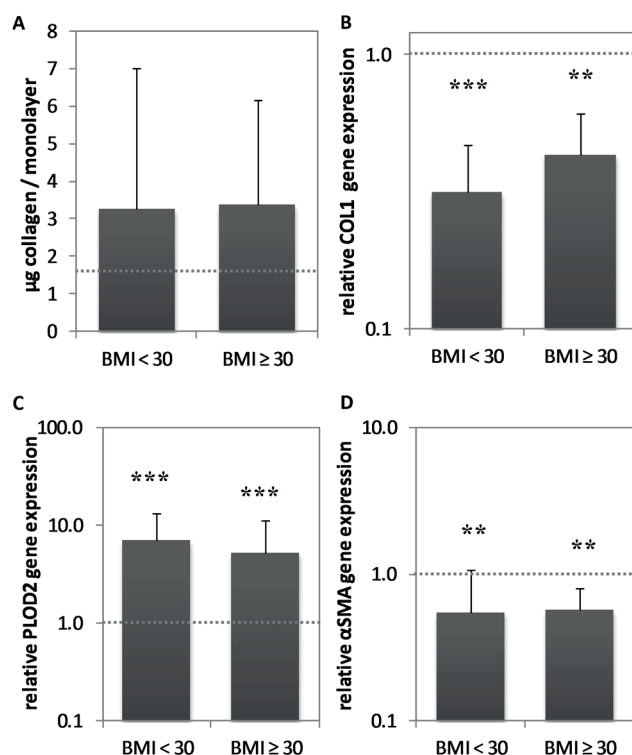


Figure 2 The effect of FCM subdivided in non obese (BMI < 30, n = 5, 1 male and 4 female) and obese (n ≥ 30, n 8, 1 male and 7 female) donors on A) collagen deposition B) collagen type 1 gene expression, C) *Plod2* gene expression, and D) *Asma* gene expression by synoviocytes. The dotted line indicates the levels in the control condition without FCM. **indicates significantly different from control condition with $p < 0.01$, ***indicates significantly different from control condition with $p < 0.005$. Bars represent the mean \pm standard deviation.

The level of TGF β 1 was positively associated with COL1A1 expression (Figure 4C). No other associations were seen.

To evaluate the effect of TGF β 1 and PGF $_{2\alpha}$ on FLS in our culture system, we added these compounds to FLS cultures without the presence of FCM. The addition of 1ng/ml TGF β 1 increased total collagen deposition, COL1A1 expression, and ASMA expression. The addition of 1 μM PGF $_{2\alpha}$ increased PLOD2 expression and total collagen deposition (Figures 5A and D-F). TGF β 1 and PGF $_{2\alpha}$ both increased the migration of the FLS, but had no effect on proliferation of the FLS (Figures 5B and C). The effects of PGF $_{2\alpha}$ best simulated the effects of FCM as seen in our experiments (as described in Figures 1 and 2).

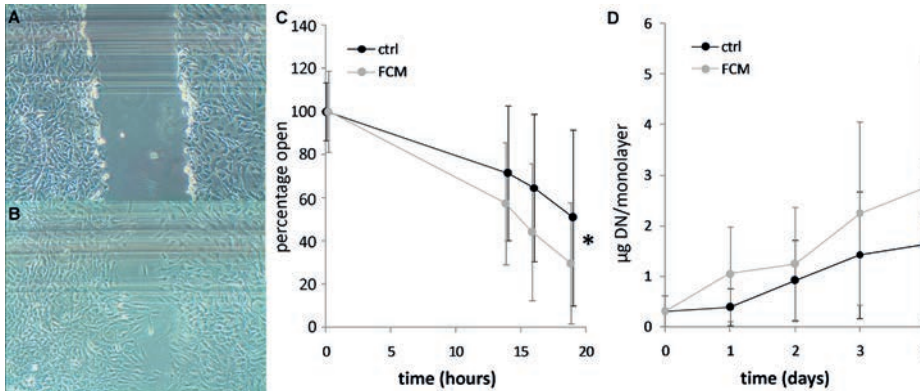


Figure 3 The effect of FCM on migration and proliferation of FLS determined by a scratch-wound assay.

(A) Pictures of the scratch were taken directly after making the scratch and (B) after migration for 19 hours. The lines at the top of A and B mark the bottom of the well as reference point for taking pictures during migration. The effect of FCM on (C) migration as percentage open and (D) proliferation as μg DNA per monolayer was tested. A total of 9 different FCM batches was tested on FLS of three different donors. * indicates $p < 0.05$ regarding the total migration and proliferation curves. Data are shown as mean migration or proliferation \pm standard deviation of 9 FCM batches.

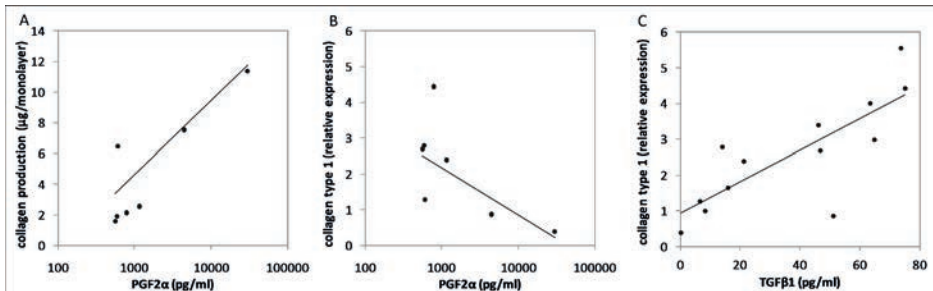


Figure 4 Associations between concentration of TGF $\beta 1$ and PGF $_{2\alpha}$ in the FCM and the effect of FCM on the FLS in culture.

A) a positive association between the level of PGF $_{2\alpha}$ in the FCM and collagen deposition by the FLS ($R = 0.89$, $p = 0.028$) B) a negative association between PGF $_{2\alpha}$ in the FCM and *Col1* gene expression ($R = -0.82$, $p = 0.023$), and C) a positive association between TGF $\beta 1$ in the FCM and *Col1* gene expression ($R = 0.77$, $p = 0.012$). The p -values were corrected for multiple testing.

Counteraction of the pro-fibrotic effect of FCM via inhibition of PGF $_{2\alpha}$ signaling.

To examine the involvement of TGF $\beta 1$ and PGF $_{2\alpha}$ in the pro-fibrotic effect of FCM, the FLS were cultured with FCM with or without a TGF $\beta 1$ receptor type I kinase inhibitor, SB505124, or a selective PGF receptor antagonist, AL8810. First, we verified whether SB505124 could indeed inhibit the effect of 1 ng/ml TGF $\beta 1$, and whether AL8810 could indeed inhibit the effect of 1 μM PGF $_{2\alpha}$. SB505124 blocked

the effect of TGF β 1 on collagen production, COL1A1 expression, and ASMA expression, confirming the efficacy of the inhibitor. AL8810 inhibited the effect of PGF $_{2\alpha}$ on collagen production and there was a trend toward normalization of PLOD2 expression ($p=0.08$) (Figures 5A and D–F). The presence of 1 μ M SB505124 or 10 μ M AL8810 alone seemed to have no influence on collagen deposition or COL1A1, PLOD2, and ASMA expression (Supplementary figure 1).

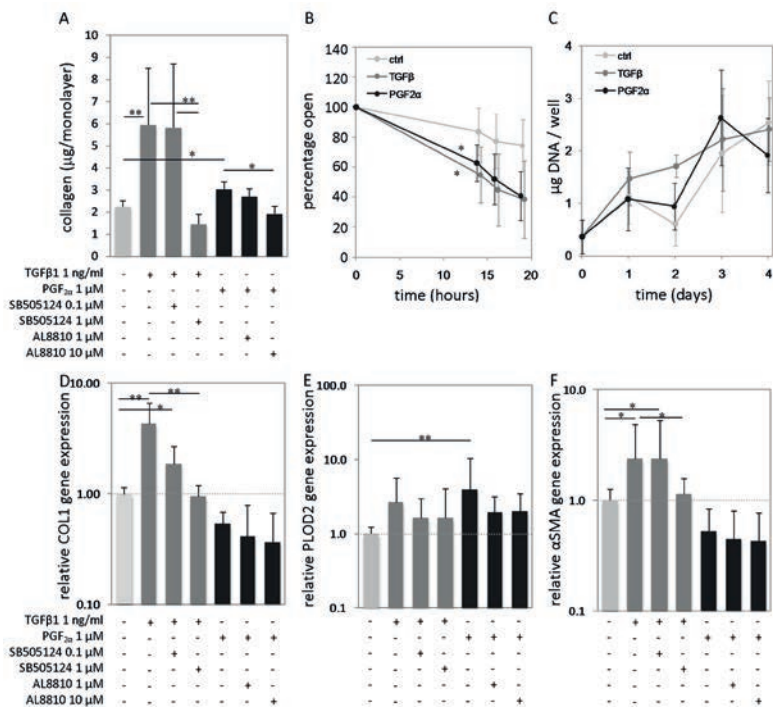


Figure 5 The effect of 1 ng/ml TGF β 1 and 1 μ M PGF $_{2\alpha}$ and their inhibitors SB505124 and AL8810 in the absence of FCM on A) collagen production, B) migration, and C) proliferation and gene expression of C) *Col1 α 1*, D) *Plod2* and E) *Asma* by FLSs relative to the control without these additions (set at 1). All analyses were done in triplicate with three FLS donors. *indicates $p<0.05$, **indicates $p<0.01$. Bars or dots represent the mean \pm standard deviation.

Inhibition of TGF β /activin receptor–like kinase 5 signaling with SB505124 did not alter the FCM-induced effects on FLS, indicating that the effect of FCM was not caused by TGF β . Blocking the PGF receptor with AL8810, on the other hand, inhibited the increase in collagen deposition that had been induced by FCM, bringing the collagen deposition back to the levels seen in control conditions without FCM (Figure 6A). The increase in PLOD2 expression induced by FCM was similarly abrogated, with a return to the levels seen in control conditions without FCM, when the FLS were co-incubated with FCM and AL8810 (Figure 6E).

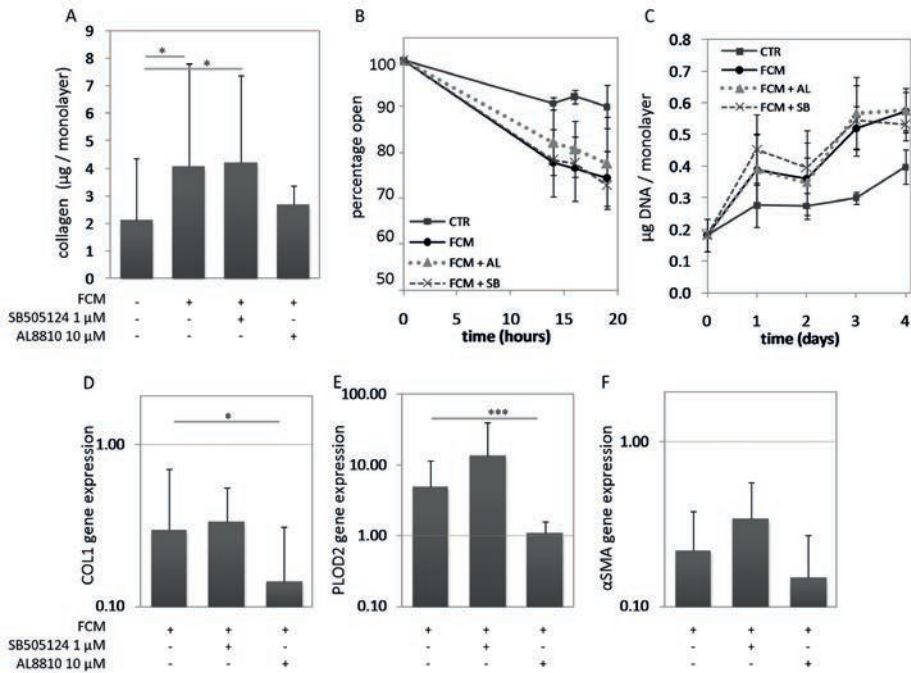


Figure 6 The effect of the TGF β /ALK5 (SB505124) or PGF $_{2\alpha}$ signalling (AL8810) inhibition on the effect of FCM in FLS cultures on A) collagen production, B) migration and C) proliferation and D) *Col1a1* gene expression, E) *Plod2* gene expression and F) *Asma* gene expression by synoviocytes. A total of 8 different FCM batches was tested using FLS of two different donors. The control without FCM was set at 1 and indicated with a dotted line for the gene expression analyses. * indicates $p < 0.05$, *** indicates $p < 0.005$. Bars or dots represent the mean \pm standard deviation of 8 different FCM batches.

The effects of FCM on the migration and proliferation of synoviocytes and on the level of ASMA expression were not counteracted by the addition of the PGF receptor inhibitor AL8810 (Figures 6B, C, and F). COL1A1 expression, which had been decreased in FLS cultures with FCM, was decreased even more in cultures with AL8810 (Figure 6D). This is consistent with the minimal decrease in COL1A1 expression that was observed when only AL8810 was added to the FLS cultures (Figure 5D).

DISCUSSION

OA is a disease of the articular joints in which synovial fibrosis is often seen^{3,4,12}. Accumulating data have been presented to suggest that OA is an inflammatory

disease in which cytokines and immune cells play a role³⁰. Adipose tissue can, in general, be considered to be an endocrine organ that secretes cytokines and growth factors and that exhibits significant infiltration of immune cells, including macrophages³¹⁻³³. In earlier studies conducted by our group and other investigators, it was shown that the IPFP is able to produce cytokines, adipokines, and growth factors, and thereby contributes to their levels in the synovial fluid^{18-20;34}. In the current study, we demonstrate that medium conditioned by samples of IPFP obtained from the joints of patients with end-stage OA stimulates fibrotic processes in FLS.

Culturing the FLS with FCM increased collagen production, the expression of PLOD2 encoding for the enzyme LH2b (involved in pyridinoline-based collagen crosslinks), and the migration and proliferation of FLS, which are hallmarks of a fibrotic process^{11;13;35}. These effects were independent of the BMI of the IPFP donor (BMI < 30 kg/m² versus BMI > 30 kg/m²).

TGFβ1, and more recently, PGF_{2α}¹⁴, have been suggested to act as pro-fibrotic factors in the joints. We found that both TGFβ1 and PGF_{2α} were present in the FCM batches used for culture with the FLS; this finding is in addition to the previously described presence of many other cytokines, adipokines, and growth factors¹⁷. When we compared the levels of TGFβ1 and PGF_{2α} in the FCM with our functional parameters, we found a positive association between PGF_{2α} levels and collagen deposition, a negative association between PGF_{2α} levels and COL1A1 expression, and a positive association between TGFβ1 levels and COL1A1 expression. These associations indicate that PGF_{2α} was responsible for some of the effects of the FCM. The absence of associations between PGF_{2α} levels and PLOD2 expression and between TGFβ1 levels and ASMA expression might be explained by the fact that the FCM contains, in addition to PGF_{2α} and TGFβ1, many other unknown factors that could also have influenced the fibrotic processes in FLS.

Furthermore, our experiments indicate that the effects of FCM on FLS are comparable to the effects of adding PGF_{2α} to FLS cultures without FCM, again indicating that the presence of PGF_{2α} contributes to the FCM effect. The profibrotic effect of FCM may be attributable not only to the PGF_{2α} present in the FCM, but also to the PGF_{2α} that is produced by FLS in response to FCM. Fibroblasts, in general, are known to produce PGF_{2α}^{36;37}. This may explain the discrepancy between our findings of PGF_{2α} increasing PLOD2 expression and AL8810 bringing PLOD2 expression back to control levels and our findings of the absence of a correlation between PGF_{2α} levels in the FCM and PLOD2 expression.

Messenger RNA (mRNA) and protein levels are, in general, associated with each other. This was true for the COL1A1 mRNA and protein levels in this study, when we cultured the FLS with TGFβ1. However, collagen deposition is regulated on

many levels, and its regulation through variation in the amount of mRNA is only the beginning. For example, after synthesis of the different collagen chains, post-translational modification through enzymes such as the lysyl and prolyl hydroxylases and lysyl oxidases can occur, while correct folding of the collagen molecules requires the involvement of chaperones such as Hsp47. These changes not only are directly involved in collagen synthesis but also can indirectly regulate collagen content. The level of collagen crosslinking, for example, can have an effect on the sensitivity of collagen to degradation by matrix metalloproteinases³⁸. Of course, degradation of collagen can have a major role in determining to what extent collagen content increases over time. In this respect, it is very exciting to see that despite a reduction in type I collagen mRNA, the presence of FCM or PGF_{2α} does result in increased collagen deposition, and that there are differences between stimulation with PGF_{2α} and stimulation with TGFβ1. Unfortunately, we were not able to quantify deposition of specific types of collagen.

To further examine the involvement of TGFβ1 and PGF_{2α} present in the FCM in the different fibrotic processes, we used a TGFβ1 receptor type I kinase inhibitor, SB505124, and a selective PGF_{2α} receptor antagonist, AL8810, together with the FCM incubation. Blockade of PGF_{2α} with AL8810 brought collagen deposition and PLOD2 expression back to the levels in control conditions without FCM, whereas the presence of the TGFβ1 inhibitor SB505124 did not alter the FCM effect on FLS. Since the addition of AL8810 decreased PLOD2 expression, our results indicate indirectly that PGF_{2α} levels are associated with PLOD2 expression, in addition to the already-shown association between PGF_{2α} and collagen production. The latter is confirmed by the fact that inhibition of the PGF_{2α} receptor with AL8810 normalized collagen deposition in FCM-treated FLS. Inhibition of TGFβ1 signaling with SB505124 in combination with FCM did not normalize collagen deposition or PLOD2 expression. From these results, we conclude that PGF_{2α} might be a more important factor than TGFβ1 in the FCM-induced fibrotic processes in FLS.

No effect of the inhibitors was seen on the FCM-induced migration and proliferation of synoviocytes, and co-incubation of FCM with AL8810 decreased COL1A1 expression even more than that with FCM alone. Thus, next to PGF_{2α}, other factors also influenced the parameters of fibrosis, since not all processes induced by FCM were counteracted by AL8810. In addition, the extra inhibition of COL1A1 expression that occurred when the FLS were cultured with FCM and AL8810 could be explained by the fact that, in our culture system, there is no direct effect of PGF_{2α} on COL1A1 expression and that other factors are involved in this relationship.

Like other organs, adipose tissue contains a resident population of cells of the innate immune system, in particular macrophages and T lymphocytes. In our earlier study, we demonstrated that macrophages were present in the IPFP, many

of which have an M2 phenotype³⁹. Alternatively activated M2 macrophages have an anti-inflammatory or repair phenotype and produce, predominantly, IL-10 but also growth

factors such as TGF β 1 and insulin-like growth factor 1, and almost no IL-12 or IL-23⁴⁰. The presence of M2 macrophages in the IPFP of patients with end-stage OA might contribute to the profibrotic effect of the FCM on FLS described in the present study. Earlier studies also found that macrophages are able to produce PGF_{2 α} ^{41;42}. In addition to macrophages, adipocytes, T lymphocytes, or other cells from the stromal vascular fraction might also contribute to PGF_{2 α} production in the IPFP⁴³.

Prostaglandins, including PGD₂, PGE₂, PGF_{2 α} , and PGI₂, are produced when phospholipids are cleaved in response to stimuli, resulting in the release of arachidonic acid, which is then metabolized by cyclooxygenase to produce prostaglandins. PGF_{2 α} is considered to be a major and stable metabolite of PGE₂⁴⁴. Reduction in PGE₂ production is the classic mode of action of anti-inflammatory agents such as nonsteroidal anti-inflammatory drugs (NSAIDs), which are commonly used in medical management of OA, and numerous studies have demonstrated a lower PGE₂ concentration in synovial fluid following NSAID treatment^{45;46}. More recently, PGF_{2 α} was also found in the synovial fluid of horses, the levels of which increased after stimulation of acute inflammation and which were shown to be decreased after the treatment of inflamed knees with an NSAID⁴⁷. NSAIDs might, therefore, also be useful in the prevention of the synovial fibrosis seen in OA.

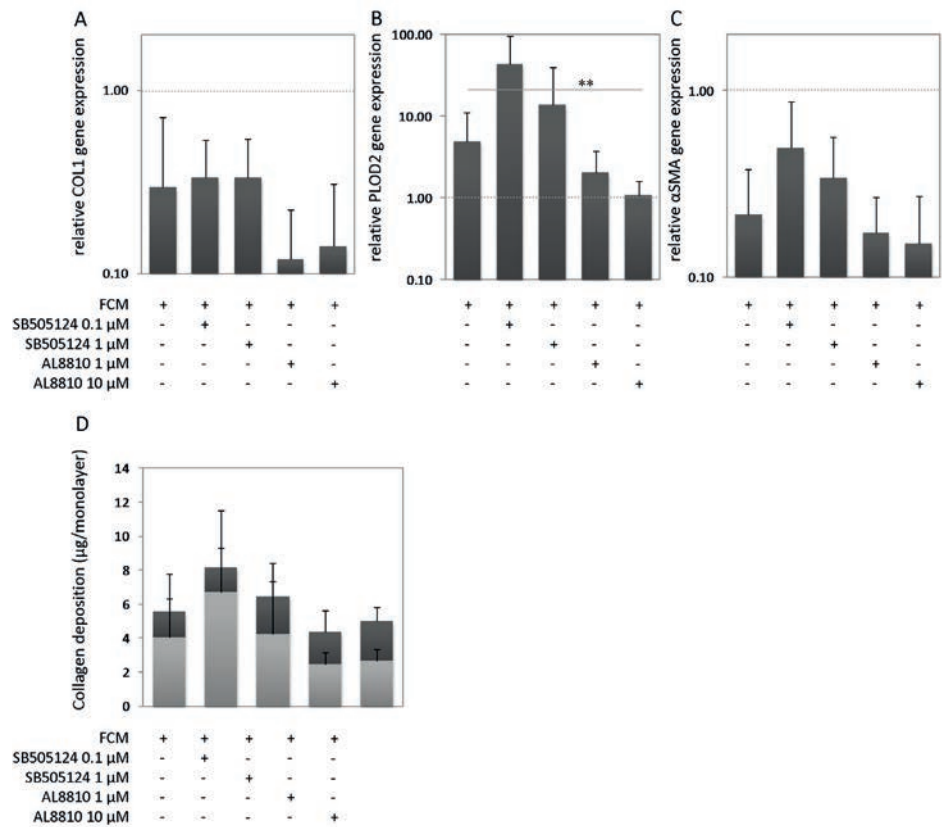
To our knowledge, this is the first study to examine the effect of adipose tissue on the synovium and to assess the potential involvement of the IPFP on the development of the synovial fibrosis often seen in OA³. The results of this study indicate that the IPFP in the knees of patients with end-stage OA not only inhibits catabolic mediators in cartilage³⁹ but also exerts pro-fibrotic effects on the synovium, and these pro-fibrotic effects can be partially explained by the presence of PGF_{2 α} . However, since not all of the fibrotic effects can be explained by the presence of PGF_{2 α} , other factors may also play a role. Additional experiments are required to examine the effect of FCM on the entire OA fibrotic process, and to investigate whether the effect that we found is specific to the IPFP in end-stage OA or whether the IPFP from an earlier stage of OA would have the same pro-fibrotic effect. Future studies should also investigate whether FLS from patients with OA in an earlier stage would respond in a manner comparable to that of FLS from patients with end-stage OA. In addition, it should be examined whether OA patients have increased levels of PGF_{2 α} in their synovial fluid and whether this is associated with severe changes in their synovium. The continuing expansion of this knowledge might eventually contribute to more optimal treatment or even the prevention of OA.

REFERENCES

1. Yusuf E, Bijsterbosch J, Slagboom PE, Rosendaal FR, Huizinga TW, Kloppenburg M. Body mass index and alignment and their interaction as risk factors for progression of knees with radiographic signs of osteoarthritis. *Osteoarthritis Cartilage* 2011;19: 1117–22.
2. Reijman M, Pols HA, Bergink AP, Hazes JM, Belo JN, Lievense AM, et al. Body mass index associated with onset and progression of osteoarthritis of the knee but not of the hip: the Rotterdam Study. *Ann Rheum Dis* 2007;66:158–62.
3. Revell PA, Mayston V, Lalor P, Mapp P. The synovial membrane in osteoarthritis: a histological study including the characterisation of the cellular infiltrate present in inflammatory osteoarthritis using monoclonal antibodies. *Ann Rheum Dis* 1988;47:300–7.
4. Hutton CW, Hinton C, Dieppe PA. Intra-articular variation of synovial changes in knee arthritis: biopsy study comparing changes in patellofemoral synovium and the medial tibiofemoral synovium. *Br J Rheumatol* 1987;26:5–8.
5. Loeuille D, Chary-Valckenaere I, Champigneulle J, Rat AC, Toussaint F, Pinzano-Watrin A, et al. Macroscopic and microscopic features of synovial membrane inflammation in the osteoarthritic knee: correlating magnetic resonance imaging findings with disease severity. *Arthritis Rheum* 2005;52:3492–501.
6. Gharaee-Kermani M, Phan SH. Role of cytokines and cytokine therapy in wound healing and fibrotic diseases. *Curr Pharm Des* 2001;7:1083–103.
7. Gabbiani G. The myofibroblast in wound healing and fibrocontractive diseases. *J Pathol* 2003;200:500–3.
8. Desmouliere A, Geinoz A, Gabbiani F, Gabbiani G. Transforming growth factor-1 induces -smooth muscle actin expression in granulation tissue myofibroblasts and in quiescent and growing cultured fibroblasts. *J Cell Biol* 1993;122:103–11.
9. Ronnov-Jessen L, Petersen OW. Induction of -smooth muscle actin by transforming growth factor-1 in quiescent human breast gland fibroblasts: implications for myofibroblast generation in breast neoplasia. *Lab Invest* 1993;68:696–707.
10. Van der Slot AJ, Zuurmond AM, Bardoel AF, Wijmenga C, Pruijs HE, Sillence DO, et al. Identification of Plod2 as telopeptide lysyl hydroxylase, an important enzyme in fibrosis. *J Biol Chem* 2003; 278:40967–72.
11. Van der Slot AJ, Zuurmond AM, van den Bogaerdt AJ, Ulrich MM, Middelkoop E, Boers W, et al. Increased formation of pyridinoline cross-links due to higher telopeptide lysyl hydroxylase levels is a general fibrotic phenomenon. *Matrix Biol* 2004;23:251–7.
12. Remst DF, Blaney Davidson EN, Vitters EL, Blom AB, Stoop R, Snabel JM, et al. Osteoarthritis-related fibrosis is associated with both elevated pyridinoline cross-link formation and lysyl hydroxylase 2b expression. *Osteoarthritis Cartilage* 2013;21:157–64.
13. Van der Slot AJ, van Dura EA, de Wit EC, De Groot J, Huizinga TW, Bank RA, et al. Elevated formation of pyridinoline cross-links by profibrotic cytokines is associated with enhanced lysyl hydroxylase 2b levels. *Biochim Biophys Acta* 2005;1741:95–102.
14. Oga T, Matsuoka T, Yao C, Nonomura K, Kitaoka S, Sakata D, et al. Prostaglandin F₂ α receptor signaling facilitates bleomycin-induced pulmonary fibrosis independently of transforming growth factor- β . *Nat Med* 2009;15:1426–30.
15. Olman MA. Beyond TGF- β : a prostaglandin promotes fibrosis. *Nat Med* 2009;15:1360–1.

16. Chen WP, Bao JP, Feng J, Hu PF, Shi ZL, Wu LD. Increased serum concentrations of visfatin and its production by different joint tissues in patients with osteoarthritis. *Clin Chem Lab Med* 2010;48:1141–5.
17. Clockaerts S, Bastiaansen-Jenniskens YM, Feijt C, De Clerck L, Verhaar JA, Zuurmond AM, et al. Cytokine production by infrapatellar fat pad can be stimulated by interleukin 1 and inhibited by peroxisome proliferator activated receptor agonist. *Ann Rheum Dis* 2012;71:1012–8.
18. Klein-Wieringa IR, Kloppenburg M, Bastiaansen-Jenniskens YM, Yusuf E, Kwekkeboom JC, El-Bannoudi H, et al. The infrapatellar fat pad of patients with osteoarthritis has an inflammatory phenotype. *Ann Rheum Dis* 2011;70:851–7.
19. Presle N, Pottie P, Dumond H, Guillaume C, Lapicque F, Pallu S, et al. Differential distribution of adipokines between serum and synovial fluid in patients with osteoarthritis: contribution of joint tissues to their articular production. *Osteoarthritis Cartilage* 2006; 14:690–5.
20. Ushiyama T, Chano T, Inoue K, Matsusue Y. Cytokine production in the infrapatellar fat pad: another source of cytokines in knee synovial fluids. *Ann Rheum Dis* 2003;62:108–12.
21. Clockaerts S, Bastiaansen-Jenniskens YM, Runhaar J, van Osch GJ, Van Offel JF, Verhaar JA, et al. The infrapatellar fat pad should be considered as an active osteoarthritic joint tissue: a narrative review. *Osteoarthritis Cartilage* 2010;18:876–82.
22. Fain JN, Madan AK, Hiler ML, Cheema P, Bahouth SW. Comparison of the release of adipokines by adipose tissue, adipose tissue matrix, and adipocytes from visceral and subcutaneous abdominal adipose tissues of obese humans. *Endocrinology* 2004; 145:2273–82.
23. Fain JN. Release of interleukins and other inflammatory cytokines by human adipose tissue is enhanced in obesity and primarily due to the nonfat cells. *Vitam Horm* 2006;74:443–77.
24. Fain JN, Tichansky DS, Madan AK. Most of the interleukin 1 receptor antagonist, cathepsin S, macrophage migration inhibitory factor, nerve growth factor, and interleukin 18 release by explants of human adipose tissue is by the non-fat cells, not by the adipocytes. *Metabolism* 2006;55:1113–21.
25. Fain JN, Cheema PS, Bahouth SW, Lloyd Hiler M. Resistin release by human adipose tissue explants in primary culture. *Biochem Biophys Res Commun* 2003;300:674–8.
26. Fain JN, Madan AK. Regulation of monocyte chemoattractant protein 1 (MCP-1) release by explants of human visceral adipose tissue. *Int J Obes (Lond)* 2005;29:1299–307.
27. Fain JN, Tagele BM, Cheema P, Madan AK, Tichansky DS. Release of 12 adipokines by adipose tissue, nonfat cells, and fat cells from obese women. *Obesity (Silver Spring)* 2010;18:890–6.
28. Bastiaansen-Jenniskens YM, de Bart AC, Koevoet W, Jansen KM, Verhaar JA, van Osch GJ, et al. Elevated levels of cartilage oligomeric matrix protein during in vitro cartilage matrix generation decrease collagen fibril diameter. *Cartilage* 2010;1:200–10.
29. Balvers MG, Verhoeckx KC, Meijerink J, Bijlsma S, Rubingh CM, Wortelboer HM, et al. Time-dependent effect of in vivo inflammation on eicosanoid and endocannabinoid levels in plasma, liver, ileum and adipose tissue in C57BL/6 mice fed a fish-oil diet. *Int Immunopharmacol* 2012;13:204–14.
30. Pelletier JP, Martel-Pelletier J, Abramson SB. Osteoarthritis, an inflammatory disease: potential implication for the selection of new therapeutic targets [review]. *Arthritis Rheum* 2001;44:1237–47.
31. Kershaw EE, Flier JS. Adipose tissue as an endocrine organ. *J Clin Endocrinol Metab* 2004;89:2548–56.
32. Frayn KN, Karpe F, Fielding BA, Macdonald IA, Coppack SW. Integrative physiology of human adipose tissue [review]. *Int J Obes Relat Metab Disord* 2003;27:875–88. INFRAPATELLAR FAT PAD AND SYNOVIAL FIBROSIS 2079
33. Galic S, Oakhill JS, Steinberg GR. Adipose tissue as an endocrine organ. *Mol Cell Endocrinology* 2010;316:129–39.

34. Distel E, Cadoudal T, Durant S, Pognard A, Chevalier X, Benelli C. The infrapatellar fat pad in knee osteoarthritis: an important source of interleukin-6 and its soluble receptor. *Arthritis Rheum* 2009;60:3374–7.
35. Shi Q, Liu X, Bai Y, Cui C, Li J, Li Y, et al. In vitro effects of pirfenidone on cardiac fibroblasts: proliferation, myofibroblast differentiation, migration and cytokine secretion. *PLoS One* 2011;6:e28134.
36. Harks EG, Peters PH, van Dongen JL, van Zoelen EJ, Theuvsen AP. Autocrine production of prostaglandin F₂ α enhances phenotypic transformation of normal rat kidney fibroblasts. *Am J Physiol Cell Physiol* 2005;289:C130–7.
37. Olson DM, Tanswell AK. Production of prostaglandins by fetal rat lung type II pneumonocytes and fibroblasts. *Biochim Biophys Acta* 1989;1003:327–30.
38. Van der Slot-Verhoeven AJ, van Dura EA, Attema J, Blauw B, Degroot J, Huizinga TW, et al. The type of collagen cross-link determines the reversibility of experimental skin fibrosis. *Biochim Biophys Acta* 2005;1740:60–7.
39. Bastiaansen-Jenniskens YM, Clockaerts S, Feijt C, Zuurmond AM, Stojanovic-Susulic V, Bridts C, et al. Infrapatellar fat pad of patients with end-stage osteoarthritis inhibits catabolic mediators in cartilage. *Ann Rheum Dis* 2012;71:288–94.
40. Verreck FA, de Boer T, Langenberg DM, van der Zanden L, Ottenhoff TH. Phenotypic and functional profiling of human proinflammatory type-1 and anti-inflammatory type-2 macrophages in response to microbial antigens and IFN- γ - and CD40L-mediated costimulation. *J Leuk Biol* 2006;79:285–93.
41. Norwitz ER, Lopez Bernal A, Starkey PM. Tumor necrosis factor- α selectively stimulates prostaglandin F₂ α production by macrophages in human term decidua. *Am J Obstet Gynecol* 1992;167:815–20.
42. O'Sullivan MG, Chilton FH, Huggins EM Jr, McCall CE. Lipopolysaccharide priming of alveolar macrophages for enhanced synthesis of prostanoids involves induction of a novel prostaglandin H synthase. *J Biol Chem* 1992;267:14547–50.
43. Iyer A, Fairlie DP, Prins JB, Hammock BD, Brown L. Inflammatory lipid mediators in adipocyte function and obesity. *Nat Rev Endocrinol* 2010;6:71–82.
44. Samuelsson B. Prostaglandins and thromboxanes. *Recent Prog Horm Res* 1978;34:239–58.
45. De Grauw JC, van de Lest CH, van Weeren PR. Inflammatory mediators and cartilage biomarkers in synovial fluid after a single inflammatory insult: a longitudinal experimental study. *Arthritis Res Ther* 2009;11:R35.
46. Mastbergen SC, Marijnissen AC, Vianen ME, Zoer B, van Roermund PM, Bijlsma JW, et al. Inhibition of COX-2 by celecoxib in the canine groove model of osteoarthritis. *Rheumatology (Oxford)* 2006;45:405–13.
47. De Grauw JC, van de Lest CH, van Weeren PR. A targeted lipidomics approach to the study of eicosanoid release in synovial joints. *Arthritis Res Ther* 2011;13:R123.



Supplementary figure 1 The effect of TGFβ/ALK5 (SB505124) or PGF_{2α} signalling (AL8810) inhibition on FLS cultures on A) collagen production, B) *Col1a1* gene expression, C) *Plod2* gene expression, and D) *Asma* gene expression. All analyses were done in triplicate on one FLS donor. Bars represent the mean + standard deviation.



CHAPTER 4

The infrapatellar fat pad from diseased joints inhibits chondrogenesis of mesenchymal stem cells

Wu Wei

Resti Rudjito

Niamh Fahy

Jan A.N. Verhaar

Stefan Clockaerts

Yvonne M. Bastiaansen-Jenniskens

Gerjo J.V.M. van Osch

Eur Cell Mater. 2015 Dec 02;30:303-14

ABSTRACT

Cartilage repair by bone marrow derived mesenchymal stem cells (MSCs) can be influenced by inflammation in the knee. Next to synovium, the infrapatellar fat pad (IPFP) has been described as a source for inflammatory factors. Here, we investigated whether factors secreted by the IPFP affect chondrogenesis of MSCs and whether this is influenced by different joint pathologies or obesity. Furthermore, we examined the role of IPFP resident macrophages. First, we made conditioned medium from IPFP obtained from osteoarthritic joints, IPFP from traumatically injured joints during anterior cruciate ligament reconstruction and subcutaneous adipose tissue. Additionally, we made conditioned medium of macrophages isolated from osteoarthritic IPFP and of polarised monocytes from peripheral blood. We evaluated the effect of different types of conditioned medium on MSC chondrogenesis. Conditioned medium from IPFP decreased collagen 2 and aggrecan gene expression and thionin and collagen type 2 staining. This anti-chondrogenic effect was the same for conditioned medium from IPFP of osteoarthritic and traumatically injured joints. Furthermore, IPFP from obese (Body Mass Index >30) donors did not inhibit chondrogenesis more than that of lean (Body Mass Index <25) donors. Finally, conditioned medium from macrophages isolated from IPFP decreased the expression of hyaline cartilage genes, as did peripheral blood monocytes stimulated with pro-inflammatory cytokines. The IPFP and the resident pro-inflammatory macrophages could therefore be targets for therapies to improve MSC-based cartilage repair.

INTRODUCTION

Articular cartilage has limited self-healing capabilities and surgical intervention using bone marrow stimulation techniques, such as the microfracture procedure, can be used to activate mesenchymal stem cells (MSCs) from the underlying bone marrow to repair the defect^{1,2}. However, instead of a normal hyaline cartilage matrix, a fibrocartilaginous cartilage matrix fills up the defect^{1,3,4}. An explanation why hyaline cartilage production is inhibited could be that the cartilage defect is located in a post-traumatic inflammatory environment⁵. In this post-traumatic inflammatory environment, circulating inflammatory factors stimulate matrix degradation and inhibit chondrogenic differentiation⁶.

Besides surgical intervention, research is currently focused on MSC-based tissue-engineered cartilage repair strategies⁷. In these strategies, repair tissues are engineered in-vitro using a combination of MSCs, scaffolds and growth factors and subsequently implanted into the cartilage defect. When implanted, the MSCs in these pre-engineered constructs will be exposed to the same post-traumatic inflammatory environment as the MSCs after the microfracture procedure. An inflammatory environment can inhibit hyaline cartilage matrix production⁸.

Another factor that could influence MSC chondrogenic differentiation is obesity. The clinical results after the microfracture procedure are reported to be worse in patients with obesity⁹. Obesity is known to cause systemic metabolic and inflammatory changes, with increased circulating inflammatory factors¹⁰.

Inflammatory factors can be produced by different tissues of the knee joint, the most well described being the synovium and cartilage. The infrapatellar fat pad (IPFP) is an adipose tissue located extra-synovially and intra-capsularly. It is richly vascularised, innervated and known to also secrete many adipokines and cytokines^{11,12}. Adipose tissue in obese patients has been shown to have an inflammatory phenotype with abundant immune cell infiltration and secretion of inflammatory cytokines¹³. Furthermore, joint trauma and joint degradation can both increase inflammation in the IPFP and the secretion of inflammatory factors^{12; 14-16}.

The IPFP contains immune cells such as macrophages^{15,17}. Macrophages play an important role in inflammation and wound healing. Macrophages can be categorized into pro-inflammatory macrophages and anti-inflammatory or wound healing macrophages^{18,19}. Inflammation or obesity often result in increased numbers of in-

flammatory macrophages. Previously we have shown that only pro-inflammatory and not anti-inflammatory macrophages inhibit MSC chondrogenesis *in vitro*²⁰.

Since the IPFP from end-stage OA patients is a source of inflammatory and catabolic cytokines¹², it is to be expected that IPFP secreted factors influence other joint tissues. Against our expectation that the factors released from IPFP would stimulate tissue degradation, our previous studies demonstrated that factors released from IPFP from end-stage OA patients inhibit catabolic mediators in cartilage¹⁵ and stimulate fibrotic processes in synovial fibroblasts²¹. This indicates that the factors released by the IPFP not only have a pro-inflammatory effect on joint environment and that this effect could be different in each type of joint tissue.

Considering the IPFP's potential to produce factors that influence the joint environment, and the knowledge that the joint environment influences cartilage repair, we hypothesized that factors secreted by the IPFP affect MSC-based cartilage repair. In this study, we investigated whether and how factors secreted by the IPFP affect the chondrogenesis of MSCs *in vitro* and whether this could be influenced by joint pathology or obesity. Furthermore, we evaluated whether macrophages present in the IPFP could be responsible for the effect seen on MSC chondrogenesis.

METHODS

Preparation of adipose tissue conditioned medium (CM)

IPFP tissue was obtained as leftover material from patients with OA who had undergone a total knee replacement (Age 66.1 years (53.9-80.2); BMI 29.3 (21.5-43.7)), or from patients during anterior cruciate ligament (LR) reconstruction (Age 29.3 (17.6-48.0); BMI 22.8 (19.3-29.0)), with time from trauma to reconstruction 5.4 months (2-12 months). Subcutaneous adipose tissue (SAT) from patients undergoing total hip replacement was used (Age 63.0 (50.2-79.1); BMI 31.3 (24.0-35.8)). Consent was given in accordance with the guidelines of the Federation of Biomedical Scientific Societies (<http://www.federa.org>) after approval by the local ethical committee (MEC 2012-267). All culture media from now onwards were supplemented with 1.5 µg/mL fungizone and 50 µg/mL gentamicin (both Gibco). To generate adipose tissue CM, adipose tissue was cut into small pieces of approximately 9 mm², washed for two times with saline and cultured at a concentration of 100 mg/ml in Dulbecco's Modified Eagle Medium with Glutamax (DMEM-HG; Gibco) supplemented with 1% insulin-transferrin-selenium (ITS+; BD Biosciences) for 24 hours at 37°C. Afterwards, the medium was harvested, centrifuged at 250G

for 8 minutes and the supernatant was stored at -80°C for culture experiments. Unconditioned medium was generated by incubation of DMEM-HG supplemented with ITS+ for 24 hours at 37°C , centrifuged at 250G for 8 minutes and stored at -80°C .

Isolation of macrophages from adipose tissue and preparation of IPFP macrophage CM

To isolate macrophages from the stromal vascular fraction of adipose tissue, six OA IPFP samples (Age 66.6 (54.1-80.2), BMI 28.9 (21.9-33.9)) were used. Adipose tissue samples were cut into pieces of around 9mm^2 and incubated overnight at 37°C with 1 mg/ml collagenase B (Roche, Germany) in DMEM-HG with 10% FCS. After centrifugation, the supernatant containing the floating adipocytes and fat was removed, cell pellet was re-suspended and filtered through a $100\text{ }\mu\text{m}$ filter followed by a $40\text{ }\mu\text{m}$ filter. The resulting cell suspension was layered on top of 15 ml Ficoll (Ficoll-Paque™ PLUS, GE Healthcare) and separated by density gradient following centrifugation at 1,000g for 15 minutes. The interphase was removed and washed with phosphate buffered saline (PBS; Gibco) containing 2% FCS followed by incubation with CD45-PE (BD Biosciences) for 1 hour and incubation in $20\text{ }\mu\text{l}$ of anti-mouse-IgG magnetic beads (Miltenyi Biotec) per 10,000,000 cells for 30 minutes in the dark at 4°C . CD45 positive cells were separated by magnetic activated cell sorting (MACS, MACS Separation columns LS and MidiMACS™ Separator, Miltenyi Biotec) according to manufacturer's instructions. Flowcytometric analysis was performed to confirm a $>90\%$ CD45+ population purity. CD45 reduced fraction contained $<10\%$ CD45+ cells. Isolated CD45+ cells were seeded at a cell density of 100,000 cells/ cm^2 in 24 wells plates and cultured overnight at 37°C in DMEM-HG supplemented with 10% FCS. Cells were then carefully washed twice with PBS to remove non-attached cells and DMEM-HG with 1% ITS+ was added. After 24 hours, IPFP CD45+ CM was harvested, centrifuged at 250g for 8 minutes and stored at -80°C for further experiments.

Human monocyte isolation, differentiation and CM preparation

Peripheral blood monocytes were isolated from buffy coats with CD14+ magnetic beads (Miltenyi Biotec) and MACS according to manufacturer's instructions. Monocytes were then seeded at 500,000 cells/ cm^2 , stimulated to M(LPS+IFN- γ) with 100 ng/ml lipopolysaccharide (LPS; Sigma Aldrich) and 10 ng/ml IFN- γ (PeproTech) or M(IL-4) with 10 ng/ml IL-4 (PeproTech)¹⁹. Subsequently, M(LPS+IFN- γ) and M(IL-4) CM were made as previously described^{20;22}. Samples of these experiments were previously used in Fahy et al²⁰, but additional gene expression analysis were performed for the current study.

Human dermal fibroblast expansion and CM preparation

Human dermal fibroblast from adult donors (HDFa) were acquired from Gibco (Cat. no. C-013-5C) and were seeded at 5000 cells/cm² in DMEM-HG containing 10% FCS. After reaching sub-confluency, HDFas were trypsinized and seeded again. For HDFa CM preparation, P4 cells were cultured until subconfluency, washed with PBS for three times and DMEM-HG with ITS+ was added. After 24 hours, CM was harvested, centrifuged at 250g for 8 minutes and stored at -80 °C for further experiments.

Isolation and culture of human MSCs

MSCs were isolated from heparinized bone marrow aspirates of patients with OA undergoing total hip replacement (9 donors; Age 61 years (32-78)). Patients gave informed consent and the study was approved by the local ethical committee of the Erasmus MC, Rotterdam (MEC 2004-142) and Albert Schweitzer Hospital, Dordrecht (MEC 2011-07). Bone marrow aspirates were plated and washed after 24 hours with PBS containing 2% fetal calf serum (FCS; Lonza). MSCs were expanded in Minimum Essential Medium-Alpha (α -MEM; Gibco) supplemented with 10% FCS, 1 ng/mL fibroblast growth factor 2 (FGF2; R&D Systems) and 25 μ g/mL ascorbic acid-2-phosphate (Sigma-Aldrich). After reaching sub-confluency, MSCs were trypsinised and seeded again at a density of 2500 cells/cm². MSCs of passage 3 or 4 were used.

Chondrogenic differentiation of MSCs

MSCs were encapsulated in 1.2% alginate (CP Kelco) in saline at a density of 4.000.000 cells/ml. Beads were formed by purging the MSC-alginate solution through a 23G needle and allowing droplets to fall into 102 mM CaCl₂ solution. Pellets were made by centrifugation of 200.000 cells in polypropylene tubes. Beads and pellets were cultured with DMEM-HG with ITS+ containing 25% IPFP CM or unconditioned medium. As chondrogenic supplements, we used 0.1 μ M Dexamethasone (Sigma-Aldrich), 10 ng/ml TGF β 1 (R&D systems), 25 μ g/mL ascorbic acid-2-phosphate (Sigma-Aldrich), 40 μ g/ml L-Proline (Sigma-Aldrich) and 1 mM sodium pyruvate (Gibco). MSC beads were cultured in 100 μ L of medium per bead and pellets were cultured in 500 μ L of medium per pellet. Medium was refreshed 3 times a week. Beads and pellets were harvested after 28 days.

For the experiments with macrophages, obese versus lean IPFP, osteoarthritic versus post-joint trauma IPFP and SAT versus IPFP, beads were first cultured in DMEM-HG containing ITS+ and chondrogenic supplements for 14 days. From day 14-17, parts of the DMEM-HG with ITS+ was replaced by conditioned medium or an equal

percentage of unconditioned medium. For the experiments with IPFP and SAT CM, we replaced 25% of the DMEM-HG containing ITS+. For the macrophages experiments, we replaced 50% of the DMEM-HG containing ITS+ with CD45 CM or 20% with M(LPS+IFN γ)/M(IL-4) CM. For the CD45 experiments, the lowest cell number used to generate CM (0.23 μ g DNA) was set at 50% and for the M(LPS+IFN γ)/M(IL-4) experiments, the average cell number used to generate CM (1.64 μ g DNA) was set at 20%. All subsequent donors were corrected accordingly to assure that medium conditioned by an equal number of cells was added. Chondrogenic supplements were always added after mixing the medium with CM or unconditioned medium. In this way, all conditions had the same final concentration of all supplements. Beads were harvested at day 17. All media were refreshed 24 hours prior to harvest.

Gene expression analysis

MSC alginate beads were harvested in ice-cold 55 mM sodium citrate and dissolved after gentle agitation at 4 °C. The solution was then centrifuged at 400g for 8 minutes at 4 °C and cell pellets were re-suspended in 650 μ l RNA-Bee (TelTest, USA) per bead. Chloroform (Sigma-Aldrich) was added to all samples at 200 μ l/mL RNA-Bee. RNA was further purified using RNeasy Micro Kit (Qiagen). RNA concentration and quality was measured using NanoDrop ND1000 UV-Vis Spectrophotometer (Isogen Life Science). RNA was reverse-transcribed to cDNA using the RevertAid First Strand cDNA Synthesis Kit (Fermentas, Germany) according to manufacturer's instructions. qRT-PCR was performed in 10 μ l reactions on cDNA using the CFX96 Touch™ Real-Time PCR Detection System (BIO-RAD, USA). Expression of glyceraldehyde-3-phosphate dehydrogenase (*GAPDH*), hypoxanthine phosphoribosyltransferase 1 (*HPRT1*), collagen type II α 1 (*COL2A1*), aggrecan (*ACAN*), collagen type I (*COL1A1*) and versican (*VCAN*) were determined with qRT-PCR. The genes *GAPDH* and *HPRT* were used as housekeepers. Gene expression was analyzed according to the $\Delta\Delta$ Ct method, with the condition treated with unconditioned medium used as control and set at 1.0. Expression levels of other conditions are expressed relative to the this control condition. The primer efficiency for *GAPDH* was 1.06, for *HPRT* 0.96, for *COL2A1* 1.02, for *ACAN* 0.95, for *COL1A1* 0.97 and *VCAN* 0.95. The mean Ct value for *GAPDH* was 22.9 and for *HPRT* 28.8. Difference in Ct values between the samples within each experiment was less than 1 Ct and there were no significant differences between the conditions (data not shown). Gene expression values after normalization to housekeepers are used to calculate *COL2A1*/*COL1A* and *ACAN*/*VCAN* ratios.

Primer sequences were as followed: *GAPDH*, forward: GTCAACGGATTGTCGTATTGGG, reverse: TGCCATGGGTGGAATCATATTGG and probe Fam: TGGC-

GCCCCAACAGCC. *HPRT* forward: TATGGACAGGACTGAACGTCTTG, reverse: CACACAGAGGGCTACAATGTG and probe Fam: GCCCCAATACGACCAAATCCGTTGAC. *COL2A1* forward: GGCAATAGCAGGTTTCACGTACA, reverse: CGATAACAGTCTTGCCCCACTT and probe Fam: CCGGTATGTTTCGTGCAGCCATCCT. *ACAN* forward: TCGAGGACAGCGAGGCC, reverse: TCGAGGGTGTAGCGTGTAGAGA and probe Fam: ATGGAACACGATGCCTTTCACCACGA. *COL1A1* forward: CAGCCGCTTCACCTACAGC, reverse: TTTTGTATTCAATCACTGTCTTGCC and probe Fam: CCGGTGTGACTCGTGCAGCCATC. *VCAN* forward: TGGAATGATGTTCCCTGCAA, reverse: AAGGTCTTGGCATTCTTCTACAACAG, probe: CTGGCCGCAAGCAACTGTTCCCTT.

Quantification of DNA and GAG content

Alginate beads were dissolved in sodium citrate and digested with papain. (Sigma Aldrich). Pellets were digested with proteinase K (Sigma Aldrich). DNA was subsequently quantified by spectrophotometric detection of ethidium bromide (Gibco) binding at 340 and 590 nm. GAG content was determined with dimethylmethylene blue (Polysciences) spectrophotometrically at 530nm and 590 nm²³ and at a pH of 1.75.

Histological evaluation of MSC chondrogenesis in pellet culture

6 µm thick paraffin sections were made of the pellets and thionin staining was performed. For immunohistochemical staining, sections were incubated with monoclonal antibody against collagen type 2 (DSHB, #II-II 6B3) and collagen type 1 (Abcam, #6308) or IgG1 isotype control (Dako Cytomation, #X0931). Sections were then incubated with Link and Label (Biogenex, HK-321-UK) and freshly prepared new-fuchsin was used as substrate.

Evaluation of macrophage subtypes in adipose tissue

10 µm cryosections were made of 13 samples of OA IPFP (Age 65.3 (54.3-74.1), BMI 28 (21.5-35.8)), 7 samples of LR IPFP (Age 29.9 (21.3-48), BMI 25.6 (19.3-38.5)) and 9 samples of SAT (Age 63.1 (±50.2-79.1), BMI 32.3 (25.9-47.2)). After fixation in acetone, sections were incubated with monoclonal antibodies against CD68 (DAKO, #EMB11), CD11c (Chemicon, #EP1347Y) and CD206 (Abcam, #64693). Mouse IgG (Dako) were used as isotype controls. Subsequently, sections were incubated with link and label (BioGenex) and freshly prepared new-fuchsin was used as substrate. A cell was considered positive when stained red. Samples were ranked based on their relative number of positive cells in three sections per sample by two blinded observers as previously described¹⁵. Ranking was performed for each marker separately and for each sample, the average rank of the two observers (WW and RR) was used in the analysis.

Statistical analysis

IBM SPSS statistics 21 (IBM Corporation) was used for statistical analysis. The Shapiro-Wilk test was used to test data for normality and the Levene's test for homogeneity of variance. No data were normally distributed. For gene analysis and GAG measurement, if not otherwise stated, the Kruskal-Wallis test was used followed by a post-hoc Bonferroni correction. For immunohistochemical ranking, the Mann-Whitney U test was used. $p < 0.05$ was considered statistically significant.

RESULTS

IPFP negatively impacts chondrogenic differentiation of MSCs

COL2A1 and *ACAN* were only detectable after TGF β 1 was added (Figure 1). IPFP from OA donors statistically significantly lowered the gene expression of MSCs for *COL2A1* ($p < 0.001$), *ACAN* ($p < 0.001$) and *VCAN*, without affecting *COL1A1* (Figure 1A). This resulted in a lower *COL2A1*/*COL1A1* ($p < 0.001$) and *ACAN*/*VCAN* ratio ($p < 0.05$) (Figure 1A). This effect was absent when CM was heated to 95°C for 10 minutes before use, indicating that the effects are caused by proteins produced by IPFP (Figure 1B). GAG content of the alginate beads were increased by IPFP (Figure 2A). To further investigate the effects of IPFP on matrix production, pellet culture was used. IPFP decreased thionin and immunohistochemical staining of collagen type 2, whereas collagen type 1 staining was not influenced (Figure 2C). Furthermore, IPFP decreased GAG content of pellets (Figure 2D-E).

Effect of obese versus lean IPFP and osteoarthritic versus traumatic joint IPFP on MSC chondrogenesis

Obesity increases the release of inflammatory factors by adipose tissue. Therefore, we hypothesized that CM from obese IPFP donors (BMI 33.1 (30-35.8)) would reduce MSC chondrogenesis more than CM from lean IPFP (BMI 23.1 (21.5-24)) donors. However, chondrogenic markers were not more inhibited by CM from obese than by CM from lean donors (Figure 3A). Next, we compared the effect of CM from LR IPFP (BMI 22.9 (22.0-25.0)) with BMI matched OA IPFP (BMI 23.1 (21.5-24.0)). Chondrogenic gene expression was not statistically significantly different between MSCs exposed to CM from LR IPFP and CM from OA IPFP. Interestingly LR IPFP CM statistically significantly increased *COL1A1* compared to control and OA IPFP CM ($p = 0.023$) (Figure 3B).

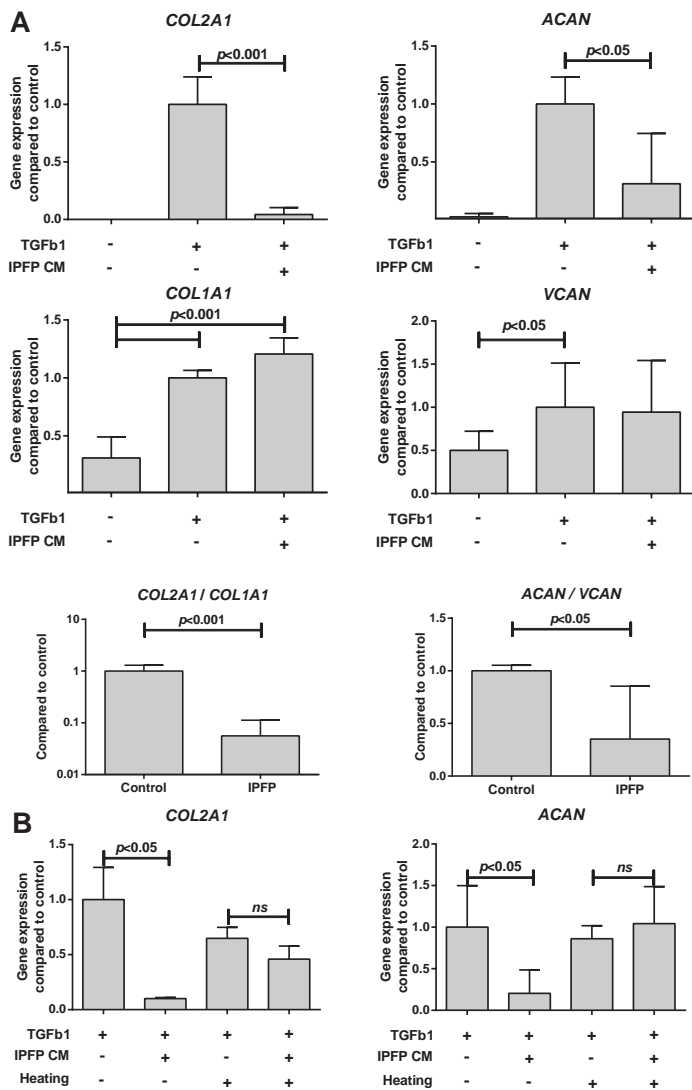


Figure 1 IPFP inhibits chondrogenic differentiation of MSCs.

A) MSC alginate beads were treated with 25% IPFP CM for 28 days of culture in chondrogenic medium with TGFβ1. The control condition was treated with 25% unconditioned medium with chondrogenic medium with TGFβ1. Relative gene expression COL2A1, ACAN, COL1A1 and VCAN normalized to the control condition and COL2A1/COL1A1 and ACAN/VCAN ratio. CM were pooled from 3-5 different IPFP donors and used to treat 3 MSC donors, with each condition performed in triplicate. B) MSC alginate beads were treated with 25% CM from IPFP from day 14-17 of chondrogenic stimulation. CM or unconditioned medium were heated for 10 minutes at 95°C and allowed to cool down to room temperature before addition to MSC alginate beads. Relative gene expression of COL2A1 and ACAN in MSCs after treatment, normalized to the control condition. One pool of CM from 3 IPFP donors was used to treat 1 MSC donor with each condition performed in triplicate. The mean Ct value in the control condition for COL2A1 was 23.2, for ACAN 27.3, for COL1A1 19.7 and for VCAN 24.3. Values represent the mean ± SD.

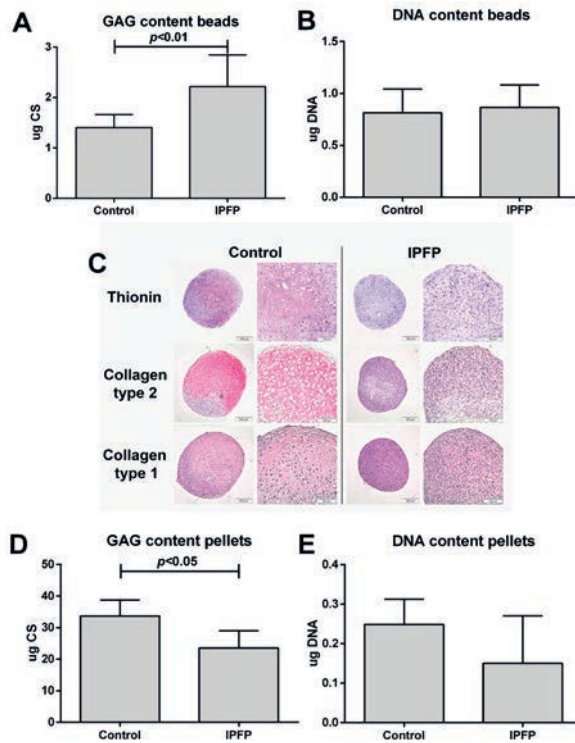


Figure 2 IPFP inhibits chondrogenic differentiation of MSCs.

All conditions were chondrogenically stimulated with TGF β 1 during the entire culture period. MSC alginate beads and pellets were treated with 25% IPFP CM whereas the control condition was treated with 25% unconditioned medium for 28 days. A) Total GAG content and B) total DNA content of alginate beads. C) Representative images of pellets from 1 MSC donor stained for glycosaminoglycans with thionin or collagen type 2 and collagen type 1 using immunohistochemistry. D) Total GAG content and E) total DNA content of pellets. Different pools of CM from 3 different IPFP donors were used for each experiment. For total GAG and DNA content in beads (Panel A), 3 MSC donors were used with each condition performed in triplicate. For the pellet culture experiment (Panel C-E), 2 MSC donor were used with 5 pellets per condition. Values represent mean \pm SD. The Mann-Whitney U test was used to determine statistical significance.

Chondrogenic differentiation of MSCs is more affected by IPFP than by SAT

To investigate whether the effect of adipose tissue of the joint (IPFP) is different from subcutaneous adipose tissue (SAT), we added CM made from SAT to MSCs during chondrogenic differentiation. SAT statistically significantly lowered gene expression of *COL2A1* and *ACAN* ($p < 0.01$), but did not influence the *COL2A1/COL1A1* and *ACAN/VCAN* ratio (Figure 4A). To investigate whether this is due to a difference in the concentration of factors released by IPFP and SAT, we increased the percentage of SAT CM added to culture up to 50%. In contrast to the effect of IPFP, the effect of SAT on chondrogenesis was not dosage dependent (Figure 4B).

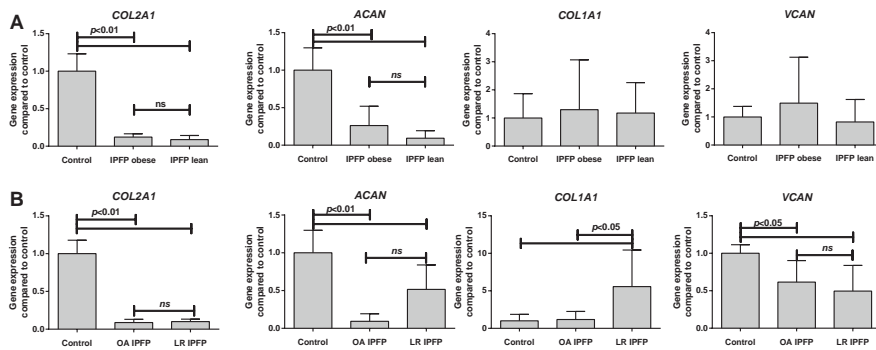


Figure 3 Effect of obese versus lean IPFP and osteoarthritic versus traumatic joint IPFP on MSC chondrogenesis.

All conditions were chondrogenically stimulated with TGF β 1 during the entire culture period. MSC alginate beads were treated with 25% IPFP CM from day 14-17. The control condition was treated with 25% unconditioned medium. Relative gene expression of COL2A1, ACAN, COL1A1 and VCAN in MSCs after treatment with CM from A) obese (BMI >30) or lean (BMI <25) OA IPFP donors and B) OA or BMI matched LR IPFP donors. Gene expression was normalized to the control condition per MSC donor. CM from 6 obese OA IPFP, 6 lean OA IPFP and 6 LR IPFP donors were used. Three different pools of CM was made with each pool a selection of three different IPFP donors. Three MSC donors were used, with each condition performed in triplicate. Values represent the mean \pm SD.

Difference between IPFP and SAT in number and phenotype of macrophages

We hypothesized that the difference in effects of IPFP and SAT on expression of chondrogenic and fibrous tissue genes could be due to the type of macrophages in the adipose tissue. We therefore first characterized the macrophages in the different adipose tissues. IPFP samples from OA donors ranked higher on CD68 ($p=0.007$ and $p=0.03$) and CD206 ($p=0.02$ and $p=0.049$) positive staining than LR IPFP and SAT samples (Figure 5B and D). We could not detect differences between obese and lean donors.

Macrophages in IPFP contribute to the effects seen on MSC chondrogenesis

To investigate whether macrophages present in the IPFP were responsible for the effect seen on MSC chondrogenesis, we added CM from macrophages isolated from IPFP to MSCs during chondrogenesis. IPFP macrophages statistically significantly lowered the COL2A1 and ACAN gene expression (Figure 6A). Since we applied a very strict selection for CD45+ cells, the remainder fraction still contained a small number of CD45+ cells. This CD45 reduced fraction appeared to be able to inhibit COL2A1 and ACAN gene expression as well (Figure 6B). To investigate whether this effect was specific for cells isolated from the IPFP, we added CM from human dermal fibroblasts (HDFa) to MSCs during chondrogenesis. CM from HDFAs did not influence MSC chondrogenesis (Figure 6B).

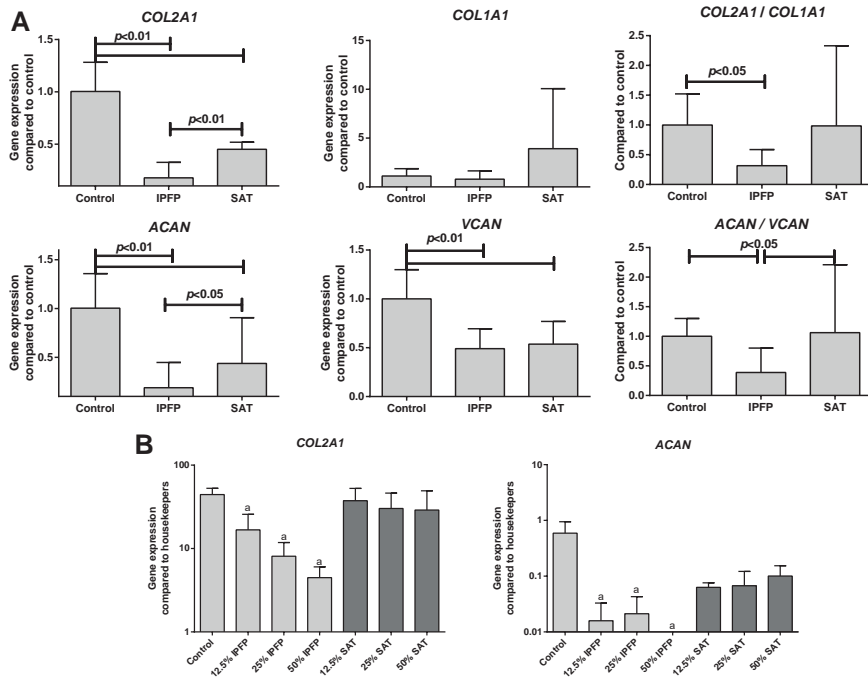


Figure 4 MSC chondrogenesis is more influenced by IPFP than subcutaneous adipose tissue (SAT). MSC alginate beads were treated with CM from IPFP or SAT from day 14-17 of culture. The control condition was treated with 25% unconditioned medium. All conditions were chondrogenically stimulated with TGF β 1 during the entire culture period. A) 25% of CM was used and CM were pooled from 3 pools of different 3 IPFP or 3 pools of different 3 SAT donors and used to treat 3 MSC donors. Each experiment was performed in triplicate. Relative gene expression of COL2A1, ACAN, COL1A1, VCAN, COL2A1/COL1A1 ratio and ACAN/VCAN ratio in MSCs after treatment. Gene expression was normalized to the control condition per MSC donor. B) Different percentages of CM were used and CM were pooled from 3 IPFP or 3 SAT donors and used to treat 1 MSC donor, with each condition performed in triplicate. Relative gene expression of COL2A1 and ACAN compared to housekeepers in MSCs after treatment. All conditions received the same final concentration of all chondrogenic supplements. Values represent the mean \pm SD. $p < 0.05$ versus Control using the Mann-Whitney-U test.

Finally we investigated whether the negative effects of IPFP derived macrophages on MSC chondrogenesis could be explained by the phenotype of the macrophage. Due to the low number of macrophages we could obtain from IPFP, we used PBMCs that were stimulate to pro- or anti-inflammatory phenotype. MSCs exposed to CM of M(LPS+IFN γ) macrophages had lower hyaline cartilage genes expression compared to control and CM of M(IL-4) macrophages (Figure 6C)

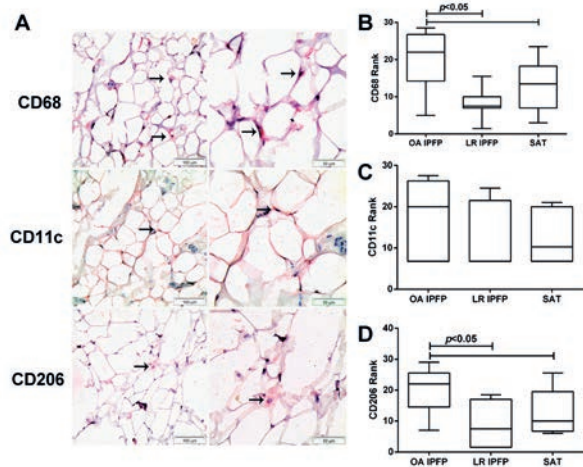


Figure 5 Macrophages with different phenotypes are present in adipose tissue samples. 13 samples of OA IPFP, 7 samples of LR IPFP and 9 samples of SAT were used. A) Representative images of immunohistochemical staining of CD68, CD11c and CD206 positive cells in OA IPFP samples. Positive cells are stained red and indicated with arrows. Ranking of positive staining in adipose tissue samples for B) CD68, C) CD11c and D) CD206.

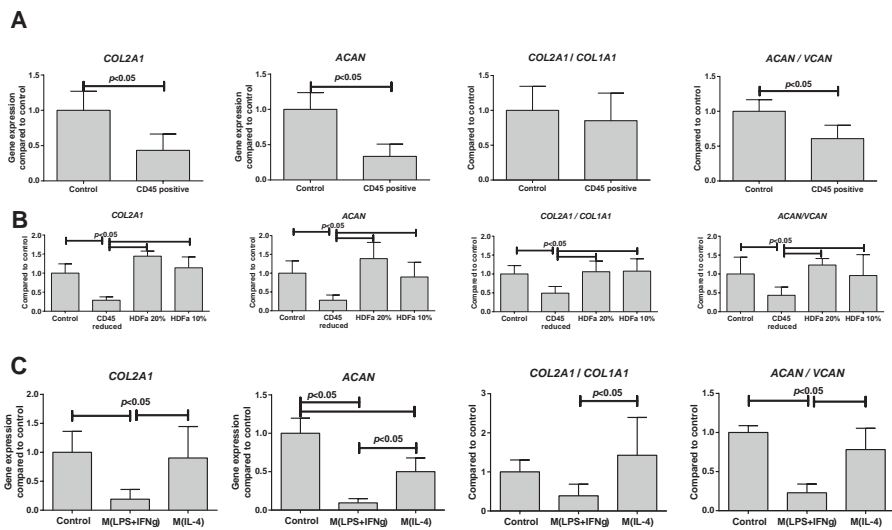


Figure 6 Macrophages in IPFP contribute to the effects seen on MSC chondrogenesis. MSC alginate beads were treated with CM from day 14-17. The control condition was treated with 25% unconditioned medium. All conditions were chondrogenically stimulated with TGFβ1 during the entire culture period. A) Effect of 50% CM from CD45+ cells from IPFP on MSC chondrogenesis; B) Effect 50% CM from CD45 reduced fraction from IPFP or CM from adult human dermal fibroblasts (HDFa) on MSC chondrogenesis; C) Effect of 20% CM from M(LPS+IFNγ) or M(IL-4) macrophages on MSC chondrogenesis. Relative gene expression of COL2A1, ACAN, COL2A1/COL1A1 ratio and ACAN/VCAN ratio in MSCs after treatment. Gene expression was normalised to the control condition per MSC donor. CM were from 6 IPFP donors, 1 HDFa donor or 3 blood donors and used to treat 1 MSC donor. Conditions with CM derived from IPFP were performed in single well and all other conditions were performed in triplicate. Values represent the mean ± SD.

DISCUSSION

IPFP secretes cytokines, growth factors and adipokines which could influence the joint environment¹¹. In this study we have shown that the IPFP released factors that inhibit chondrogenic differentiation of MSCs and the production of hyaline cartilage matrix. This anti-chondrogenic effect was the same for patients with end stage OA and patients with joint trauma. Furthermore, the IPFP of obese patients did not inhibit chondrogenesis more than IPFP of lean patients. Finally, we have indications that macrophages residing in the IPFP might play an important role in this anti-chondrogenic effect.

Repair tissue formed after marrow stimulation techniques, such as the microfracture procedure, is mainly fibrocartilage which is of less biomechanical quality than native hyaline cartilage²⁴. In the present study, the decrease in *COL2A1*/*COL1A1* and *ACAN*/*VCAN* ratios suggests that IPFP not only inhibits chondrogenesis, but also shifts the production from hyaline to fibro-cartilage. Fibrocartilage also contains proteoglycans, but instead of aggrecan this is versican. This could be an explanation why we found no reduction in glycosaminoglycan production in alginate beads after IPFP CM treatment, despite a decrease in aggrecan core-protein gene expression. However, this could also be caused by interference of the DMMB assay by alginate especially when low amount of GAG is involved^{23;25}. Analyses on matrix with DMMB and immunohistochemistry can be used more reliably on pellets²⁶. The reduced thionin staining and immunohistochemical staining for collagen type 2 in pellets treated with IPFP CM supports the gene expression results in alginate beads. Our findings indicate that fibrocartilage production by MSCs, taking place after microfracture procedure, could be partly due to factors secreted by the IPFP.

The secretion of factors by IPFP could be influenced by the disease state of the joint. The microfracture procedure and MSC based treatments are recommended for the treatment of post-traumatic, rather than end-stage OA cartilage defects²⁷. Higher levels of inflammatory cytokines were found in post-traumatic than end-stage OA knees^{28;29}. Gandhi et al¹⁶ reported that post-traumatic IPFP expresses more pro-inflammatory genes compared to end-stage OA IPFP. We found differences in macrophage number and in particular CD206 positive cells between IPFP from OA and LR knees, albeit factors secreted by both OA and LR IPFP inhibited chondrogenesis. However, we cannot exclude that these effects are due to different cytokines or adipokines.

Another factor that could influence both IPFP and the results of microfracture is obesity⁹. In obese patients, macrophages in adipose tissue are changed towards a chronic inflammatory phenotype with increased production of pro-inflammatory cytokines¹⁰. An inflamed obese IPFP would possibly be an explanation for the worse results of microfracture in obese patients. In contrast to this hypothesis, we did not detect an increased anti-chondrogenic effect of IPFP from obese compared to lean donors. To investigate whether the OA process could be of more influence to the factors secreted by IPFP than being obese, experiments with IPFP donors with a low or high BMI but without OA would be required. It is however difficult to obtain sufficient IPFP from non-OA donors.

Independent from joint pathology or obesity, differences have been reported between IPFP and other adipose tissue. IPFP expresses more inflammatory genes, release more inflammatory factors and contains more immune cells than SAT¹⁷. In our study, the anti-chondrogenic effect of IPFP was stronger than that of SAT and even after increasing the dosage of SAT CM, the anti-chondrogenic effect was not increased to the level of IPFP. This suggests that the IPFP releases anti-chondrogenic factors not produced by subcutaneous adipose tissues.

IPFP secretes pro-inflammatory factors and adipokines, such as TNF- α , IL1 β , IL6 and adipokines, such as leptin, resistin and adiponectin¹². These factors could be produced by the fibroblasts, adipocytes and immune cells residing in the IPFP. A large proportion of the immune cells in the IPFP are macrophages^{15;17}. Immunohistochemical analysis on IPFP and SAT indicated that IPFP contained more macrophages than SAT. Previously we have shown that only pro-inflammatory macrophages inhibit chondrogenesis²⁰ and in the current study, only the pro-inflammatory macrophages shifts MSCs to produce fibrocartilage matrix. As a proof of principle, we showed that isolated macrophages from the IPFP were anti-chondrogenic. Although we could not exclude that other cells in the IPFP could also secrete anti-chondrogenic factors, our study does suggest that macrophages in the IPFP play a vital role in inhibiting production of hyaline cartilage and the shift towards fibrocartilage matrix production.

Next to directly negatively affecting chondrogenesis of MSCs, IPFP can influence other joint structures and thereby indirectly influence chondrogenesis. IPFP factors have been shown to stimulate fibrotic processes²¹ and production of pro-inflammatory factors in synovial fibroblasts³⁰. In this way, synovium can then inhibit chondrogenesis²⁰. In contrast to the effect on synovium, the IPFP inhibits catabolic mediators in cartilage explants stimulated with or without IL1 β ¹⁵. This shows that different tissues in the joint can react differently to factors secreted

by the IPFP and the interplay between all joint tissues will determine the eventual effect on cartilage repair. The use of co-cultures of several joint tissues would be required to elucidate this in future studies and to show the potential effect of modulation.

In summary, we have shown that the IPFP is a source of factors that inhibit chondrogenic differentiation of MSCs and shifted the production from hyaline to fibrocartilage matrix. This anti-chondrogenic effect of adipose tissue was specific for IPFP and not subcutaneous adipose tissue. Furthermore, this anti-chondrogenic effect was not more in obese donors than lean donors and was not different between donors with post-joint trauma or end-stage OA. Finally, the IPFP and specifically the macrophages in the tissue could therefore be targets for future therapies to improve the joint environment for MSC chondrogenesis and thereby improve the outcome of microfracture procedure and future MSC-based treatments for the repair of cartilage defects.

REFERENCES

1. Shapiro F, Koide S, Glimcher MJ. 1993. Cell origin and differentiation in the repair of full-thickness defects of articular cartilage. *J Bone Joint Surg Am* 75:532-553.
2. Steadman JR, Miller BS, Karas SG, et al. 2003. The microfracture technique in the treatment of full-thickness chondral lesions of the knee in National Football League players. *J Knee Surg* 16:83-86.
3. Frisbie DD, Oxford JT, Southwood L, et al. 2003. Early events in cartilage repair after subchondral bone microfracture. *Clin Orthop Relat Res*:215-227.
4. Kaul G, Cucchiari M, Remberger K, et al. 2012. Failed cartilage repair for early osteoarthritis defects: a biochemical, histological and immunohistochemical analysis of the repair tissue after treatment with marrow-stimulation techniques. *Knee Surg Sports Traumatol Arthrosc* 20:2315-2324.
5. Irie K, Uchiyama E, Iwaso H. 2003. Intraarticular inflammatory cytokines in acute anterior cruciate ligament injured knee. *Knee* 10:93-96.
6. Heldens GT, Blaney Davidson EN, Vitters EL, et al. 2012. Catabolic factors and osteoarthritis-conditioned medium inhibit chondrogenesis of human mesenchymal stem cells. *Tissue Eng Part A* 18:45-54.
7. Hunziker EB, Lippuner K, Keel MJ, et al. 2015. An educational review of cartilage repair: precepts & practice—myths & misconceptions—progress & prospects. *Osteoarthritis Cartilage* 23:334-350.
8. Wehling N, Palmer GD, Pilapil C, et al. 2009. Interleukin-1beta and tumor necrosis factor alpha inhibit chondrogenesis by human mesenchymal stem cells through NF-kappaB-dependent pathways. *Arthritis Rheum* 60:801-812.
9. Mithoefer K, Williams RJ, 3rd, Warren RF, et al. 2005. The microfracture technique for the treatment of articular cartilage lesions in the knee. A prospective cohort study. *J Bone Joint Surg Am* 87:1911-1920.
10. Lumeng CN, Saltiel AR. 2011. Inflammatory links between obesity and metabolic disease. *J Clin Invest* 121:2111-2117.
11. Clockaerts S, Bastiaansen-Jenniskens YM, Runhaar J, et al. 2010. The infrapatellar fat pad should be considered as an active osteoarthritic joint tissue: a narrative review. *Osteoarthritis Cartilage* 18:876-882.
12. Clockaerts S, Bastiaansen-Jenniskens YM, Feijt C, et al. 2012. Cytokine production by infrapatellar fat pad can be stimulated by interleukin 1beta and inhibited by peroxisome proliferator activated receptor alpha agonist. *Ann Rheum Dis* 71:1012-1018.
13. Grant RW, Dixit VD. 2015. Adipose tissue as an immunological organ. *Obesity* (Silver Spring).
14. Gierman LM, Wopereis S, van El B, et al. 2013. Metabolic profiling reveals differences in concentrations of oxylipins and fatty acids secreted by the infrapatellar fat pad of donors with end-stage osteoarthritis and normal donors. *Arthritis Rheum* 65:2606-2614.
15. Bastiaansen-Jenniskens YM, Clockaerts S, Feijt C, et al. 2012. Infrapatellar fat pad of patients with end-stage osteoarthritis inhibits catabolic mediators in cartilage. *Ann Rheum Dis* 71:288-294.
16. Gandhi R, Takahashi M, Virtanen C, et al. 2011. Microarray analysis of the infrapatellar fat pad in knee osteoarthritis: relationship with joint inflammation. *J Rheumatol* 38:1966-1972.
17. Klein-Wieringa IR, Kloppenburg M, Bastiaansen-Jenniskens YM, et al. 2011. The infrapatellar fat pad of patients with osteoarthritis has an inflammatory phenotype. *Ann Rheum Dis* 70:851-857.
18. Mosser DM, Edwards JP. 2008. Exploring the full spectrum of macrophage activation. *Nat Rev Immunol* 8:958-969.
19. Murray PJ, Allen JE, Biswas SK, et al. 2014. Macrophage activation and polarization: nomenclature and experimental guidelines. *Immunity* 41:14-20.

20. Fahy N, de Vries-van Melle ML, Lehmann J, et al. 2014. Human osteoarthritic synovium impacts chondrogenic differentiation of mesenchymal stem cells via macrophage polarisation state. *Osteoarthritis Cartilage* 22:1167-1175.
21. Bastiaansen-Jenniskens YM, Wei W, Feijt C, et al. 2013. Stimulation of fibrotic processes by the infrapatellar fat pad in cultured synoviocytes from patients with osteoarthritis: a possible role for prostaglandin f2alpha. *Arthritis Rheum* 65:2070-2080.
22. Grotenhuis N, Vd Toom HF, Kops N, et al. 2014. In vitro model to study the biomaterial-dependent reaction of macrophages in an inflammatory environment. *Br J Surg* 101:983-992.
23. Enobakhare BO, Bader DL, Lee DA. 1996. Quantification of sulfated glycosaminoglycans in chondrocyte/alginate cultures, by use of 1,9-dimethylmethylene blue. *Anal Biochem* 243:189-191.
24. Furukawa T, Eyre DR, Koide S, et al. 1980. Biochemical studies on repair cartilage resurfacing experimental defects in the rabbit knee. *J Bone Joint Surg Am* 62:79-89.
25. Zheng CH, Levenston ME. 2015. Fact versus artifact: avoiding erroneous estimates of sulfated glycosaminoglycan content using the dimethylmethylene blue colorimetric assay for tissue-engineered constructs. *Eur Cell Mater* 29:224-236; discussion 236.
26. Yang IH, Kim SH, Kim YH, et al. 2004. Comparison of phenotypic characterization between "alginate bead" and "pellet" culture systems as chondrogenic differentiation models for human mesenchymal stem cells. *Yonsei Med J* 45:891-900.
27. Gomoll AH, Farr J, Gillogly SD, et al. 2011. Surgical management of articular cartilage defects of the knee. *Instr Course Lect* 60:461-483.
28. Beekhuizen M, Gierman LM, van Spil WE, et al. 2013. An explorative study comparing levels of soluble mediators in control and osteoarthritic synovial fluid. *Osteoarthritis Cartilage* 21:918-922.
29. Tsuchida AI, Beekhuizen M, Rutgers M, et al. 2012. Interleukin-6 is elevated in synovial fluid of patients with focal cartilage defects and stimulates cartilage matrix production in an in vitro regeneration model. *Arthritis Res Ther* 14:R262.
30. Eymard F, Pigenet A, Citadelle D, et al. 2014. Induction of an inflammatory and prodegradative phenotype in autologous fibroblast-like synoviocytes by the infrapatellar fat pad from patients with knee osteoarthritis. *Arthritis Rheumatol* 66:2165-2174.



CHAPTER 5

Anti-chondrogenic and pro-catabolic effect of infrapatellar fat pad and its residing macrophages can be modulated by triamcinolone acetone

Wu Wei

Serdar Capar

Nicole Kops

Jan A.N. Verhaar

Stefan Clockaerts

Gerjo J.V.M. van Osch

Yvonne M. Bastiaansen-Jenniskens

Submitted

ABSTRACT

Background

Prolonged inflammation inhibits successful cartilage repair. An inflamed infrapatellar fat pad (IPFP), and in particular the residing pro-inflammatory macrophages, secrete factors that inhibit chondrogenic differentiation and stimulate tissue degradation. We aimed to reduce inflammation in the IPFP thereby creating an environment more suitable for cartilage repair

Hypothesis

The anti-chondrogenic and catabolic effect of IPFP can be reduced by influencing macrophage phenotype with anti-inflammatory medication

Study design

Controlled laboratory study

Methods

IPFP explants obtained from 12 donors during total knee arthroplasty were cultured with celecoxib, triamcinolone acetonide (TAA), pravastatin and fenofibrate for 24 hours. The effect of the medications on IPFP gene expression and macrophage surface markers was evaluated. The effects of conditioned medium (CM) from IPFP explants treated with medications on chondrogenesis of human bone marrow mesenchymal stem cells (MSC) and catabolic processes in osteoarthritic synovial fibroblasts were evaluated.

Results

TAA significantly decreased gene expression of tumor necrosis factor- α (*TNFA*), interleukin(IL)-1 β (*IL1B*) and *IL6* and increased expression of *IL10*, cluster of differentiation (CD)206 (*CD206*) and *CD163* in IPFP explants, whereas celecoxib, pravastatin, and fenofibrate had no effect on IPFP inflammation. TAA also significantly increased anti-inflammatory CD14+/CD163+ and CD14+/CD206+ cells in the IPFP. The decrease of collagen type 2 (*COL2A1*) expression in chondrogenic MSCs as a result of CM from IPFP explants could be reduced by treating IPFP with TAA during the production of the CM. The increased matrix metalloproteinase (*MMP*)1 and *MMP13* expression in MSCs and osteoarthritic synovial fibroblasts as result of CM from IPFP explants could be significantly reduced by treating IPFP with TAA.

Conclusions

TAA decreases IPFP inflammation by increasing the anti-inflammatory macrophages in IPFP. TAA can be used to decrease the anti-chondrogenic effect of IPFP on MSC chondrogenesis. Furthermore, TAA decreases the catabolic effect of IPFP on MSCs and synovial fibroblasts.

Clinical relevance

TAA might be used to modulate the IPFP and therefore improve the joint environment for cartilage repair procedures.

INTRODUCTION

Joint injuries are common and often result in cartilage defects and inflammation of the joint. Joint inflammation in turn may prevent successful cartilage defect repair and without successful repair, cartilage defects can eventually lead to the development of osteoarthritis (OA)¹. To improve cartilage repair and prevent the development of OA, restoration of the joint homeostasis is necessary.

Currently, non-steroid anti-inflammatory drugs such as celecoxib and glucocorticoids such as triamcinolone acetonide (TAA) are used to reduce inflammation and reduce the symptoms of OA². Furthermore, statins and fibrates are also shown to have anti-inflammatory properties besides their metabolic modulatory properties³⁻⁵. The effect of anti-inflammatory medication on the synovium membrane, cartilage and bone are often studied^{6,7}. However, the infrapatellar fat pad (IPFP) also seems to play an important role in joint homeostasis⁸.

The IPFP is an adipose tissue located extra-synovially, but intracapsularly within the knee joint. The IPFP secretes factors that inhibit chondrogenic differentiation of mesenchymal stem cells (MSCs)⁹ and stimulate fibrotic and catabolic processes in synovial fibroblasts^{10,11}. Furthermore, cytokine secretion by the IPFP increases in response to inflammation⁴ and IPFP aggravates further degeneration of traumatized cartilage¹². The IPFP contains many pro- and anti-inflammatory macrophages^{9,13}. Pro-inflammatory or M1 macrophages are indicated to contribute to the anti-chondrogenic effect of the IPFP⁹. M2 macrophages on the other hand can have an anti-inflammatory or tissue repair phenotype and they did not inhibit^{9,14} and could even enhance MSC chondrogenesis¹⁵.

To improve the joint environment for cartilage repair procedures, we hypothesized that medication can be used to modulate the IPFP and its resident macrophages. In this way, secretion of anti-chondrogenic factors by the IPFP might reduce. Furthermore, catabolic and anti-chondrogenic processes in synovium might also be reduced since the IPFP influences the synovium^{5,10,11}.

In the current study, we investigated the effect of celecoxib, TAA, pravastatin and fenofibrate on IPFP inflammation. We choose these four medications due to their wide-spread clinical use. Due to the presence of many macrophages in the IPFP and the importance of macrophages in inflammation, we investigated whether macrophage phenotype within the IPFP was modulated by the medications. Finally, we investigated whether the anti-chondrogenic effect of IPFP on MSCs and

the pro-fibrotic and pro-catabolic effect on synovial fibroblasts could be reduced by treating the IPFP with these medications.

MATERIALS AND METHODS

Treatment of infrapatellar fat pad and preparation of conditioned medium (CM)

IPFP tissue was obtained as leftover material from 12 patients with OA who had undergone a total knee arthroplasty. Consent was given in accordance with the guidelines of the Federation of Biomedical Scientific Societies (<http://www.federa.org>), with approval by the local ethical committee (Erasmus MC University Medical Center, The Netherlands, MEC 2012-267). The inner part of the IPFP was cut into small pieces of approximately 9 mm², washed two times with saline and cultured at a concentration of 100 mg/ml. As a result, each sample contained 0.5 g IPFP tissue divided over 10 explants. Explants were cultured in Dulbecco's Modified Eagle Medium with Glutamax (DMEM-HG; Gibco™, Thermo Fisher Scientific, Waltham, Massachusetts, USA) supplemented with 1% insulin-transferrin-selenium (ITS+; BD Biosciences, Franklin Lakes, New Jersey, USA) at 37°C. All culture media were supplemented with 1.5 µg/mL fungizone and 50 µg/mL gentamicin (both Gibco™). Triamcinolone acetonide (TAA; #T6501), celecoxib (#PZ0008), pravastatin (#P4498) and fenofibrate (#F6020) were acquired from Sigma-Aldrich (St. Louis, Missouri, USA). Dimethyl sulfoxide (DMSO; Sigma-Aldrich) was used to dissolve all four medications. Used end-concentration are indicated in the respective graphs. Medications were further diluted in DMEM-HG and added to IPFP explants direct from the start of culture. The used end concentrations for the medications were based on literature¹⁶ and our previous work^{17,18}. To take into account any possible effect of DMSO, we added extra DMSO to the conditions where the medications were more diluted. As a result, all conditions had 0,1% DMSO in the culture medium. After 24 hours of culture, medium was harvested, centrifuged at 250 g for 8 minutes and supernatant was stored in aliquots of 1 ml at -80 °C for analysis and culture experiments. IPFP explants were further used for fluorescence-activated cell sorting (FACS) analysis or were snap-frozen in liquid nitrogen for gene analysis. Unconditioned medium was generated by incubation of DMEM-HG supplemented with ITS+ for 24 hours at 37°C, centrifuged at 250 g for 8 minutes and stored at -80 °C.

Analysis of macrophage phenotype in IPFP

Cultured IPFP explants were digested for 3 hours at 37°C in Hanks' Balanced Salt solution (Gibco™) with Ca^{2+} and Mg^{2+} , containing 2 mg/ml Collagenase IV (Gibco™) and 0.2 mg/ml Dispase II (Roche, Penzberg, Upper Bavaria, Germany). We used 0.5 g of cultured IPFP per condition. After incubation, the digest was neutralized by adding fetal calf serum (FCS; Lonza, Basel, Switzerland) to a final solution concentration of 5%. Subsequently, the solution was filtered through a 100 µm filter followed by twice a 40 µm filter. Cells were then centrifuged for 8 minutes at 250 g, re-suspended in FACSflow (#342003 BD Biosciences) and counted. Approximately 200.000 cells were stained for each condition. Cells were re-suspended in 40 µL of FACSflow and incubated for 15 minutes at room temperature in the dark with a mixture of the following antibodies against CD14 (APC-H7, #561384), CD206 (FITC, #551135), CD163 (PerCP-Cy™5.5, #563887), CD80 (PECy™7, #561135), and CD86 (PE, #560957, all BD Biosciences). Cells were fixed in 1.8% paraformaldehyde for 20 minutes in the dark. Subsequently, paraformaldehyde was removed, cells were suspended in FACSflow, and analyzed with FACSJazz™ (BD Biosciences) and FlowJo V.10 (FlowJo LLC, Ashland, Oregon)

Isolation and culture of human MSCs

Human MSCs were isolated from bone marrow aspirates from 3 end-stage hip OA patients undergoing total hip arthroplasty. Written informed consent was attained and the study was approved by the local ethical committee (Erasmus MC University Medical Center, The Netherlands, MEC 2004-142) and Albert Schweitzer Hospital, The Netherlands (MEC 2011-07). Aspirates were plated in expansion medium consisting of Minimum Essential Medium-Alpha (α -MEM; Gibco™) supplemented with 10% FCS, 1 ng/ml fibroblast growth factor 2 (FGF2; R&D Systems) and 25 µg/mL ascorbic acid-2-phosphate (Sigma-Aldrich). After 24 hours, plates were washed with PBS containing 2% FCS. MSCs were then expanded in expansion medium, trypsinised after reaching sub-confluency and seeded again at a density of 2500 cells/cm². MSCs of passage 4 were encapsulated in 1.2% alginate (CP Kelco, Atlanta, Georgia, USA) in saline at a density of 4.000.000 cells/ml. Beads were formed by purging the MSC-alginate solution through a 23G needle allowing droplets to fall into 102 mM CaCl_2 solution. Beads were first cultured for 14 days with 100 µL of DMEM-HG with ITS+ per alginate bead supplemented with 0.1 µM Dexamethasone (Sigma-Aldrich), 25 µg/mL ascorbic acid-2-phosphate (Sigma-Aldrich), 40 µg/ml L-Proline (Sigma-Aldrich), and 1 mM sodium pyruvate (Gibco™). 10 ng/ml of TGFβ1 (R&D systems; Minneapolis, Minnesota, USA) was used to induce chondrogenesis. Medium was refreshed 3 times a week. After 14 days, beads were cultured with 25% IPFP CM or unconditioned medium. Supplements and TGFβ1

were always added after mixing the medium with CM or unconditioned medium. This way, all the conditions had the same final amount of supplements and TGF β 1. Beads were harvested after 3 additional days of culture and medium was refreshed 24 hours prior to harvest.

Isolation and culture of human fibroblast like synoviocytes

Human synovium was obtained as leftover material from 3 end-stage knee OA patients who had undergone a total knee arthroplasty (Erasmus MC University Medical Center, The Netherlands, MEC 2008-181). The synovium was separated from the underlying fat, cut into small pieces and digested overnight with 1 mg/ml collagenase B (Roche, Germany) in Iscove's modified Dulbecco's medium (IMDM; Gibco™) containing 10% FCS. The cell suspension was then filtered through a 100 μ m filter, followed by centrifugation at 250 g for 8 minutes. The resulting cell pellet was re-suspended and cells were plated at 3500 cells/cm² in IMDM with 10% FCS. After reaching sub-confluency, cells were trypsinised and re-seeded. Fibroblast like synoviocytes (FLS) of passage 3 were plated as monolayer at 50.000 cells/cm² in IMDM with 10% FCS and allowed to attach. After 72 hours, cells were washed 3 times with saline and DMEM-HG containing ITS+ with 25% IPFP CM or unconditioned medium were added. 25 μ g/mL ascorbic acid-2-phosphate was also added to the culture medium. After 4 days of culture, medium was removed and cells were harvest in RLT buffer (Qiagen, Venlo, The Netherlands) with 1% β -mercaptoethanol. Medium was refreshed 24 hours prior to harvest.

RNA extraction and gene expression analysis

Frozen IPFP explants were homogenized with a Mikro-Dismembrator (Braun Biotech International GmbH, Melsungen, Germany) re-suspended in 1.8 ml RNA-Bee (TelTest, Friendswood, Texas, USA). MSC alginate beads were dissolved in ice-cold 55 mM sodium citrate at 4 °C. The solution was then centrifuged at 400 g for 8 minutes at 4 °C and cell pellets were re-suspended in 600 μ l RNA-Bee per bead. Chloroform (Sigma-Aldrich) was added to all samples at 200 μ L/mL RNA-Bee. FLS were harvested in RLT buffer.

RNA from IPFP explants, MSCs and FLS was further purified using RNeasy Micro Kit (Qiagen) according to manufacturer's instructions. RNA concentration and quality was measured using NanoDrop ND1000 UV-Vis Spectrophotometer (Isogen Life Science, Veldzicht, The Netherlands). RNA was reverse-transcribed to cDNA using the RevertAid First Strand cDNA Synthesis Kit (Thermo Fisher) according to manufacturer's instructions. qRT-PCR was performed in 10 μ L reactions on cDNA using the CFX96 Touch™ Real-Time PCR Detection System (Biorad, Hercules, California, USA). Expression of glyceraldehyde-3-phosphate dehydrogenase (*GAPDH*),

tumor necrosis factor alpha (*TNFA*), interleukin-1 β (*IL1B*), *IL6*, cluster of differentiation (*CD*)206, *CD163* matrix metalloproteinase (*MMP*)-1, *MMP-13*, collagen type II (*COL2A1*), aggrecan (*ACAN*), collagen type I (*COL1A1*), procollagen-lysine 2-oxoglutarate 5-dioxygenase 2 (*PLOD2*), and α -smooth muscle actin (*ASMA*) were determined with qRT-PCR. Gene expression was calculated according to the $\Delta\Delta C_t$ method and *GAPDH* was used as housekeeper. C_t values between the samples within each experiment differ less than 1 C_t and there were no significant differences between the conditions. 0.1% DMSO and treatment with medication did not interfere with *GAPDH* level. Unless otherwise stated, the condition treated with unconditioned medium and DMSO was used as control and set at 1.0. Expression levels of other conditions are expressed relative to the control condition. Primer sequences can be found in the supplementary methods,

Statistical analysis

IBM SPSS statistics 21 (IBM Corporation, Armonk, New York, USA) was used for statistical analysis. All data was not normally distributed according to the Shapiro-Wilk test and Levene's test for homogeneity of variance.

If not otherwise stated, statistical significance between conditions was determined using the Mann-Whitney U test. $p < 0.05$ was considered statistically significant.

RESULTS

Triamcinolone acetone reduces IPFP inflammation

Of the four medications tested, only 100 μ M TAA significantly reduced *TNFA* ($p < 0.001$), *IL1B* ($p < 0.001$) and *IL6* ($p < 0.001$) and increased the expression of genes encoding for proteins related to anti-inflammatory processes, namely *IL10* ($p < 0.05$), *CD206* ($p < 0.001$) and *CD163* ($p < 0.001$) in IPFP explants (Figure 1). DMSO as diluent of the medications did not significantly influence gene expression in IPFP explants (Supplementary figure 1).

Triamcinolone acetone reduces IPFP inflammation, even at lower concentrations

Because TAA was the only medication that significantly decreased the expression of genes encoding for pro-inflammatory proteins and increased the expression of genes associated with anti-inflammatory processes, we decided to focus on the effects of this medication. To reduce possible negative effects of 100 μ M TAA, we investigated whether a lower concentration of TAA would give the same anti-

inflammatory results. At a concentration of 0.1 μM , TAA still significantly reduced *TNFA* ($p < 0.05$) and *IL1B* ($p < 0.05$) and increased *CD206* ($p < 0.05$) and *CD163* ($p < 0.05$) (Figure 2). 10 and 1 μM of TAA also significantly increased *IL10* ($p < 0.05$). *IL6* expression was only significantly reduced with 10 μM of TAA or higher. *TNFA* and *IL1B* expression were not significantly different between the four concentration tested.

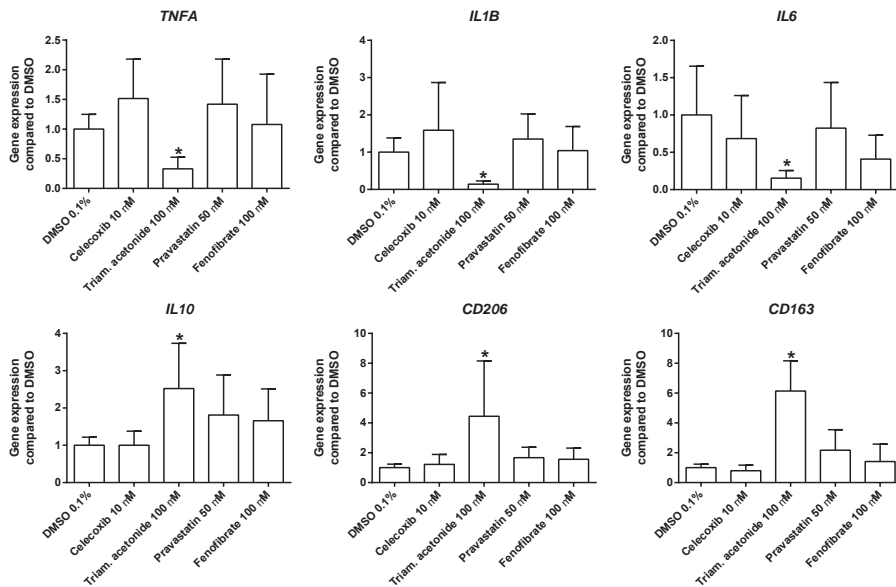


Figure 1 Triamcinolone acetate reduces IPFP inflammation

IPFP explants were treated for 24 hours with DMSO, celecoxib, triamcinolone acetate, pravastatin or fenofibrate. Gene expression of *TNFA*, *IL1B*, *IL6*, *IL10*, *CD206*, and *CD163* in IPFP explants after treatment, compared to the DMSO 0.1% treated condition. The gene expression of DMSO 0.1% treated sample was set at 1. IPFP from 3 donors were cultured with 2 samples per donor ($n=6$). Values are mean \pm SD. * $p < 0.05$ versus DMSO treated condition.

Triamcinolone acetate modulates macrophage phenotype in IPFP

Next we investigated whether TAA modulates the phenotype of the macrophages in the IPFP, since macrophages are known to be important in inflammation. We investigated the effect of 10 and 1 μM on macrophages because these two concentrations already decreased pro-inflammatory and increased anti-inflammatory genes expression. 10 μM of TAA significantly increased the percentage of CD14+/CD206+ and CD14+/CD163+ cells in the IPFP, indicating macrophages with an M2-like phenotype (Figure 3). However, TAA did not alter the percentage of CD14+/CD80+ and CD14+/CD86+ cells in the IPFP (Figure 3), indicating that the percentage of macrophages with an M1-like phenotype did not change.

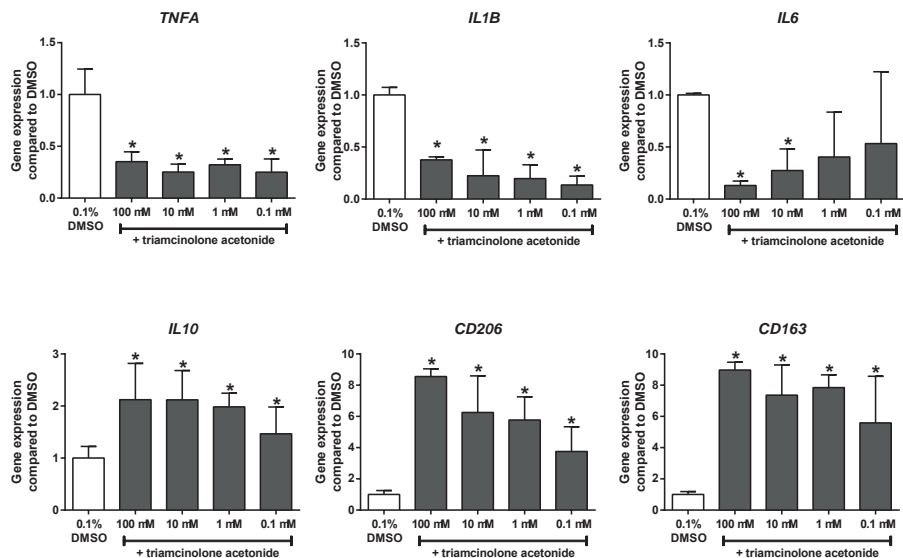


Figure 2 Triamcinolone acetonide reduced IPFP inflammation in dose range of 0.1-100 μ M. IPFP explants were treated for 24 hours with triamcinolone acetonide in the concentrations 0.1 μ M-100 μ M. Gene expression of *TNFA*, *IL1B*, *IL6*, *IL10*, *CD206*, and *CD163* in IPFP explants after treatment, compared to the condition treated with 0.1% DMSO only. Gene expression in 0.1% DMSO only was set at 1. IPFP from 2 donors were cultured with 3 samples per donor (n=6). Values are mean \pm SD. * p <0.05 versus 0.1% DMSO treated samples

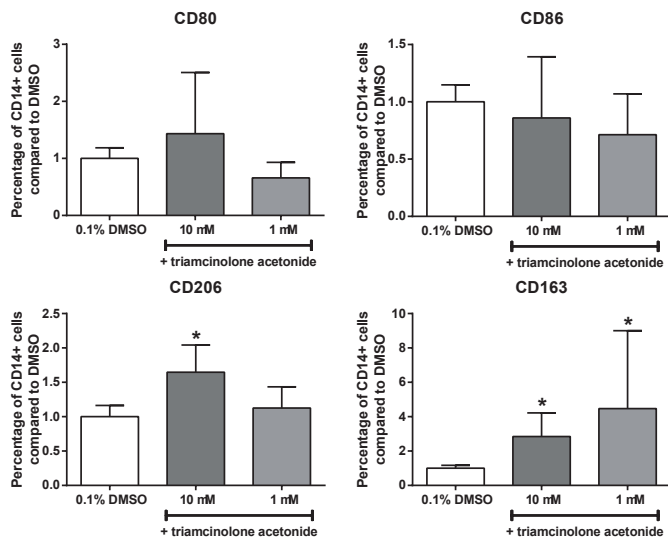


Figure 3 Triamcinolone acetonide modulates macrophages in IPFP. IPFP explants were treated for 24 hours with triamcinolone acetonide in the concentrations 10 μ M and 1 μ M. In these explants, percentage of CD80, CD86, CD206 and CD163 positive cells within the CD14 positive population (indicating macrophages) was determined using flow cytometry. Relative percentage of positive cells after treatment, compared to the condition treated with 0.1% DMSO only. Condition treated with 0.1% DMSO only was set at 1. Values are from 5 IPFP donors with 1-3 samples per donor (n=12). Values are mean \pm SD. * p <0.05 versus 0.1% DMSO.

Triamcinolone acetonide reduces anti-chondrogenic and pro-catabolic effects of IPFP

Finally, we investigated whether TAA can reduce the negative effect of IPFP on chondrogenesis of MSCs and the fibrotic and catabolic processes in fibroblast like synoviocytes (FLS). Factors secreted by untreated IPFP significantly decreased *COL2A1* ($p<0.05$) in chondrogenically stimulated MSCs (Figure 4A). Treatment of the IPFP with 1 μ M and 10 μ M TAA while making the CM significantly reduced this effect, although not entirely. Factors produced by IPFP significantly increased *MMP1* and *MMP13* in MSCs ($p<0.05$)(Figure 4A) and FLS ($p<0.05$)(Figure 4B). Treatment of the IPFP with TAA during making of the CM significantly reduced the expression of these genes in MSCs and FLS. Since TAA was also present in the medium conditioned by IPFP, we also added TAA directly to the chondrogenic stimulated MSC alginate beads and the FLS. *COL2A1* and *ACAN* were significantly reduced in MSCs by TAA. *COL1A1*, *ASMA*, *MMP1*, and *MMP13* were significantly reduced and *PLOD2* significantly increased in FLS by TAA treatment (Supplementary figure 2). This suggests that TAA mainly acts by reducing the anti-chondrogenic effect of other cells on MSCs and not through stimulation of chondrogenesis in MSCs.

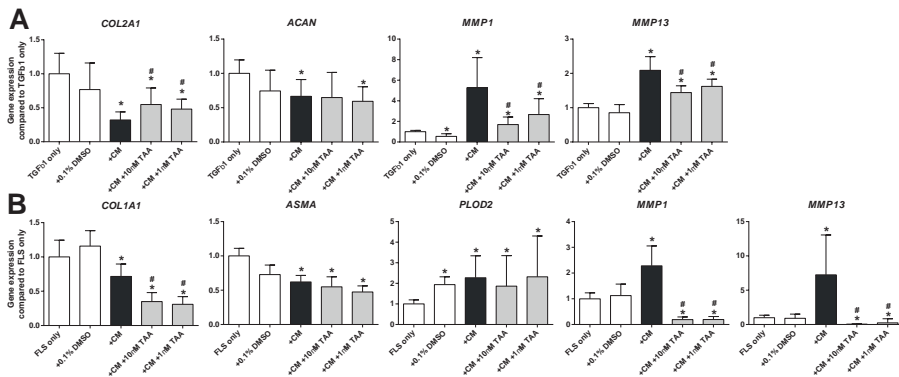


Figure 4 Triamcinolone acetonide reduces the anti-chondrogenic and pro-catabolic effects of IPFP.

FLS and chondrogenic stimulated MSC alginate beads were treated with CM from IPFP treated without or with TAA in the concentrations 10 μ M and 1 μ M. A) *COL2A1*, *ACAN*, *MMP1*, and *MMP13* expression in chondrogenic stimulated MSC alginate beads relative to the condition treated with TGFβ1 only. B) *COL1A1*, *PLOD2*, *ASMA*, *MMP1*, and *MMP13* expression in FLS relative to the condition with only FLS in culture. Gene expression in TGFβ1 only and FLS only conditions were set at 1. 3 different pools of CM of each from 3 IPFP donors were used to treat 3 MSC donors and 3 FLS donors, with each condition performed in triplicate (n=9). Values represent mean \pm SD. * $p<0.05$ versus non-treated controls (TGFβ1 only or FLS only). # $p<0.05$ versus treated with CM only.

DISCUSSION

In this study, we investigated whether anti-inflammatory medications can reduce IPFP inflammation and thereby prevent the negative effect of IPFP on chondrogenic MSCs⁹ and synovial fibroblasts^{10;11}. We have tested four commonly used medications and found that TAA, a glucocorticoid, reduced IPFP inflammation and modulated IPFP macrophage phenotype. Furthermore, TAA reduced the anti-chondrogenic effect of IPFP on MSCs and the pro-catabolic effect on FLS.

Inflammation plays a major inhibitory role in joint repair¹ and macrophages play an important role in inflammation¹⁹. Next to the synovium, which is often studied in relation to joint inflammation, the IPFP can become inflamed. The IPFP contains a large number of macrophages, and was proposed to stimulate synovial fibrosis¹⁰ and inhibit of chondrogenesis during cartilage repair⁹. In the current study, TAA not only decreased expression of genes encoding for pro-inflammatory proteins in IPFP but also increased the percentage of macrophages expressing CD163 and CD206 protein on their surface in the IPFP. Anti-inflammatory or M2-like macrophages express CD163 and CD206. Furthermore, they express factors that reduce inflammation or stimulate tissue repair, such as IL10 or CCL18^{18; 20}. The increase of M2-like macrophages in IPFP could either directly or indirectly affect the M1-like macrophages. As a result, the change in favour of M2-like macrophages might have contributed to the altered gene expression of inflammatory cytokines. In this way, the anti-chondrogenic effect of IPFP on MSC and pro-catabolic effect on FLS can be reduced.

The used medication was chosen for their anti-inflammatory effects. However, celecoxib, pravastatin and fenofibrate did not influence IPFP inflammation focusing on genes known to be expressed by different macrophage phenotypes. We therefore decided not to continue with celecoxib, pravastatin, and fenofibrate in the current study, as inflammation driven by the macrophages seem to play a large role in the negative effect of IPFP on joint tissues^{9; 10}. We cannot exclude however that celecoxib, pravastatin and fenofibrate might have an effect on anti-chondrogenic and catabolic properties of IPFP through inhibition of other pathways less related to inflammation and via other cells than the macrophages.

TAA is currently injected intra-articularly as treatment of pain and inflammation in early-OA. Although symptomatic relief does occur, no structural modifying effect on cartilage is seen⁶. TAA does reduce catabolic processes in OA synovium explants co-cultured with cartilage explants¹⁷ and in-vivo rat studies have shown

that intra-articular injection of TAA can reduce post-traumatic arthrofibrosis^{21;22}. TAA injected intra-articularly directly after joint trauma could also reduce synovitis²³. Furthermore, unlike other glucocorticoids, it is not toxic to cartilage or synovium²⁴⁻²⁶. There are cases of adipose tissue atrophy described after TAA injection²⁷. A systematic review by Brinks et al showed that these adverse events are rare and if present, are relatively mild²⁸. Repeated injections of TAA however, increased collagen type 2 and aggrecan release and turnover in knee cartilage of horses²⁹. To reduce the negative effects of TAA on cartilage, a dosage as low as possible is preferred. In our current study, expression of *GAPDH* was not influenced by treatment with any of the concentrations, suggesting that the concentrations of TAA we used had no gross overall effect on cell metabolism. Furthermore, TAA influenced IPFP inflammation at a concentration of 0.1 μM , and reduced the anti-chondrogenic and pro-catabolic effects of IPFP at 1 μM . This suggests that a lower dose of TA is sufficient to modulate the IPFP.

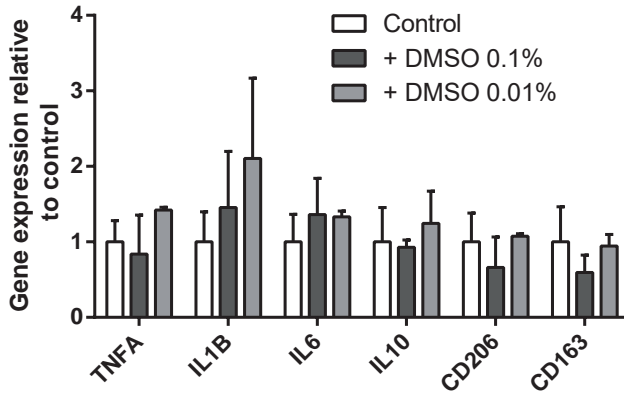
In rabbits, a single intra-articular injection of the glucocorticoid dexamethasone reduces IPFP cellularity and fibrosis 48 hours after joint trauma. However it did not reduce *IL1B* expression nor were effects on IPFP cellularity and fibrosis still present after 9 weeks³⁰. Therefore, a higher dosage and/or multiple intra-articular injections of medication might be needed before a prolonged effective level is reached in the IPFP. Multiple injections that result in a higher concentration of TAA, might however, be negative for cartilage and MSCs³¹. To reduce the number of injections and the side-effects of a high dosage, a slow-release drug delivery system directly in the IPFP could be a solution. Besides a sustained delivery system, the time of delivery is also crucial. Directly after joint trauma, levels of pro-inflammatory factors in the synovial fluid peak^{32;33}. The level of these pro-inflammatory factors drops over time, but are still higher in injured knees than in uninjured knees up to 1 year after injury³⁴. The timing of addition of TAA is therefore important as well as the required dosage, which could change over time depending on the expected level of inflammation.

Taken together, TAA reduces IPFP inflammation and the anti-chondrogenic and pro-catabolic effect of the IPFP on the joint. This is possibly caused by modulation of macrophages in the IPFP. Therefore TAA is a promising medication to modulate the joint environment, thereby creating a better environment for successful cartilage repair.

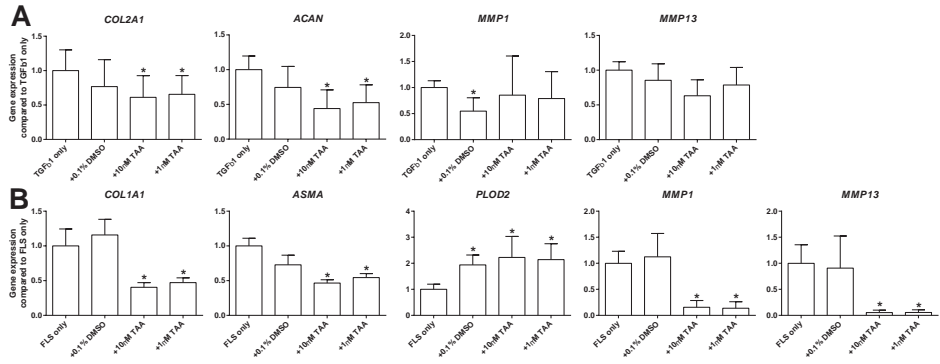
REFERENCES

1. Zhang Y, Pizzute T, Pei M. 2014. Anti-inflammatory strategies in cartilage repair. *Tissue Eng Part B Rev* 20:655-668.
2. Bannuru RR, Schmid CH, Kent DM, et al. 2015. Comparative effectiveness of pharmacologic interventions for knee osteoarthritis: a systematic review and network meta-analysis. *Ann Intern Med* 162:46-54.
3. Abe M, Matsuda M, Kobayashi H, et al. 2008. Effects of statins on adipose tissue inflammation: their inhibitory effect on MyD88-independent IRF3/IFN-beta pathway in macrophages. *Arterioscler Thromb Vasc Biol* 28:871-877.
4. Clockaerts S, Bastiaansen-Jenniskens YM, Feijt C, et al. 2012. Cytokine production by infrapatellar fat pad can be stimulated by interleukin 1beta and inhibited by peroxisome proliferator activated receptor alpha agonist. *Ann Rheum Dis* 71:1012-1018.
5. van Eekeren IC, Clockaerts S, Bastiaansen-Jenniskens YM, et al. 2013. Fibrates as therapy for osteoarthritis and rheumatoid arthritis? A systematic review. *Ther Adv Musculoskelet Dis* 5:33-44.
6. Evans CH, Kraus VB, Setton LA. 2014. Progress in intra-articular therapy. *Nat Rev Rheumatol* 10:11-22.
7. Scotti C, Gobbi A, Karnatzikos G, et al. 2016. Cartilage Repair in the Inflamed Joint: Considerations for Biological Augmentation Toward Tissue Regeneration. *Tissue Eng Part B Rev* 22:149-159.
8. Clockaerts S, Bastiaansen-Jenniskens YM, Runhaar J, et al. 2010. The infrapatellar fat pad should be considered as an active osteoarthritic joint tissue: a narrative review. *Osteoarthritis Cartilage* 18:876-882.
9. Wei W, Rudjito E, Fahy N, et al. 2015. The infrapatellar fat pad from diseased joints inhibits chondrogenesis of mesenchymal stem cells. *Eur Cell Mater* 30:303-314.
10. Bastiaansen-Jenniskens YM, Wei W, Feijt C, et al. 2013. Stimulation of fibrotic processes by the infrapatellar fat pad in cultured synoviocytes from patients with osteoarthritis: a possible role for prostaglandin f2alpha. *Arthritis Rheum* 65:2070-2080.
11. Eymard F, Pigenet A, Citadelle D, et al. 2014. Induction of an inflammatory and prodegradative phenotype in autologous fibroblast-like synoviocytes by the infrapatellar fat pad from patients with knee osteoarthritis. *Arthritis Rheumatol* 66:2165-2174.
12. He J, Jiang Y, Alexander PG, et al. 2017. Infrapatellar fat pad aggravates degeneration of acute traumatized cartilage: a possible role for interleukin-6. *Osteoarthritis Cartilage* 25:138-145.
13. Bastiaansen-Jenniskens YM, Clockaerts S, Feijt C, et al. 2012. Infrapatellar fat pad of patients with end-stage osteoarthritis inhibits catabolic mediators in cartilage. *Ann Rheum Dis* 71:288-294.
14. Fahy N, de Vries-van Melle ML, Lehmann J, et al. 2014. Human osteoarthritic synovium impacts chondrogenic differentiation of mesenchymal stem cells via macrophage polarisation state. *Osteoarthritis Cartilage* 22:1167-1175.
15. Sesia SB, Duhr R, Medeiros da Cunha C, et al. 2015. Anti-inflammatory/tissue repair macrophages enhance the cartilage-forming capacity of human bone marrow-derived mesenchymal stromal cells. *J Cell Physiol* 230:1258-1269.
16. Toyoda T, Kamei Y, Kato H, et al. 2008. Effect of peroxisome proliferator-activated receptor-alpha ligands in the interaction between adipocytes and macrophages in obese adipose tissue. *Obesity (Silver Spring)* 16:1199-1207.
17. Beekhuizen M, Bastiaansen-Jenniskens YM, Koevoet W, et al. 2011. Osteoarthritic synovial tissue inhibition of proteoglycan production in human osteoarthritic knee cartilage: establishment and characterization of a long-term cartilage-synovium coculture. *Arthritis Rheum* 63:1918-1927.

18. Utomo L, van Osch GJ, Bayon Y, et al. 2016. Guiding synovial inflammation by macrophage phenotype modulation: an in vitro study towards a therapy for osteoarthritis. *Osteoarthritis Cartilage* 24:1629-1638.
19. Hamidzadeh K, Christensen SM, Dalby E, et al. 2017. Macrophages and the Recovery from Acute and Chronic Inflammation. *Annu Rev Physiol* 79:567-592.
20. Murray PJ, Allen JE, Biswas SK, et al. 2014. Macrophage activation and polarization: nomenclature and experimental guidelines. *Immunity* 41:14-20.
21. Clark DD, Weckesser EC. 1971. The influence of triamcinolone acetonide on joint stiffness in the rat. *J Bone Joint Surg Am* 53:1409-1414.
22. Efrid W, Kellam P, Yeazell S, et al. 2014. An evaluation of prophylactic treatments to prevent post traumatic joint stiffness. *J Orthop Res* 32:1520-1524.
23. Sieker JT, Ayturk UM, Proffen BL, et al. 2016. Immediate Administration of Intraarticular Triamcinolone Acetonide After Joint Injury Modulates Molecular Outcomes Associated With Early Synovitis. *Arthritis Rheumatol* 68:1637-1647.
24. Sherman SL, James C, Stoker AM, et al. 2015. In Vivo Toxicity of Local Anesthetics and Corticosteroids on Chondrocyte and Synoviocyte Viability and Metabolism. *Cartilage* 6:106-112.
25. Sherman SL, Khazai RS, James CH, et al. 2015. In Vitro Toxicity of Local Anesthetics and Corticosteroids on Chondrocyte and Synoviocyte Viability and Metabolism. *Cartilage* 6:233-240.
26. Sola M, Dahners L, Weinhold P, et al. 2015. The viability of chondrocytes after an in vivo injection of local anaesthetic and/or corticosteroid: a laboratory study using a rat model. *Bone Joint J* 97-B:933-938.
27. Imagawa K, Ohkuma S. 2010. A case of fat injection for treating subcutaneous atrophy caused by local administration of corticosteroid. *Tokai J Exp Clin Med* 35:66-69.
28. Brinks A, Koes BW, Volkers AC, et al. 2010. Adverse effects of extra-articular corticosteroid injections: a systematic review. *BMC Musculoskelet Disord* 11:206.
29. Celeste C, Ionescu M, Robin Poole A, et al. 2005. Repeated intraarticular injections of triamcinolone acetonide alter cartilage matrix metabolism measured by biomarkers in synovial fluid. *J Orthop Res* 23:602-610.
30. Heard BJ, Solbak NM, Chung M, et al. 2016. The infrapatellar fat pad is affected by injury induced inflammation in the rabbit knee: use of dexamethasone to mitigate damage. *Inflamm Res* 65:459-470.
31. Wyles CC, Houdek MT, Wyles SP, et al. 2015. Differential cytotoxicity of corticosteroids on human mesenchymal stem cells. *Clin Orthop Relat Res* 473:1155-1164.
32. Bigoni M, Sacerdote P, Turati M, et al. 2013. Acute and late changes in intraarticular cytokine levels following anterior cruciate ligament injury. *J Orthop Res* 31:315-321.
33. Catterall JB, Stabler TV, Flannery CR, et al. 2010. Changes in serum and synovial fluid biomarkers after acute injury (NCT00332254). *Arthritis Res Ther* 12:R229.
34. Lieberthal J, Sambamurthy N, Scanzello CR. 2015. Inflammation in joint injury and post-traumatic osteoarthritis. *Osteoarthritis Cartilage* 23:1825-1834.



Supplementary figure 1 DMSO does not significantly affect gene expression in IPFP explants. IPFP explants were treated for 24 hours with DMSO. Gene expression of *TNFA*, *IL1B*, *IL6*, *IL10*, *CD206* and *CD163* compared to control. Gene expression of control was set at 1. Results are from 3 donors with 2 samples per donor (n=6). Values are mean \pm SD. * p <0.05 versus control.



Supplementary figure 2 Triamcinolone acetate has an effect on MSC and FLS. FLS and chondrogenic stimulated MSC alginate beads were treated with TAA in the concentrations 10 μ M and 1 μ M. A) *COL2A1*, *ACAN*, *MMP1*, and *MMP13* expression in chondrogenic stimulated MSC alginate beads relative to the condition treated with TGFβ1 only. B) *COL1A1*, *PLOD2*, *ASMA*, *MMP1*, and *MMP13* in FLS relative to the condition with only FLS in culture. Gene expression in TGFβ1 only and FLS only conditions were set at 1. TAA was used to treat 3 MSC donors and 3 FLS donors, with each condition performed in triplicate (n=9). Values represent mean \pm SD. * p <0.05 versus non-treated controls (TGFβ1 only or FLS only).

PART II

Systemic effects of adipose tissue



CHAPTER 6

Statins and fibrates do not affect development of spontaneous cartilage damage in STR/Ort mice

Wu Wei

Stefan Clockaerts

Yvonne M. Bastiaansen-Jenniskens

Lobke M. Gierman

Sander M. Botter

Sita M.A. Bierma-Zeinstra

Harrie Weinans

Jan A.N. Verhaar

Margreet Kloppenburg

Anne-Marie Zuurmond

Gerjo J.V.M. van Osch

ABSTRACT

Objective

Since statins and fibrates are capable of improving the metabolic profile of patients as well as decreasing inflammation, they are considered as potential drugs for preventing OA. The goal of the present study was to investigate the effect of these drugs in the STR/Ort spontaneous OA mouse model.

Design

Male STR/Ort mice received control diet or control diet containing two different dosages of simvastatin or fenofibrate or a combination of both. Mice were euthanized after 16 weeks of treatment at the age of 24 weeks. Serum analysis for metabolic and inflammatory markers, histologic OA grading and μ CT analysis of subchondral bone plate were performed.

Results

Simvastatin treatment did not have a statistically significant effect on any of the measured parameters. Fenofibrate treated mice gained less body weight and had lower serum amyloid A (SAA) levels, but higher IL1 α and MIP1 α than other mice. Mice treated with 200 mg/kg BW/day fenofibrate had less subchondral bone plate volume than control, but no statistically significant reduction in cartilage damage. In the combination treatment group, body weight and SAA were lower than control.

Overall, bodyweight, synovium membrane cell layers and SAA levels correlated to subchondral bone plate changes and subchondral bone plate changes correlated to cartilage damage.

Conclusions

Statins and fibrates did not affect development of cartilage damage in the STR/Ort spontaneous osteoarthritis mouse model. Fenofibrates however, had an effect on body weight, serum inflammation markers and subchondral bone plate morphology.

INTRODUCTION

The current non surgical treatment options for osteoarthritis (OA) are limited to non pharmacological interventions such as life style changes, exercise or weight reduction, with pharmacological treatment of symptoms if needed. No effective disease modifying drug is currently on the market for OA¹. OA is a common joint disease that affects the entire joint, including the articular cartilage, subchondral bone and the synovial membrane. High age and obesity are both major risk factors of OA. Prevalence and incidence figures are expected to rise with increasing life expectancy and growing obesity^{2,3}.

The metabolic syndrome is a concurrence of obesity, hyperinsulinemia, dyslipidemia and hypertension⁴. Metabolic OA is considered one of the subtypes of OA and is associated with the metabolic syndrome. Besides hyperglycaemia and increased serum lipids, also the vascular pathology associated with the metabolic syndrome might have negative effects on the cartilage⁵.

Statins are hydroxymethylglutaryl coenzyme-A reductase inhibitors that decrease serum cholesterol levels, reduce systemic inflammation, and decrease the amount of cardiovascular events^{6,7}. Fibrates are ligands of Peroxisome Proliferator Activated Receptor (PPAR) α . These drugs decrease serum triglycerides and also exert anti-inflammatory effects on different tissues. Like statins, they decrease inflammatory processes in cartilage, synovium and intra-articular adipose tissue in in-vitro studies⁸⁻¹⁴. Chronic low grade inflammation plays an important role in the pathogenesis of OA and metabolic syndrome⁴. Since statins and fibrates can potentially inhibit inflammatory processes in the joint as well as improve the metabolic profile of patients, they might offer a potential therapeutic or preventive strategy for OA. Recently, we associated the use of statins with decreased incidence and slower progression of knee OA in the Rotterdam Study on x-rays¹⁵. Kadam et al associated the use of statin with decreased incidence of clinical OA in the General Practice Research Database from the United Kingdoms¹⁶. No direct association between the use of fibrates and incidence of OA has been described yet¹⁷. Before starting a clinical trial that directly addresses the question whether statins and fibrates are able to prevent OA or OA progression, an *in-vivo* animal study should be performed.

In the STR/Ort mouse strain, 80% of the male mice spontaneously develop OA in the tibiofemoral joint at the age of 6 month, particularly at the medial condyles with similar histopathological lesions as in humans¹⁸. STR/Ort mice also spontaneously

develop obesity¹⁹. Furthermore, serum levels of total cholesterol, high density lipoprotein (HDL) cholesterol, LDL cholesterol, triglycerides, nonesterified fatty acids, glucose and insulin are reported to be increased in STR/Ort mice compared to C57BL/6J mice¹⁹. In addition it has been suggested that STR/Ort mice develop OA spontaneously due to the reduction of endogenous PPAR α or PPAR γ signalling, and thus possibly increasing inflammation and altering osteoblast phenotype²⁰.

For these reasons, the STR/Ort mouse model seems eminently suited to investigate the effects of statins and fibrates on OA development. In this study, we investigated whether administration of simvastatin or fenofibrate or a combination of both would prevent or delay the development of OA in the tibiofemoral joint. We evaluated the effect of this treatment on serum cholesterol, triglyceride, the inflammation marker serum Amyloid A (SAA) and the inflammatory cytokines in the blood. Cartilage damage was evaluated with histology and joint bone morphology with micro computed tomography (μ CT).

METHODS

Animals

Four-week-old male STR/Ort mice (n=72) acquired from Harlan Italy (Udine, Italy) were maintained at the animal testing facilities of the Erasmus MC University Medical Center, The Netherlands. Mice were housed in groups of three mice per cage under standard conditions and had access to water and food ad libitum. The study protocol was approved by the institutional Animal Care and Use Committee (Erasmus MC University Medical Center, The Netherlands, AEC 116-10-01)

Diets and drug intake

Mice were fed semi-synthetic non-irradiated mice reference diet (AbDiets, Woerden, The Netherlands) for 4 weeks before feeding the experimental diets. Body weight (BW) was measured every two weeks and food was replaced 2-3 times per week. Average BW per mouse and average food intake per cage per day could thus be determined and we could calculate the amount of drugs (mg/kg) needed to be mixed with reference diet for the mice to receive the intended target dosage (mg/kg BW/day). At the age of 8 weeks, the mice were divided into 6 experimental groups of n = 12. Group 1 (control) continued to receive the non-supplemented reference diet. Group 2 and 3 received reference diet mixed with either 300 or 750 mg/kg simvastatin (Eurogenerics, Brussel, Belgium), which corresponds to dosages of 40 and 100 mg/kg BW/day. Groups 4 and 5 received reference diet mixed

with either 600 or 1500 mg/kg fenofibrate (Eurogenerics, Brussel, Belgium), which corresponds to dosages of 80 and 200 mg/kg BW/day. Finally, group 6 received a combination of simvastatin (300 mg/kg) and fenofibrate (600 mg/kg) with dosages 40 and 80 mg/kg BW/day respectively. Target dosages of each drug were based upon what is often used in the literature to study the anti-inflammatory or lipid lowering effects of these drugs²¹. All experimental diets were provided and mixed by AB Diets (Woerden, The Netherlands) and were stored at 4°C for a maximum of 26 weeks. At the age of 6 months the mice were sacrificed via isoflurane anesthesia and heart puncturing.

One mouse in the simvastatin 40mg/kg BW/day treatment group rapidly lost weight and was euthanized 2 weeks before the end of the study. Nevertheless, having completed >90% of the study period, we decided to include the data from this mouse in all analyses.

Serum analysis

Blood was collected through a cheek puncture prior to the start of experimental diet. At end point, blood was collected through a heart puncture. Blood was stored for 1 hour at room temperature, followed by 30 minutes at 4°C, then centrifuged for 5 minutes at 12.000 rpm and serum was removed and immediately stored at -80°C. Total plasma cholesterol (Roche Diagnostics kit no.1489437) and plasma triglyceride (Roche diagnostics kit no.1488872) were determined after defrosting. Serum Amyloid A (SAA) was also determined in each sample by ELISA (Tridelta development, Maynooth, Ireland) according to the manufacturer's instruction. Mouse inflammatory cytokines (FGF basic, GM-CSF, IFN- γ , Interleukin(IL)-1 α , IL-1 β , IL-2, IL-4, IL-5, IL-6, IL-10, IL-12p40/p70, IL-13, IL-17, IP-10, KC, MCP-1 MIG, MIP-1 α , TNF- α and VEGF) were measured using a magnetic 20-plex bead assay (Invitrogen, Frederick, MD, USA) according to manufacturer's instructions.

Due to technical problems during sample processing, the serum samples of one mouse in the control group and two of the simvastatin 40mg/kg BW/day treatment group were lost.

μ CT analysis

The left hind legs of all animals were excised and fixed in 4% buffered formalin for μ CT and histology. We used the Skyscan 1176 X-ray microtomograph and complementary dedicated software (Bruker micro-CT, Kontich, Belgium) to analyze the subchondral bone morphology in the proximal tibia of the left knee. The following scan settings were used: voltage 100 kV; current 100 μ A; filter 0.5 mm aluminium; image pixel size 17.92 μ m; exposure time 2360 ms; frame averaging 3; with 0.4 degree rotation through 180 degrees. Following scanning, datasets were recon-

structed using NRecon (Bruker-Skyscan). Segmentation was performed with a local threshold algorithm²² and using CTAnalyser (Bruker-Skyscan), the medial and lateral subchondral bone plate (region of interest depth: 1.61 mm ventro-dorsal, starting from the anterior intercondylar area; region of interest width: adjusted according to total medio-lateral width in each tibia, then split in half in the middle of the intercondylar eminence, yielding a lateral and a medial part) were selected as regions of interest. Finally, CTAnalyser was used to calculate subchondral bone plate bone volume (BV) and subchondral bone plate thickness, as described previously²³.

Histological analysis

After μ CT scanning, the legs were decalcified in 10% formic acid in distilled water for 10 days and embedded in paraffin and 6 μ m thick coronal (frontal) histological sections were cut at 100 μ m intervals through the joint. Sections were stained with thionine. Two independent blinded observers scored cartilage damage at the medial and lateral sides of both the femur and the tibia according to the semi-quantitative scoring system devised by the Osteoarthritis Research Society International (OARSI) histopathology initiative²⁴. Briefly, this scoring system has a range from 0 to 6, with 0 means normal cartilage, 1 small fibrillations without loss of cartilage and 3-6 erosions to the calcified cartilage extending from <25% to >75%. Only slides where all four (i.e. the medial and lateral sides of both the femur and tibia) locations were visible were used. The mean score of three different slides was determined and in case of a >0.5 score discrepancy between the first observers, a third independent observer rescored the slides. To determine whether treatment has an effect on synovial inflammation, the number of cell layers of the synovium membrane on the medial side of the patella was counted. The mean number of cell layers of three different slides was used in the statistical analysis.

Due to technical error during analysis, the knees of one control mouse and one combination treated mouse were lost.

Data analysis

Statistical analysis was performed in IBM SPSS statistics 20 (IBM Corporation, Armonk, New York, USA) and R: A language and environment for statistical computing 3.0.2 (R Development Core Team, Vienna, Austria). Data was tested for normality using the Shapiro-Wilk test and for homogeneity of variance using the Levene's test. The one way ANOVA with post-hoc Bonferroni correction was then used for BW at end point, serum total cholesterol and bone parameters because these parameters were normally distributed and had homogeneity of variance.

For other serum parameters, food intake and histological data, the Kruskal-Wallis with post-hoc Bonferroni correction was used. The 95% confidence interval (CI) of the difference between conditions when the Kruskal-Wallis test was used, was calculated using the bootstrap method. To assess the relationship between BW at end point, serum total cholesterol and μ CT data, the Pearson's correlation coefficient was used because these parameters were normally distributed. For all other association analyses, the Spearman's correlation coefficient was used. $p < 0.05$ was considered statistically significant.

RESULTS

Simvastatin treatment had no statistically significant effect on serum parameters or OA characteristics

Body weight As expected, the mean BW of the mice in the control group increased during the study, reaching a mean of 36.8 (\pm 3.2) grams after 16 weeks (Figure 1). In the simvastatin only treated groups, BW at end point did not statistically significantly differ from control (95% CI: -3.4 to 4.0 and -2.6 to 4.7 for the difference between control and 40 or 100 mg/kg BW/day of simvastatin respectively). Food intake was not statistically significantly influenced by the addition of simvastatin to the food and the mice received a median of 77% of the intended dosage of drug (Table 1).

Serum No statistical significant difference was observed in serum total cholesterol (95% CI: -0.7 to 0.4 and -0.6 to 0.6), serum total triglyceride (95% CI: -2.4 to 1.1 and -1.0 to 1.6) and SAA levels (95% CI: -286.4 to 680.1 and -570.0 to 728.4) after both dosages of simvastatin only treatments (Figure 2). Using the multiplex assay, IL1 α , MIP1 α and IL10 were detectable in the serum and compared to control mice, these were not statistically significantly different after simvastatin treatment.

OA cartilage damage Microscopic evaluation demonstrated variability in cartilage loss and the amount of subchondral bone in all the groups (Figure 3). Cartilage damage was most profound in the medial compartment of the joint. The median OARSI scores in the simvastatin 100 mg/kg BW/day treated group at the medial femur and tibia were lower than the untreated control group, although this difference was not statistically significant (95% CI: -0.6 to 3.8 for medial femur and -1.8 to 4.6 for medial tibia OARSI score). We could not detect a statistically significant reduction of synovial hyperplasia in the mice after simvastatin treatment compared to controls (95% CI: -0.7 to 1.0 and -0.7 to 1.0 for the difference between control and 40 or 100 mg/kg BW/day of simvastatin respectively; Figure 3).

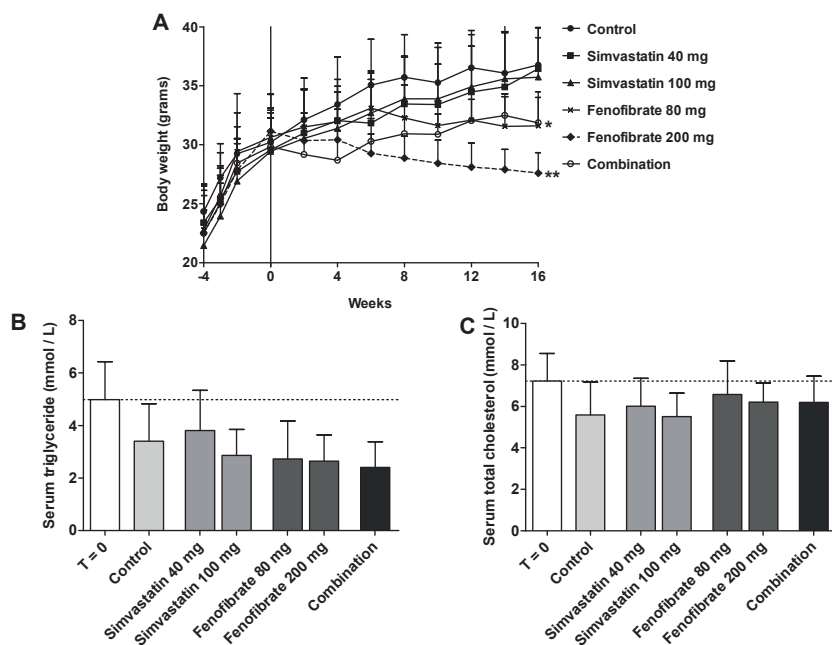


Figure 1 Effect of treatment on body weight and serum metabolic markers.

T = 0 weeks represent start of experimental treatment at the age of 8 weeks. Control group received reference diet for 16 weeks. Treatment groups received simvastatin and/or fenofibrate mixed into their diet for 16 weeks. Indicated dosages are intended drug intake/kg body weight/day. Combination group received simvastatin 40 mg and fenofibrate 80 mg. A) Body weight, B) Serum triglyceride, C) Serum total cholesterol. Values indicate mean \pm SD (n=11-12 mice per group). Horizontal dashed line: mean value of T = 0. * p <0.01 versus Control group. ** p <0.001 versus Control group

Table 1 Total food intake and drug intake per mouse*

Treatment Group (Intended drug intake)	Average total food intake per mouse in grams**	P Value	Actual drug intake per kg body weight per day in mg (% of intended drug intake)
Control	492.1 \pm 15.7		
Simvastatin 40 mg	467.1 \pm 13.8	1.000	30.7 \pm 1.8 (77)
Simvastatin 100 mg	460.2 \pm 4.2	0.265	76.2 \pm 2.6 (76)
Fenofibrate 80 mg	557.5 \pm 18.8	0.009	74.5 \pm 2.0 (93)
Fenofibrate 200 mg	524.9 \pm 8.6	0.265	189.3 \pm 5.5 (95)
Combination	484.3 \pm 11.8	1.000	33.5 \pm 1.4 (84)\$ 67.0 \pm 2.8 (84)#

*Treatment groups received simvastatin and/or fenofibrate mixed with their diet for 16 weeks. Indicated dosages are intended drug intake/kg body weight/day. Combination group received simvastatin 40 mg and fenofibrate 80 mg. Data are mean \pm SD; Kruskal-Wallis test with post-hoc Bonferonni correction was performed; P values indicate the statistical difference between treatment and control group;

**Average total food intake per mouse for 16 weeks

\$ Simvastatin 40 mg

Fenofibrate 80 mg

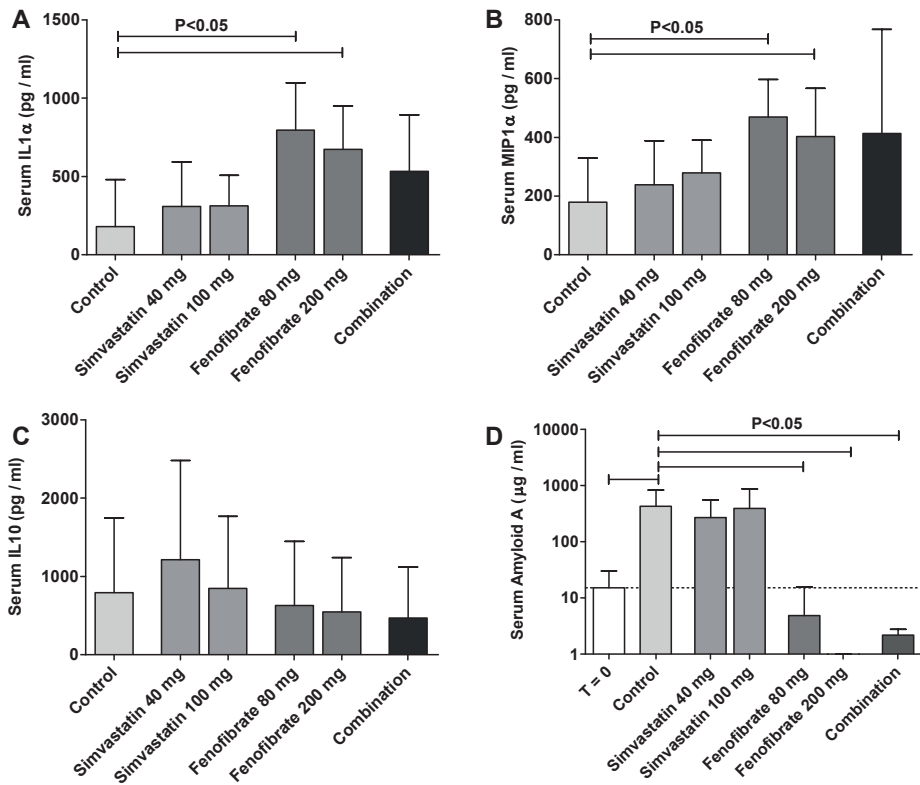


Figure 2 Effect of simvastatin and/or fenofibrate on serum inflammatory markers.

Control group received reference diet. Treatment groups received simvastatin and/or fenofibrate mixed with their diet for 16 weeks. Indicated dosages are intended drug intake/kg body weight/day. Combination group received simvastatin 40 mg and fenofibrate 80 mg. A) Serum IL1 α , B) Serum MIP1 α , C) Serum IL10 and D) Serum Amyloid A levels. T = 0: values before treatment at the age of 8 weeks. Horizontal dashed line indicates the mean value at the start of treatment (T = 0). Values indicate mean + SD (n=11-12 mice per group)

Twenty one percent of the mice developed patella subluxation and the prevalence of subluxation was not different between groups. Excluding the mice with patella dislocation from the analyses did not alter the results (Supplementary table 1).

μ CT analysis Both the subchondral bone volume (95% CI: -0.1 to 0.1 and -0.1 to 0.2) and plate thickness (95% CI: -40.6 to 42.1 and -24.3 to 60.2) did not statistically significantly differ between mice treated with simvastatin and control mice (Figure 4).

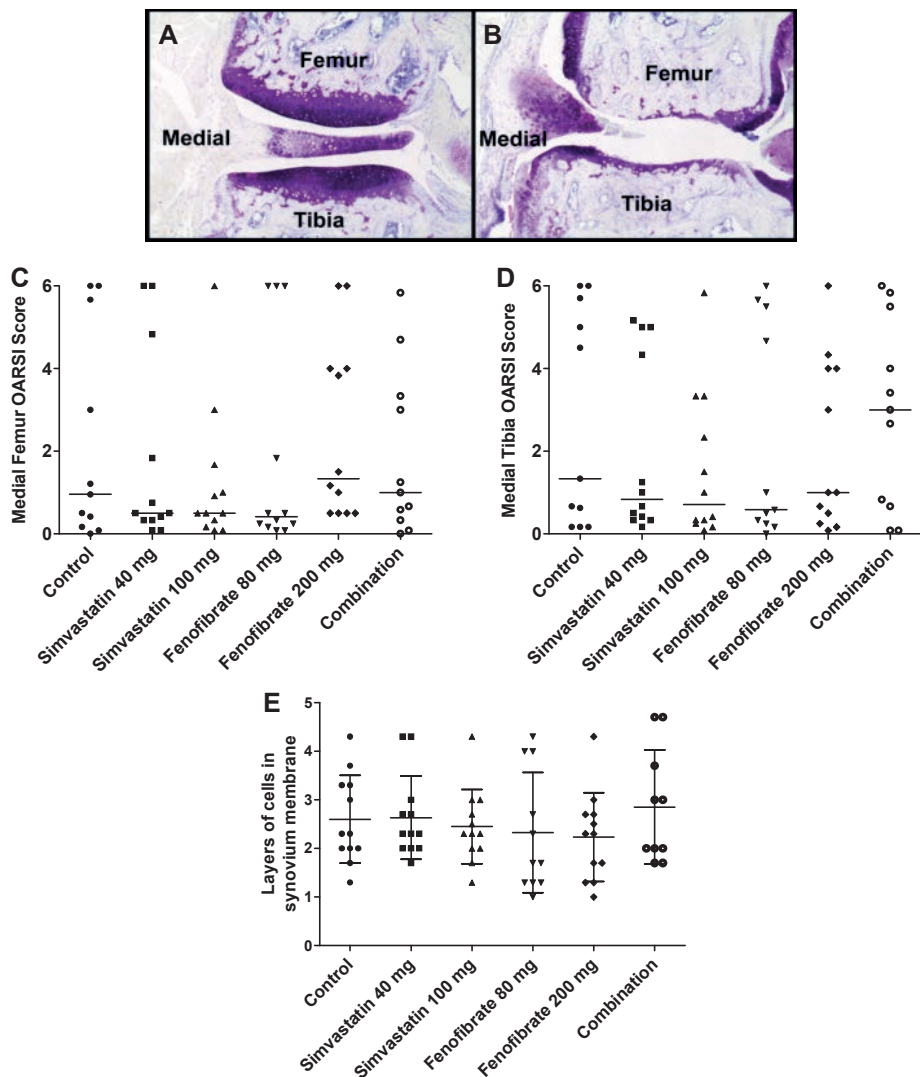


Figure 3 Histological analysis of effect of simvastatin and/or fenofibrate treatment on cartilage damage in STR/Ort mice.

The coronal sections of cartilage in the weight-bearing area of the tibiofemoral compartment of the left knee were stained with thionine and severity of cartilage damage was scored on a scale of 0-6 using the OARSI histological scoring scale. Control group received reference diet for 16 weeks. Treatment groups received simvastatin and/or fenofibrate mixed with their diet for 16 weeks. Indicated dosages are intended drug intake/kg body weight/day. Combination group received simvastatin 40 mg and fenofibrate 80 mg. A) Representative picture of score 0: normal cartilage B) Representative picture of score 6: Vertical clefs/erosion to the calcified cartilage extending to >75% of the surface. Pictures are taken at 40x magnification. C) Quantification of OARSI scores of the medial femur. D) Quantification of OARSI scores of the medial tibia. E) Number of cell layers in the synovial membrane. Each dot represents an individual mouse (n=11-12 mice per group) Horizontal line indicates median value per group in C and D. Mean \pm SD is shown in E.

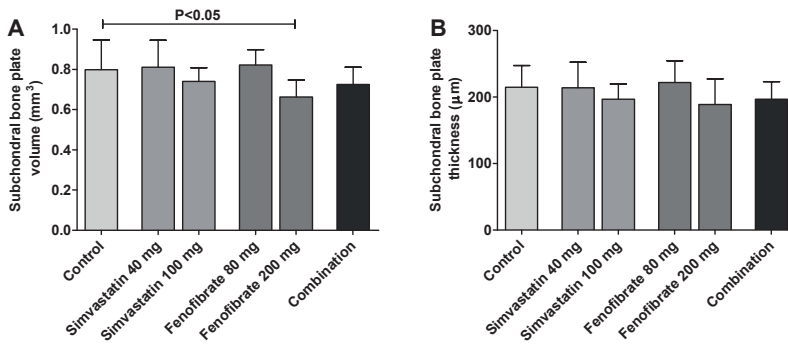


Figure 4 Effect of simvastatin and/or fenofibrate treatment on subchondral bone plate bone volume and thickness of the tibia plateau in STR/Ort mice.

Control group received reference diet for 16 weeks. Treatment groups received simvastatin and/or fenofibrate mixed with their diet for 16 weeks. Indicated dosages are intended drug intake/kg body weight/day. Combination group received simvastatin 40 mg and fenofibrate 80 mg. A) Subchondral bone plate bone volume B) Subchondral bone plate thickness, Values indicate mean + SD (n=11-12 mice per group)

Fenofibrate treatment reduced body weight, SAA and subchondral bone

Body weight Mice treated with 200 mg/kg BW/day fenofibrate had the lowest mean BW at end point compared to the control group ($p<0.001$; Figure 1). All fenofibrate treated mice ate more compared to the control group, although only the fenofibrate 80 mg/kg BW/day treated group ate statistically significantly more (Table 1). No signs of diarrhoea were observed. The mice received a median of 94% of the intended drug dosage.

Serum markers We did not detect a statistically significant effect of fenofibrate treatment on serum total triglyceride (95% CI: -0.5 to 2.2 and -0.8 to 2.0 for the difference between control and 80 or 200 mg/kg BW/day of fenofibrate respectively) and on serum total cholesterol (95% CI: -0.9 to 0.3 and -0.8 to 0.4; Figure 2). SAA levels in fenofibrate treated groups did not change after start of treatment and at end point were significantly lower than in the control group (95% CI: 9.5 to 828.0 and 10.8 to 829). On the multiplex assay only IL1 α , MIP1 α and IL10 were detectable in the serum (Figure 2). IL1 α and MIP1 α levels were significantly higher in fenofibrate treated mice than in control mice.

OA cartilage damage We could not detect a statistically significant reduction of medial femur (95% CI: -2.8 to 3.4 and -3.5 to 2.6) and tibia (95% CI: -4.3 to 4.6 and -3.4 to 4.3) OARSI scores and synovial hyperplasia (95% CI: -1.7 to 1.8 and -0.6 to 1.3) in the fenofibrate treated mice compared to controls (Figure 3).

μ CT analysis Mice treated with 200 mg/kg BW/day fenofibrate had a lower subchondral bone volume and plate thickness than the control group although only the lower subchondral bone volume was statistically significant (Figure 4).

Effects of combination treatment of simvastatin and fenofibrate

The mean BW of the mice treated with a combination of simvastatin and fenofibrate at the end of the study was lower than the mean BW in the control group ($p=0.003$, Figure 1). The mice received 84% of the intended dosage simvastatin and fenofibrate (Table 1).

Only serum amyloid A was statistically significantly different between mice treated with a combination of simvastatin and fenofibrate and controls (Figures 2, 3 and 4)

Correlation between body weight, serum markers, cartilage damage, synovial hyperplasia and bone changes.

Body weight at end point correlated with serum total triglyceride ($p<0.001$), IL1 α ($p<0.001$) and MIP1 α ($p=0.001$) and subchondral bone volume ($p=0.01$). In none of the treatment groups, serum inflammation markers correlated statistically significantly with OA cartilage damage (Table 2). SAA levels did not differ between mice with and without cartilage damage. SAA levels correlated to subchondral bone volume ($p=0.008$) Both subchondral bone volume ($p=0.002$), plate thickness ($p<0.001$) and synovial hyperplasia ($p<0.001$) correlated with cartilage damage. (Table 2)

Table 2 Correlation between body weight serum markers, OARSI cartilage scores, synovial hyperplasia and μ CT data.

	Body Weight (end point)	OARSI Score			Synovium cell layers	Subchondral bone plate volume	Subchondral bone plate volume
		Total	Femur	Tibia			
Body weight (end point)		0.14	0.04	0.19	0.32	0.31	0.22
Serum							
Total cholesterol	0.09	0.07	0.02	0.05	0.04	-0.26	-0.23
Total triglyceride	0.45	0.12	0.10	0.10	0.28	0.03	0.04
Amyloid A	0.21	-0.01	-0.08	0.08	0.12	0.34	0.19
IL1 α	-0.52	-0.07	-0.09	-0.04	-0.09	-0.09	-0.13
MIP1 α	-0.44	-0.09	-0.13	-0.02	-0.05	-0.01	-0.06
IL10	0.11	-0.08	-0.14	0.03	-0.01	-0.01	-0.11
Synovium cell layers	0.33	0.62				0.32	0.42
Subchondral bone plate volume	0.31			0.37			
Subchondral bone plate thickness	0.22			0.49			

Serum markers were measured at end point after 16 weeks of treatment; OARSI scores for the total joint, both femur and tibial compartments; Correlations between body weight at end point, serum total cholesterol and μ CT data were calculated using the Pearson correlation coefficient; Correlations between all other parameters were calculated using the Spearman correlation coefficient; Significant correlations ($p<0.05$) are shown in bold.

DISCUSSION

In this study we investigated whether drugs often used to reduce the morbidity and mortality of metabolic syndrome and obesity could serve as a therapy to prevent or treat OA. We did not find a statistically significant reduction of the severity of cartilage damage in STR/Ort mice with neither simvastatin, fenofibrate nor the combination treatment, although fenofibrate treatment prevented a high subchondral bone volume.

The STR/Ort strain was carefully chosen for this study because these mice have been described to develop OA and metabolic syndrome spontaneously at a relatively young age¹⁹, thus resembling patients with metabolic OA⁴. Since statins and fibrates are used to improve the metabolic profile of patients, the use of this strain seemed to match the subgroup of metabolic OA patients that could benefit from treatment with these drugs. In addition to hyperlipidemia and obesity, other possible causes for OA predisposition in the STR/Ort strain have been discussed, such as the role of patella subluxation^{18;25}. When patella subluxation occurs, it is a major biomechanical risk factor and disease modifying effects of simvastatin or fenofibrate would be highly unlikely. In our study, patella subluxation occurred in 21% of the mice throughout all the groups. Although all mice with patella subluxation had extensive cartilage damage, not all mice with extensive cartilage damage had patella subluxation. This suggests that patella subluxation is not the main cause of OA in these mice and is not likely to mask the effects of simvastatin or fenofibrate.

In a previous human cohort study we found that statin use was associated with a lower incidence and reduced progression of knee OA on x-rays¹⁵. In an other study statin use was associated with lower incidence of clinical OA¹⁶. In the present study with STR/Ort mice, simvastatin did not lower the serum total cholesterol level. This could be explained by a different cholesterol metabolism pathway in mice than in humans²⁶⁻²⁸. The absence of a statistically significant effect of simvastatin on OA in our study could indicate that cholesterol and OA might be linked to each other and that lowering cholesterol by statins is important to reduce OA development. Furthermore, different types of statins were included in the human clinical studies. These different types of statins have been described to have different therapeutic effects²⁹. The serum levels of total cholesterol in the control mice in our study were comparable to a previous study¹⁹. Serum cholesterol can be increased with a high fat diet in mice and decreases after treatment with statin^{30;31}. In addition, we have previously reported that statin treatment decreased the development of OA

in mice on a high fat diet³². This suggests that the effect of statin treatment could also depend on the type of diet. However, this conclusion should be drawn with caution, because the studies of Fraulob³¹ and Gierman³² used rosuvastatin and the study of Paraskevast³⁰ atorvastatin, whereas we administered simvastatin. As with humans, these different types of statins have been described to have different therapeutic effects in mice²¹.

The result of our study that simvastatin could not statistically significantly reduce OA cartilage damage is also not consistent with a previous study by Yudoh et al¹⁴, who reported a statistically significant decrease in OA cartilage score in STR/Ort mice after 12 and 24 weeks of simvastatin (40 mg/kg BW/day) treatment. This inconsistency could be due to differences in strains: Yudoh and colleagues used STR/OrtCrlj mice obtained from Charles River Japan whereas we used STR/OrtOlaHsd mice obtained from Harlan, Italy. Response to simvastatin could have been different between these two populations of mice. Furthermore, in the study by Yudoh et al, the cartilage damage in the untreated group at the age of 24 weeks was less severe than in the control group in our study. This indicates that simvastatin might be more effective in slowly developing or less severe OA. Lastly, Yudoh et al administrated the drugs by daily gavage instead of mixing it with the food and therefore a different therapeutic level might be reached in the mice.

Fenofibrate is another lipid lowering drug, widely used to lower serum lipids in patients with hypertriglyceridemia. Serum triglyceride was not lowered after treatment with fenofibrate in our study, but the treated mice gained less weight. BW was however moderately correlated to serum triglyceride suggesting that weight reduction could reduce serum triglyceride. Control mice continued to gain BW over time, reaching a mean weight of 36.8 ± 3.2 grams at the age of 24 weeks. This is comparable to previous studies^{19;33}. The reduction in BW gain by fenofibrate treatment however, did not protect the mice from developing cartilage damage. This absence of correlation between BW and incidence of cartilage damage confirms our earlier findings³² that obesity does not increase OA cartilage damage by biomechanical overloading.

In our study, serum cholesterol and serum triglyceride were both not correlated with cartilage damage. This suggests that in the STR/Ort mice lipid metabolism is not the primary cause of spontaneous OA cartilage damage development. Next to their effect on lipid metabolism, statins and fibrates are known to have an effect on inflammation^{8;9;11-13}. SAA, a marker for systemic inflammation, increased in control mice with aging. SAA has been associated with inflammatory processes in

atherosclerosis and rheumatoid arthritis³⁴⁻³⁶, is increased in obesity³⁷ and clinical studies have shown that SAA can be lowered by fenofibrate and simvastatin treatment³⁸⁻⁴⁰. In the present study with STR/Ort mice, SAA levels were only lowered after fenofibrate treatment. SAA is described to be induced by the cytokines IL1 β , IL6 and TNF- α and it can activate the NF- κ B pathway^{34;35;41}. Kyostio-Moore et al⁴² reported elevated inflammatory cytokines in the serum of STR/Ort mice including IL1 β , IL12p70 and IL5, and these changes were correlated with cartilage damage. We were able to detect IL1 α , MIP1 α and IL10 in the serum of the mice, but other cytokines were not detected. Surprisingly, IL1 α , and MIP1 α levels were significantly higher in mice that received fenofibrate treatment. This suggests that different aspects of inflammation might occur that possibly counteract each other. Furthermore, we found no correlation between individual serum inflammatory markers and synovial hyperplasia, suggesting that systemic inflammation is not directly related to local inflammatory changes in the knee in our STR/Ort mice.

Fenofibrate lowers lipid levels by activating PPAR α . It has been suggested that STR/Ort mice have reduced endogenous PPAR α signalling. This reduction of PPAR α signalling could be associated with increased osteogenic differentiation and reduced adipogenic and chondrogenic differentiation of bone marrow derived mesenchymal stem cells and thus be associated with the development of OA in these mice²⁰. In our study, PPAR α activation with 200mg/kg BW/day fenofibrate did indeed reduce the total bone volume in the subchondral bone. We could however, not detect a significant reduction of cartilage damage in our study. Changes in cartilage and subchondral bone during OA development are thought to be correlated to each other⁴³ and we did find a moderate correlation between cartilage damage and subchondral bone parameters. The absence of a statistically significant reduction of cartilage damage might be due to the limited sensitivity of the histological cartilage damage scoring or to the high variation in incidence of spontaneous OA cartilage damage in these mice. In the present study, 60% of the animals had developed OA cartilage damage at 24 weeks of age, which is less than the 80% reported in other studies that we used for our power calculation¹⁸. Moreover, since we used a spontaneous model of OA development, individual mice developed OA at a different speed²⁵ which might explain the large variation in cartilage damage in the control group.

Alternatively, it is possible that the mice treated with fenofibrate are at a different phase in OA development. During OA development in mice, a biphasic subchondral bone turnover process is taking place, with initial loss of subchondral bone, followed by increased volume and thickening of the subchondral bone plate^{23;44}.

In the fenofibrate treated mice, initial OA development could have been delayed as demonstrated by the lower subchondral bone volume whereas the other mice already progressed to a thickening of the subchondral plate. Further investigation with time series is needed to confirm this hypothesis.

Possible side effects of statins and fenofibrates are muscle pain and elevated liver enzymes. Furthermore, toxicology studies performed on mice showed that administration of very high dosages of simvastatin or fenofibrate for 72 weeks could possibly induce liver carcinomas^{45; 46}. In our study, we did not analyse the livers of our mice at age 20 weeks for the presence of liver carcinomas, so we cannot exclude the presence of these tumours. We included one group of mice that was treated with a combination of simvastatin and fenofibrate. This combination has been shown in clinical studies to be more effective in decreasing cardiovascular mortality⁴⁷, treating dyslipidemia⁴⁸ and decreasing inflammation⁴⁹ compared to monotherapy. Because the combination is demonstrated to be more effective⁴⁷⁻⁴⁹, a lower dose of both drugs can be used and therefore less side effects will occur⁵⁰. Unfortunately, we did not see synergistic effects of the combination treatment in our study. Simvastatin and fenofibrate are both metabolised in the liver and thereby lowering the levels that are reached locally in the knee or subchondral bone. Methods to increase the levels of both drugs locally, such as intra-articularly or subcutaneously injections might provide options to increase the local effects and reduce the systemic side effects.

In summary, we could not detect a statistically significant decrease of simvastatin or fenofibrate treatment on the development of cartilage damage in 6 months old STR/Ort mice. On the other hand, the effect of fenofibrate on subchondral bone morphology and the correlation between subchondral bone morphology and cartilage damage suggests there might be a mild effect on OA development that is masked by the insensitivity of the cartilage score or the high variation in cartilage damage in mice of 6 months old. Furthermore, our data suggest that biomechanical changes due to overweight or patella subluxation and spontaneous metabolic changes are not the primary cause of OA in the STR/Ort mouse. Complex inflammatory processes occur in these mice that did not affect the cartilage directly.

Nonetheless, we do not exclude that lipid lowering drugs can still be beneficial in other subtypes of OA such as high fat diet induced metabolic OA as indicated by our previous studies. This emphasizes the importance of further subtyping OA to find possibilities for pharmacological treatment of OA.

REFERENCES

1. Bijlsma JW, Berenbaum F, Lafeber FP. 2011. Osteoarthritis: an update with relevance for clinical practice. *Lancet* 377:2115-2126.
2. Aspden RM, Scheven BA, Hutchison JD. 2001. Osteoarthritis as a systemic disorder including stromal cell differentiation and lipid metabolism. *Lancet* 357:1118-1120.
3. Oliveria SA, Felson DT, Reed JI, et al. 1995. Incidence of symptomatic hand, hip, and knee osteoarthritis among patients in a health maintenance organization. *Arthritis Rheum* 38:1134-1141.
4. Zhuo Q, Yang W, Chen J, et al. 2012. Metabolic syndrome meets osteoarthritis. *Nat Rev Rheumatol* 8:729-737.
5. Hoeven TA, Kavousi M, Clockaerts S, et al. 2012. Association of atherosclerosis with presence and progression of osteoarthritis: the Rotterdam Study. *Annals of the Rheumatic Diseases*.
6. Devaraj S, Chan E, Jialal I. 2006. Direct demonstration of an antiinflammatory effect of simvastatin in subjects with the metabolic syndrome. *J Clin Endocrinol Metab* 91:4489-4496.
7. Abe M, Matsuda M, Kobayashi H, et al. 2008. Effects of statins on adipose tissue inflammation: their inhibitory effect on MyD88-independent IRF3/IFN-beta pathway in macrophages. *Arterioscler Thromb Vasc Biol* 28:871-877.
8. Baker J, Walsh P, Byrne D, et al. Pravastatin suppresses matrix metalloproteinase expression and activity in human articular chondrocytes stimulated by interleukin-1 β . *Journal of Orthopaedics and Traumatology*:1-5.
9. Clockaerts S, Bastiaansen-Jenniskens YM, Feijt C, et al. 2011. Peroxisome proliferator activated receptor alpha activation decreases inflammatory and destructive responses in osteoarthritic cartilage. *Osteoarthritis Cartilage* 19:895-902.
10. Clockaerts S, Bierma-Zeinstra SM. 2011. Comment on: Statins and the joint: multiple target for a global protection? *Semin Arthritis Rheum* 40:588.
11. Dombrecht EJ, Van Offel JF, Bridts CH, et al. 2007. Influence of simvastatin on the production of pro-inflammatory cytokines and nitric oxide by activated human chondrocytes. *Clin Exp Rheumatol* 25:534-539.
12. Lazzarini PE, Capocchi PL, Nerucci F, et al. 2004. Simvastatin reduces MMP-3 level in interleukin 1beta stimulated human chondrocyte culture. *Ann Rheum Dis* 63:867-869.
13. Lazzarini PE, Lorenzini S, Selvi E, et al. 2007. Simvastatin inhibits cytokine production and nuclear factor-kB activation in interleukin 1beta-stimulated synoviocytes from rheumatoid arthritis patients. *Clin Exp Rheumatol* 25:696-700.
14. Yudoh K, Karasawa R. 2010. Statin prevents chondrocyte aging and degeneration of articular cartilage in osteoarthritis (OA). *Aging (Albany NY)* 2:990-998.
15. Clockaerts S, Van Osch GJ, Bastiaansen-Jenniskens YM, et al. 2012. Statin use is associated with reduced incidence and progression of knee osteoarthritis in the Rotterdam study. *Ann Rheum Dis* 71:642-647.
16. Kadam UT, Blagojevic M, Belcher J. 2013. Statin Use and Clinical Osteoarthritis in the General Population: A Longitudinal Study. *J Gen Intern Med*.
17. van Eekeren IC, Clockaerts S, Bastiaansen-Jenniskens YM, et al. 2013. Fibrates as therapy for osteoarthritis and rheumatoid arthritis? A systematic review. *Ther Adv Musculoskelet Dis* 5:33-44.
18. Mason RM, Chambers MG, Flannelly J, et al. 2001. The STR/ort mouse and its use as a model of osteoarthritis. *Osteoarthritis and Cartilage* 9:85-91.
19. Uchida K, Urabe K, Naruse K, et al. 2009. Hyperlipidemia and hyperinsulinemia in the spontaneous osteoarthritis mouse model, STR/Ort. *Exp Anim* 58:181-187.

20. Watters JW, Cheng C, Pickarski M, et al. 2007. Inverse relationship between matrix remodeling and lipid metabolism during osteoarthritis progression in the STR/Ort mouse. *Arthritis Rheum* 56:2999-3009.
21. Zadelaar S, Kleemann R, Verschuren L, et al. 2007. Mouse models for atherosclerosis and pharmaceutical modifiers. *Arterioscler Thromb Vasc Biol* 27:1706-1721.
22. Waarsing JH, Day JS, Weinans H. 2004. An improved segmentation method for in vivo microCT imaging. *J Bone Miner Res* 19:1640-1650.
23. Botter SM, van Osch GJ, Clockaerts S, et al. 2011. Osteoarthritis induction leads to early and temporal subchondral plate porosity in the tibial plateau of mice: an in vivo microfocal computed tomography study. *Arthritis Rheum* 63:2690-2699.
24. Glasson SS, Chambers MG, Van Den Berg WB, et al. 2010. The OARSI histopathology initiative - recommendations for histological assessments of osteoarthritis in the mouse. *Osteoarthritis Cartilage* 18 Suppl 3:S17-23.
25. Naruse K, Urabe K, Jiang SX, et al. 2009. Osteoarthritic changes of the patellofemoral joint in STR/OrtCrly mice are the earliest detectable changes and may be caused by internal tibial torsion. *Connect Tissue Res* 50:243-255.
26. Kleemann R, Princen HM, Emeis JJ, et al. 2003. Rosuvastatin reduces atherosclerosis development beyond and independent of its plasma cholesterol-lowering effect in APOE*3-Leiden transgenic mice: evidence for antiinflammatory effects of rosuvastatin. *Circulation* 108:1368-1374.
27. Sparrow CP, Burton CA, Hernandez M, et al. 2001. Simvastatin has anti-inflammatory and antiatherosclerotic activities independent of plasma cholesterol lowering. *Arterioscler Thromb Vasc Biol* 21:115-121.
28. Endo A, Tsujita Y, Kuroda M, et al. 1979. Effects of ML-236B on cholesterol metabolism in mice and rats: lack of hypocholesterolemic activity in normal animals. *Biochim Biophys Acta* 575:266-276.
29. Weng TC, Yang YH, Lin SJ, et al. 2010. A systematic review and meta-analysis on the therapeutic equivalence of statins. *J Clin Pharm Ther* 35:139-151.
30. Paraskevas KI, Pantopoulou A, Vlachos IS, et al. 2011. Comparison of fibrate, ezetimibe, low- and high-dose statin therapy for the dyslipidemia of the metabolic syndrome in a mouse model. *Angiology* 62:144-154.
31. Fraulob JC, Souza-Mello V, Aguila MB, et al. 2012. Beneficial effects of rosuvastatin on insulin resistance, adiposity, inflammatory markers and non-alcoholic fatty liver disease in mice fed on a high-fat diet. *Clin Sci (Lond)* 123:259-270.
32. Gierman LM, van der Ham F, Koudijs A, et al. 2012. Metabolic stress-induced inflammation plays a major role in the development of osteoarthritis in mice. *Arthritis Rheum* 64:1172-1181.
33. Sokoloff L, Mickelsen O, Silverstein E, et al. 1960. Experimental obesity and osteoarthritis. *Am J Physiol* 198:765-770.
34. Okamoto H, Katagiri Y, Kiire A, et al. 2008. Serum amyloid A activates nuclear factor-kappaB in rheumatoid synovial fibroblasts through binding to receptor of advanced glycation end-products. *J Rheumatol* 35:752-756.
35. McNiff PA, Stewart C, Sullivan J, et al. 1995. Synovial fluid from rheumatoid arthritis patients contains sufficient levels of IL-1 beta and IL-6 to promote production of serum amyloid A by Hep3B cells. *Cytokine* 7:209-219.
36. King VL, Thompson J, Tannock LR. 2011. Serum amyloid A in atherosclerosis. *Curr Opin Lipidol* 22:302-307.
37. Trayhurn P, Wood IS. 2004. Adipokines: inflammation and the pleiotropic role of white adipose tissue. *Br J Nutr* 92:347-355.

38. Gervois P, Kleemann R, Pilon A, et al. 2004. Global Suppression of IL-6-induced Acute Phase Response Gene Expression after Chronic in Vivo Treatment with the Peroxisome Proliferator-activated Receptor- α Activator Fenofibrate. *Journal of Biological Chemistry* 279:16154-16160.
39. Horiuchi Y, Hirayama S, Soda S, et al. 2010. Statin therapy reduces inflammatory markers in hypercholesterolemic patients with high baseline levels. *J Atheroscler Thromb* 17:722-729.
40. Hu Y, Tong G, Xu W, et al. 2009. Anti-inflammatory effects of simvastatin on adipokines in type 2 diabetic patients with carotid atherosclerosis. *Diab Vasc Dis Res* 6:262-268.
41. Ramadori G, Van Damme J, Rieder H, et al. 1988. Interleukin 6, the third mediator of acute-phase reaction, modulates hepatic protein synthesis in human and mouse. Comparison with interleukin 1 beta and tumor necrosis factor-alpha. *Eur J Immunol* 18:1259-1264.
42. Kyostio-Moore S, Nambiar B, Hutto E, et al. 2011. STR/ort mice, a model for spontaneous osteoarthritis, exhibit elevated levels of both local and systemic inflammatory markers. *Comp Med* 61:346-355.
43. Mahjoub M, Berenbaum F, Houard X. 2012. Why subchondral bone in osteoarthritis? The importance of the cartilage bone interface in osteoarthritis. *Osteoporos Int* 23 Suppl 8:841-846.
44. Botter SM, Glasson SS, Hopkins B, et al. 2009. ADAMTS5^{-/-} mice have less subchondral bone changes after induction of osteoarthritis through surgical instability: implications for a link between cartilage and subchondral bone changes. *Osteoarthritis Cartilage* 17:636-645.
45. Drugs.com. 2013. Fenofibrate Official FDA information, side effects and uses, from Drugs.com.
46. Drugs.com. 2013. Simvastatin orally disintegrating tablet Official FDA information, side effects and uses, from Drugs.com.
47. Tenenbaum A, Medvedofsky D, Fisman EZ, et al. 2012. Cardiovascular events in patients received combined fibrate/statin treatment versus statin monotherapy: Acute Coronary Syndrome Israeli Surveys data. *PLoS One* 7:e35298.
48. Derosa G, Maffioli P, Salvadeo SA, et al. 2009. Fenofibrate, simvastatin and their combination in the management of dyslipidaemia in type 2 diabetic patients. *Curr Med Res Opin* 25:1973-1983.
49. Wagner AM, Sanchez-Quesada JL, Benitez S, et al. 2011. Effect of statin and fibrate treatment on inflammation in type 2 diabetes. A randomized, cross-over study. *Diabetes Res Clin Pract* 93:e25-28.
50. Franssen R, Vergeer M, Stroes ES, et al. 2009. Combination statin-fibrate therapy: safety aspects. *Diabetes Obes Metab* 11:89-94.



CHAPTER 7

High fat diet accelerates cartilage repair in DBA/1 mice

Wu Wei

Yvonne M. Bastiaansen-Jenniskens

Mathijs Suijkerbuijk

Nicole Kops

Pieter K. Bos

Jan A.N. Verhaar

Anne-Marie Zuurmond

Francesco Dell'Accio

Gerjo J.V.M. van Osch

J Orthop Res. 2017 Jun;35(6):1258-64.

ABSTRACT

Obesity is a well-known risk factor for osteoarthritis, but it is unknown what it does on cartilage repair. Here we investigated whether a high fat diet (HFD) influences cartilage repair in a mouse model of cartilage repair. We fed DBA/1 mice control or HFD (60% energy from fat). After two weeks, a full thickness cartilage defect was made in the trochlear groove. Mice were sacrificed, 1, 8 and 24 weeks after operation. Cartilage repair was evaluated on histology. Serum glucose, insulin and amyloid A were measured 24h before operation and at endpoints. Immunohistochemical staining was performed on synovium and adipose tissue to evaluate macrophage infiltration and phenotype. One week after operation, mice on HFD had defect filling with fibroblast-like cells and more cartilage repair as indicated by a lower Pineda score. After 8 weeks, mice on a HFD still had a lower Pineda score. After 24 weeks, no mice had complete cartilage repair and we did not detect a significant difference in cartilage repair between diets. Bodyweight was increased by HFD, whereas serum glucose, amyloid A and insulin were not influenced. Macrophage infiltration and phenotype in adipose tissue and synovium were not influenced by HFD. In contrast to common wisdom, HFD accelerated intrinsic cartilage repair in DBA/1 mice on the short term. Resistance to HFD induced inflammatory and metabolic changes could be associated with accelerated cartilage repair.

INTRODUCTION

Traumatic articular cartilage injury, a common pathology of the knee¹, results in considerable morbidity and disabilities and could eventually lead to osteoarthritis (OA). Articular cartilage has low self-repair capabilities² and the microfracture procedure is used to induce intrinsic cartilage repair by mesenchymal stem cells (MSCs)³. The microfracture procedure leads to significant symptomatic improvements in most patients^{4,5}. The clinical improvements are reported to be less in patients with obesity⁶ and these patients are now often excluded from treatments⁷. However, there is no information about the structure of the newly formed cartilage or mechanisms explaining the relationship between obesity and worse clinical outcome.

Obesity is a major health problem in the Western society and the number of persons with obesity is increasing. Obesity could lead to systemic metabolic and inflammatory changes such as hyperglycemia, hyperinsulinemia, increased serum amyloid A and infiltration of adipose tissue by pro-inflammatory macrophages⁸. Obesity is a well-known major risk factor for the development of OA⁹. Furthermore, obesity exaggerated post-traumatic arthritis¹⁰ and rheumatoid arthritis¹¹ and could lead to impaired wound healing after an operation¹². However, it is unknown what the precise effect is of obesity on intrinsic cartilage defect repair.

To optimize cartilage repair treatment results in obese patients, it is therefore essential to investigate whether and how obesity negatively influences cartilage repair. To answer this question, we performed an in-vivo mouse study to investigate the direct effect of obesity on intrinsic cartilage repair. In our study, a high fat diet (HFD) was used to increase weight and mimic human obesity in mice¹³. HFD has been shown to increase weight and to be detrimental to cartilage and cause OA in the C57/BL6 strain of mice^{12,14}. Furthermore, HFD decreases the chondrogenic differentiation potential of MSCs from C57/BL6 mice¹⁵.

Our hypothesis was that HFD would negatively influence intrinsic cartilage repair. Since C57/BL6 mice had been shown not to possess intrinsic repair capabilities of cartilage defects¹⁶, they were unsuitable for our study. Therefore, we used male DBA/1 mice which possess capabilities to repair a full thickness cartilage defect¹⁶ and gain weight on a HFD¹⁷. This strain of mice is therefore suitable to study the possible negative effects of a HFD on cartilage repair.

METHOD

Animals and diet

Eight-weeks-old male DBA/10IaHsd mice were acquired from Harlan UK and maintained at the animal testing facilities of the Erasmus MC University Medical Center, The Netherlands. Mice were housed in groups of three or four mice per cage under 12 hours light-dark cycle and had access to water and food ad libitum. The study protocol was approved by the institutional Animal Care and Use Committee (Erasmus MC University Medical Center, The Netherlands, AEC 116-12-05). Mice were allowed to acclimatize, were fed regular chow for two weeks and were allocated randomly to the diet groups. At the age of 10 weeks, mice were fed with a HFD (D12492; Research Diets, 60% kcal from fat) or control diet (D12450B; Research Diets, 10% kcal from fat). Both diets contained 4057 kcal per kilogram dry weight. Mice were weighted every two weeks and the mice continued to receive their respective diets until they were killed.

Operative procedure

At the age of 12 weeks mice were anesthetized with an isoflurane/O₂ mixture and a full thickness cartilage defect was created as previous described¹⁶. The left hind leg was shaved and disinfected using alcohol. An incision using a nr 11 microsurgical scalpel was made medially and proximally from the insertion of the patellar tendon on the tibia towards the attachment of the quadriceps muscle. The joint capsule was opened with a small incision and the joint was fully extended to dislocate the patella laterally. The knee joint was then fully flexed to expose the trochlear groove articular surface. A full thickness cartilage defect was then made using a 25G needle by scratching the articular surface. The joint was flushed with saline and closed using 6-0 Vicryl (Ethicon). The skin was closed using 6-0 Ethilon (Ethicon). The mice were given one dose of analgesic subcutaneously preoperatively (Temgesic, 0.05 mg/kg). Mice were allowed to move freely post operation and to be full weight bearing. Mice were sacrificed 1, 8 and 24 weeks after operation with a heart puncture under isoflurane/O₂ anesthesia. All mice reached end-point without disease. 34% of the operated mice had a patella dislocation and were excluded from the analysis. These mice were equally distributed over both groups: patella dislocation rate was 35% for the control group and 32% for the HFD fed group. We continued to operate mice until there were at least 5 mice per group. The time points and minimum number of mice per group needed were based on previous study by Eltawil et al¹⁶. The final number of mice on a control diet included for analysis was 8 mice at 1 week, 9 mice at 8 weeks and 6 mice at 24

weeks. For the mice on a HFD, the number of mice included was 6 mice at 1 week, 9 mice at 8 weeks and 6 mice at 24 weeks.

Serum collection and analysis

Blood was collected through a cheek puncture one day before the operation and through a heart puncture at end points. We collected three drops of blood during the cheek puncture and 1 ml of blood through the heart puncture. There was no noticeable difference in bleeding tendency between animals. Mice were fasted for 4 hours before blood collection. Blood was stored for 1 hour at room temperature, followed by 30 minutes at 4°C, then centrifuged for 5 minutes at 250g. Serum was removed and immediately stored at -80°C. Serum glucose was determined using a blood glucose meter (FreeStyle Freedom Lite, Abbott Laboratories). Serum insulin (Alpco, #80-INSMS-E01) and serum amyloid A (SAA, Alpco, #41-SAAMS-E01) were determined by Enzyme-Linked Immuno Sorbent Assay (ELISA) according to the manufacturer's instructions.

Tissue preparation for histological analysis

The skin of both hind legs of all animals was opened. The patella with surrounding synovium was removed, placed in Tissue Tek® (Sakura Finetek, the Netherlands) and snap frozen in liquid nitrogen. 6 µm thick cryosections were made of the patella with surrounding synovium. Subcutaneous adipose tissue of 5 mice per diet at time point 8 weeks after the operation were fixed in 4% buffered formalin for 1 hour, embedded in paraffin and 6 µm thick paraffin sections were made. The knees of all animals were excised and fixed in 4% buffered formalin for 7 days, decalcified in 10% formic acid in distilled water for 7 days and embedded in paraffin. 6 µm thick paraffin sections were made of the knees as described by Eltawil et al¹⁶.

Evaluation of cartilage repair

Paraffin sections were stained with thionin or immunohistochemically stained with a monoclonal antibody against collagen type 2. For immunohistochemical staining, collagen type 2 antibody (DSHB, # II-II 6B3) or IgG1 isotype control (Dako Cytomation #X0931) were first pre-coupled with biotin-SP F(ab)₂ (Jackson, #115-066-062). Sections were then incubated with the coupled antibody complex, followed by Label (Biogenex, HK-321-UK) and freshly prepared new-fuchsin was used as substrate. Pictures were taken using an Olympus SC30 camera. The size of the defect and percentage of defect filled was quantified using ImageJ software (National Institutes of Health, Bethesda, MD, USA). The number of cells in the defect was determined in ImageJ and expressed as per 100µm². Cartilage repair was assessed using the scoring system devised by Pineda et al¹⁸, in which filling,

reconstruction of osteochondral junction, matrix staining and cell morphology were taken into account. The Pineda scoring system has a range of 0 to 14, in which 0 means complete repair and 14 no repair at all. Osteoarthritic damage in the cartilage surrounding the defect was assessed using a modified Mankin scoring system¹⁹. Both scoring systems were performed by two independent observers (WW and MS) while being blinded to the group assignment. The mean score of three different slides was determined and in case of a >1 score discrepancy between the two observers, rescoring was performed together by the two observers.

Evaluation of local and systemic inflammation

Cryosection of the patella with surrounding synovium were fixed in acetone and stained with hematoxylin and eosin (H&E). For immunohistochemical staining, sections were incubated with monoclonal antibody against F4/80 (eBioscience, #14-4801), polyclonal antibodies against iNOS (Abcam, #15323) and CD206 (Abcam, #64693). Rat IgG2a antibody (eBioscience, #14-4321-82) were used as isotype control for F4/80 and rabbit IgG antibody (Dako Cytomation #X0903) were used as isotype control for iNOS and CD206. Subsequently, F4/80 sections were incubated with biotinylated rabbit-anti-rat IgG (Vector, #BA-4000) and iNOS and CD206 sections were incubated with Rabbit-Link (Biogenex, HK-326-UR). All sections were afterwards incubated with Label (BioGenex, HK-321-UK) and freshly prepared new-fuchsin was used as substrate. A cell was considered positive when stained red.

Synovial inflammation was evaluated using the histological scoring system devised by Krenn et al²⁰. To determine whether HFD had an effect on synovial macrophage phenotype, immunohistochemically stained samples were ranked based on their relative number of positive cells in three sections per sample by two independent observers (WW and MS). Scoring and ranking were performed for each marker separately and the average rank for each sample between the two observers was used in the analysis.

Paraffin sections of subcutaneous adipose tissue were deparafinized, treated with proteinase k solution (Sigma-Aldrich) for antigen retrieval and followed by the same immunohistochemical staining procedure for F4/80 as the synovium. Two independent observers (WW and MS) counted the number of crown like structures per area of random 100 adipocytes for 3 sections per sample and the average number between the two observers was used in the analysis.

Statistical analysis

Statistical analysis was performed in IBM SPSS statistics 20 (IBM Corporation, Armonk, New York, USA). The Shapiro-Wilk test was used to test data for normality and the Levene's test for homogeneity of variance. Histological data was analyzed using the Mann-Whitney-U test. Weight, serum data and defect filling were normally distributed and unless otherwise stated, statistical differences between diets were determined using an unpaired T-test. Differences were considered statistically significant when $p < 0.05$.

RESULTS

High fat diet accelerates cartilage repair early after cartilage damage

One week after the creation of the defect, in mice on a HFD, spindle shaped cells had partially filled the defect (Figure 1A). A higher percentage of the defect was filled in the mice on a HFD than on control diet (Figure 1A and D), although this

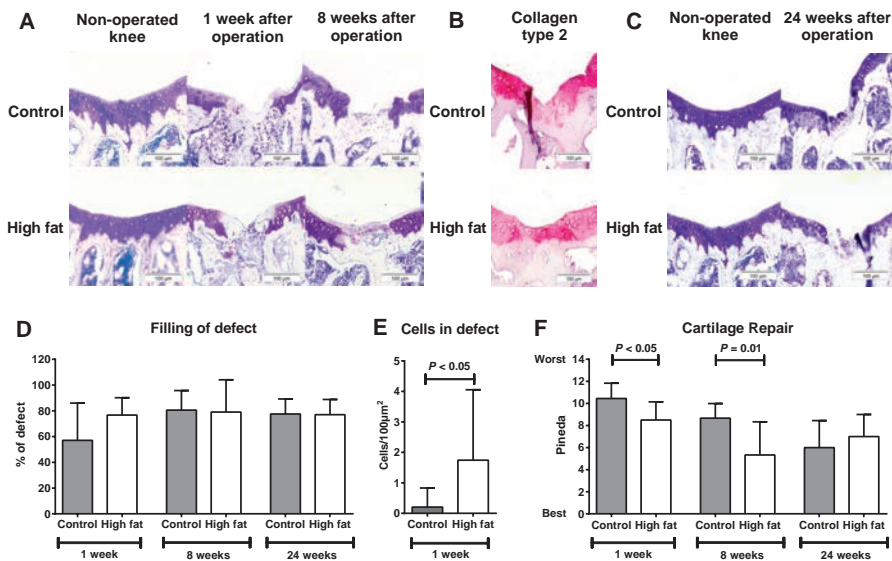


Figure 1 High fat diet feeding improves cartilage repair.

10 weeks old male DBA/1 mice were fed with control or high fat diet. After 2 weeks of feeding, full thickness cartilage defects were created. A) Representative pictures of thionin stained knees; non-operated, 1 weeks and 8 weeks after defect creation, B) immunohistological staining with antibodies against collagen type 2, 8 weeks after defect creation. This is the from the same knee as the thionin staining. There is an artifact shown in the staining. C) Representative pictures of thionin stained knees; 24 weeks after defect creation and corresponding non-operated knees, D) percentage of defect filled, E) number of cells in the defect per 100μm², F) cartilage repair evaluated using the Pineda scoring method. Values are mean ± SD (n=6-9 mice per group).

was not statistically significant (Figure 1D; 95% CI: 63-91% versus 38-77%; $p=0.15$). After 8 weeks, almost all the mice had filling of the defect (Figure 1D), however only the HFD fed mice had defects filled with chondrocyte-like cells surrounded with positive thionin and collagen type 2 staining (Figure 1A and B). In addition, the number of cells in the defect was higher in HFD fed mice compared to the control mice (Figure 1E). Finally, the Pineda score was lower 1 week ($p=0.04$) and 8 weeks ($p=0.01$) after operation in mice on a HFD compared to control diet (Figure 1F and Table 1).

Table 1 High fat diet improves cartilage repair

	Control diet					High fat diet				
	F	R	M	C	Total	F	R	M	C	Total
1 week	2.0 (± 1.1)	2.0 (± 0.0)	3.4 (± 0.7)	3.1 (± 0.9)	10.5 (± 1.4)	1.3 (± 0.5)	2.0 (± 0.0)	2.7 (± 0.8)	2.3 (± 0.5)	8.5 (± 0.7)
8 weeks	0.8 (± 0.8)	1.9 (± 0.3)	3.1 (± 0.3)	2.8 (± 0.4)	8.7 (± 1.3)	0.8 (± 1.3)	1.3 (± 0.7)	2.0 (± 1.1)	2.1 (± 1.3)	5.3 (± 3.0)
24 weeks	0.8 (± 0.8)	1.2 (± 0.4)	1.9 (± 0.9)	2.1 (± 1.0)	6.0 (± 2.4)	0.8 (± 0.8)	1.8 (0.4)	2.2 (0.8)	2.2 (0.8)	7.0 (± 2.0)

Cartilage repair evaluated using the Pineda scoring method. The different components of the Pineda scoring method are showed. Lower score represents better cartilage repair results. F: Filling of the defect (-1-4), R: Reconstruction of osteochondral junction (0-2), M: Matrix staining (0-4) and C: Cell morphology (0-4). Values are mean (\pm SD). Bold indicates $p<0.05$ versus Control diet.

High fat diet does not cause major systemic or local metabolic and inflammatory changes in DBA/1 mice

24 hours before the operation, high fat diet fed mice were heavier (26.2 grams versus 23.3 grams; $p=0.004$) and had higher serum glucose ($p=0.01$) than mice receiving a control diet (Figure 2A-B). Serum insulin and amyloid were not different between the two groups. Eight weeks after the operation the mice on HFD were still heavier and had higher fasting serum glucose, although the glucose level was not different from 1 week after operation. (Figure 2B). Serum insulin and amyloid A were not affected by HFD (Figure 2C and D). As seen on histology, HFD induced adipocyte hypertrophy (Figure 2E). There was less than one crown like structure (CLS) per 100 adipocytes and there was no significant difference between control and HFD fed mice. Finally, we investigated whether HFD influenced local inflammation in the joint and specifically the synovium. The synovium was more inflamed 1 week after the operation compared to 8 weeks (Figure 3A-B). There was no detectable synovial inflammation in the non-operated knees. No statistically significant effect of the HFD on synovitis and rank of F4/80, iNOS or CD206 positive cells was detected (Figure 3B-E).

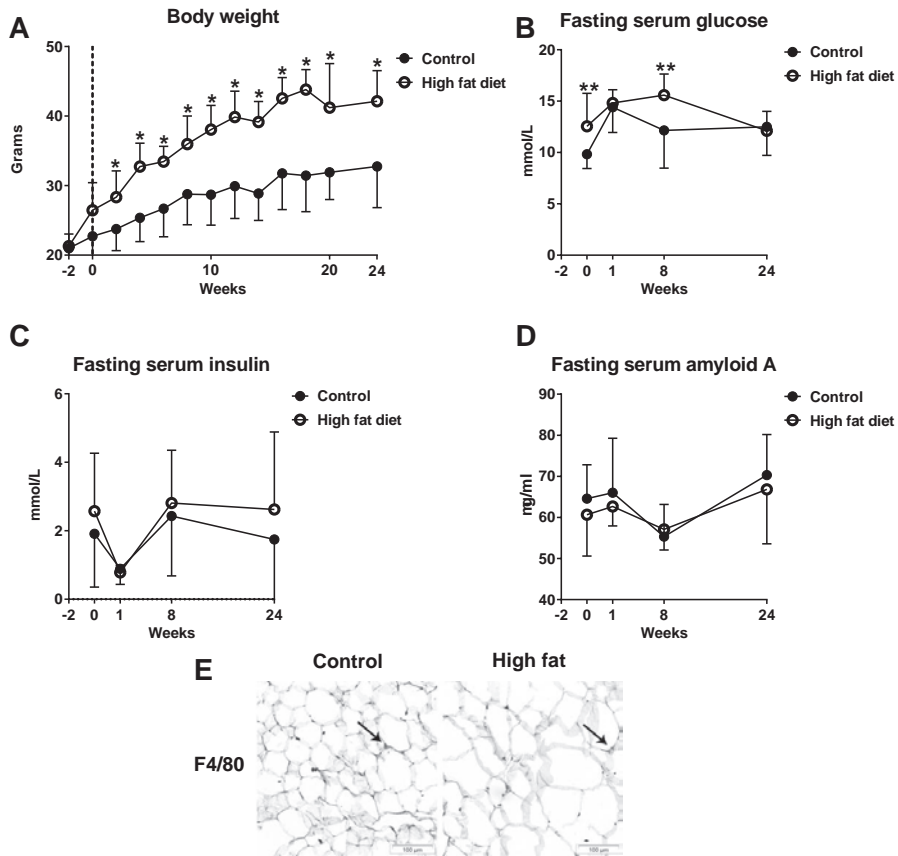


Figure 2 High fat diet increases body weight, but does not cause major systemic metabolic and inflammatory changes in DBA/1 mice.

Mice were fasted for 4 hours prior to serum collection. A) Body weight of the mice. Fasting serum B) glucose, C) insulin and D) amyloid A at 1, 8 and 24 weeks after operation. Timepoint 0 represents 24 hours before operation. E) Representative pictures of subcutaneous adipose tissue stained with antibodies against F4/80 at 8 weeks after operation. Positive cells are indicated with arrows. Bar values are mean \pm SD (n=6-9 mice per group). * p <0.01 versus control diet. ** p <0.05 versus control diet.

Long term effects of high fat diet and cartilage damage in DBA/1 mice

Long term feeding with HFD significantly increased the weight of the mice (Figure 2A, 41.1 grams versus 30.3 grams; $p=0.008$), but did not influence serum metabolic and inflammatory markers (Figure 2B-D). A small loss of thionin staining of the cartilage surrounding the defect in the operated knees was visible (Figure 1C). There was however no major cartilage loss or structural changes indicating osteoarthritis after 24 weeks in the operated knees, not even in combination with a HFD (Table 2, Figure 1C). There was no cartilage loss in the non-operated knees (Figure 1C, Table 2)

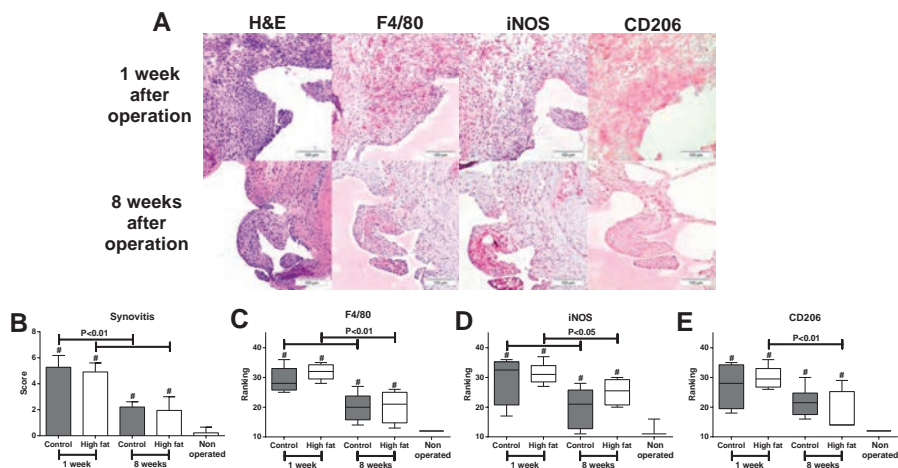


Figure 3 High fat diet does not influence operation induced synovial inflammation. A) Representative pictures of synovium with immunohistochemical staining with antibodies against F4/80, iNOS and CD206, 1 and 8 weeks after operation. B) Synovitis score and ranking score of positive cells for C) F4/80, D) iNOS and E) CD206. Bar values are mean \pm SD (n=6-9 per group). # p <0.01 versus non-operated knees

Table 2: Long term effects of high fat diet on osteoarthritis development.

	Control diet	High fat diet	P-Value
Modified Mankin score (non-operated knee)	0 (No OA)	0 (No OA)	1.0
Modified Mankin score (operated knee)	1.5 (\pm 0.5)	1.7 (\pm 0.5)	1.0
P-Value	p <0.01	p <0.01	

Osteoarthritis scores 24 weeks after operation. Values are mean (\pm SD) (n=6 mice per group)

DISCUSSION

Obesity, a major risk factor for joint diseases⁹, has been reported to negatively influence the clinical results of cartilage repair procedures^{6;21}. The present study is to our knowledge the first one that investigated the direct effect of a HFD induced weight gain on intrinsic repair of cartilage defects in an experimental mouse model for cartilage repair. In contrast to our hypothesis, mice on a HFD had a better Pineda score than the mice on a control diet. This difference was already detectable 1 week after making the defect, but became more obvious after 8 weeks. We could not detect a significant difference in cartilage repair anymore between the two diet groups after 24 weeks, suggesting that HFD only accelerated and not improved cartilage repair.

Previous reports on HFD have all shown detrimental effects of an HFD on cartilage. Wu et al¹² showed that HFD reduced ear wound healing and accelerated the progression to OA after destabilization of the medial meniscus. Louer et al¹⁰ showed that HFD accelerated post-traumatic arthritis. However, these studies used young adult C57BL/6 mice and this strain of mice, in contrast to DBA/1 mice, does not possess cartilage repair capabilities^{16;22;23}. Next to DBA/1 mice, MRL/MpJ mice are known to possess cartilage repair capabilities^{24;25}. Interestingly, these mice gained weight and fat mass, but did not develop the major metabolic changes seen in C57BL/6 mice after being fed a HFD^{17;26}. Our mice gained weight, even only after 2 weeks of HFD and continued to increase weight during the 24 weeks of the study, but did not develop major metabolic changes. This suggests that the degree of metabolic response to HFD and ability to repair cartilage damage might be associated.

Individual differences in response to being obese are also known in humans. Accumulation of macrophages in crown like structures (CLS) in obese subjects is associated with hyperinsulinemia and increased systemic inflammation^{27; 28} and metabolically healthy obese subjects do not have these CLS in their adipose tissue. The absence of CLS in the adipose tissue of the DBA/1 mice on a HFD again indicates that the DBA/1 mice are resistant to HFD-induced metabolic and inflammatory changes.

Previously we have shown that the level of inflammatory response to a HFD was associated with the development of OA²⁹. An initial higher inflammatory response in CRP-C57BL/6 mice to a HFD with increased serum levels of human C-reactive protein (hCRP) was correlated to OA development. Furthermore, rosiglitazone, a peroxisome proliferator-activated receptors (PPAR) γ agonist with anti-inflammatory properties, decreased HFD associated inflammation and OA development, even though it increased weight gain in these mice. In the present study, HFD did not induce systemic and local inflammatory changes in male DBA/1 mice based on the serum amyloid A measurements and immunohistological staining for macrophages in the synovium and adipose tissue. These mice also did not develop more OA, even in the presence of a cartilage defect. This again suggests that susceptibility to developing inflammatory changes might be associated to the development of OA. However, this may only account for HFD induced inflammatory changes, because inhibition of spontaneous occurring obesity related inflammatory changes in STR/Ort mice with fenofibrates did not inhibit the development of OA³⁰.

The male DBA/1 mice on a control diet in our study showed cartilage repair after 8 weeks, albeit not to the same degree as described by Eltawil et al¹⁶. Although

the mice used were of the same DBA/10laHsd strain from the same company, we have made the defects at the age of 12 weeks instead of 8 weeks, as in the study by Etawil et al. Intrinsic cartilage repair capabilities might have been reduced with increasing age, however younger DBA/1 mice would very likely have adapted to a HFD and not gained weight¹¹. The choice to use 12 weeks old DBA/1 mice might make translation of the results of our study to older individuals difficult. However, the current model has limited us not to use older mice. Finally, we used D12450B as the control diet as advised by the diet manufacturer (Research Diets). This control diet contains 10% kcal from fat and 35% kcal from sucrose. Etawil et al used chow which has lower amount of kcal from sucrose. We cannot exclude that the high sucrose could have reduced cartilage repair.

Furthermore, cartilage repair could be influenced by weight bearing activities after surgery³¹. Although it has been shown that HFD does not influence activity level in C57BL/6 mice, we cannot exclude that HFD could have influenced activity level of the mice in our study¹².

Although HFD had no effect on inflammation, it slightly increased the serum glucose before creation of the defect and serum glucose levels remained higher 8 weeks after the defect was made. This higher glucose level may have improved the initial cartilage repair process after cartilage damage, because differentiation to chondrocytes and synthesis of extracellular matrix requires a large amount of nutrients. An abundance of nutrients might also have increased the activity of mammalian target of rapamycin (mTOR), which is known to support skeletal growth and extracellular matrix production³².

However, a higher mTOR expression in cartilage is also correlated to cartilage damage and mTOR inhibition by rapamycin could prevent post-traumatic OA development³³. Increased mTOR expression could have played a role in initial cartilage repair in DBA/1 mice, but in the long term mTOR might have been suppressed to increase autophagy and protect the cartilage.

Next to hyperglycemia, a HFD can lead to hypercholesterolemia. Recently it has been shown that cholesterol metabolism and cartilage development and repair could be related. Statins are used to reduce serum cholesterol through inhibition of the enzyme HMG-CoA and statins could be a potential therapy for developmental diseases such as achondroplasia and might stimulate chondrogenic potential of intervertebral disc cells.^{34; 35} However, it is known that a HFD does not increase serum total cholesterol in male DBA/1 mice¹⁷. It could be that the enzyme HMG-CoA or another enzyme in the mevalonate pathway is less active in DBA/1 mice and that this could be related to increased cartilage repair in this mouse strain.

Besides serum metabolic changes, cartilage repair could also be directly influenced by the fat content of HFD. HFD contains mainly saturated and mono-unsaturated fatty acids which reduces, rather than stimulates, the chondrogenic potential of MSCs from C57BL/6 mice¹⁵. However, MSCs isolated from DBA/1 mice have been reported to have a better chondrogenic potential than those isolated from C57BL/6 mice³⁶. The effect of HFD on MSC chondrogenesis could therefore be different in different strain of mice.

In conclusion, our study shows that HFD and increased body weight in the DBA/1 mice do not negatively impair cartilage repair, but can even accelerate it. The precise mechanism in how HFD influences cartilage repair in DBA/1 is unknown. However, our data suggests that resistance to HFD induced inflammatory and metabolic changes could be associated with accelerated cartilage repair and reduced OA susceptibility. Further research is necessary to elucidate the complex relationships between a high fat diet, metabolic and inflammatory changes, cartilage degeneration and regeneration. For the clinical practice, our study suggests that not all obese patients should be excluded from treatment. Investigation of their metabolic and inflammatory state could be helpful in making the decision to start cartilage repair treatments.

REFERENCES

1. Widuchowski W, Widuchowski J, Trzaska T. 2007. Articular cartilage defects: study of 25,124 knee arthroscopies. *Knee* 14:177-182.
2. Newman AP. 1998. Articular cartilage repair. *Am J Sports Med* 26:309-324.
3. Shapiro F, Koide S, Glimcher MJ. 1993. Cell origin and differentiation in the repair of full-thickness defects of articular cartilage. *J Bone Joint Surg Am* 75:532-553.
4. Mithoefer K, McAdams T, Williams RJ, et al. 2009. Clinical efficacy of the microfracture technique for articular cartilage repair in the knee: an evidence-based systematic analysis. *Am J Sports Med* 37:2053-2063.
5. Negrin L, Kutscha-Lissberg F, Gartlehner G, et al. 2012. Clinical outcome after microfracture of the knee: a meta-analysis of before/after-data of controlled studies. *Int Orthop* 36:43-50.
6. Mithoefer K, Williams RJ, 3rd, Warren RF, et al. 2005. The microfracture technique for the treatment of articular cartilage lesions in the knee. A prospective cohort study. *J Bone Joint Surg Am* 87:1911-1920.
7. Gomoll AH, Farr J, Gillogly SD, et al. 2010. Surgical management of articular cartilage defects of the knee. *J Bone Joint Surg Am* 92:2470-2490.
8. Lumeng CN, Saltiel AR. 2011. Inflammatory links between obesity and metabolic disease. *J Clin Invest* 121:2111-2117.
9. Zhuo Q, Yang W, Chen J, et al. 2012. Metabolic syndrome meets osteoarthritis. *Nat Rev Rheumatol* 8:729-737.
10. Louer CR, Furman BD, Huebner JL, et al. 2012. Diet-induced obesity significantly increases the severity of posttraumatic arthritis in mice. *Arthritis Rheum* 64:3220-3230.
11. Hamaguchi K, Itabashi A, Kuroe Y, et al. 2012. Analysis of adipose tissues and stromal vascular cells in a murine arthritis model. *Metabolism* 61:1687-1695.
12. Wu CL, Jain D, McNeill JN, et al. 2014. Dietary fatty acid content regulates wound repair and the pathogenesis of osteoarthritis following joint injury. *Ann Rheum Dis*.
13. Buettner R, Scholmerich J, Bollheimer LC. 2007. High-fat diets: modeling the metabolic disorders of human obesity in rodents. *Obesity (Silver Spring)* 15:798-808.
14. Griffin TM, Huebner JL, Kraus VB, et al. 2012. Induction of osteoarthritis and metabolic inflammation by a very high-fat diet in mice: effects of short-term exercise. *Arthritis Rheum* 64:443-453.
15. Wu CL, Diekmann BO, Jain D, et al. 2013. Diet-induced obesity alters the differentiation potential of stem cells isolated from bone marrow, adipose tissue and infrapatellar fat pad: the effects of free fatty acids. *Int J Obes (Lond)* 37:1079-1087.
16. Eltawil NM, De Bari C, Achan P, et al. 2009. A novel in vivo murine model of cartilage regeneration. Age and strain-dependent outcome after joint surface injury. *Osteoarthritis Cartilage* 17:695-704.
17. Svenson KL, Von Smith R, Magnani PA, et al. 2007. Multiple trait measurements in 43 inbred mouse strains capture the phenotypic diversity characteristic of human populations. *J Appl Physiol* (1985) 102:2369-2378.
18. Pineda S, Pollack A, Stevenson S, et al. 1992. A semiquantitative scale for histologic grading of articular cartilage repair. *Acta Anat (Basel)* 143:335-340.
19. van der Sluijs JA, Geesink RG, van der Linden AJ, et al. 1992. The reliability of the Mankin score for osteoarthritis. *J Orthop Res* 10:58-61.
20. Krenn V, Morawietz L, Haupl T, et al. 2002. Grading of chronic synovitis—a histopathological grading system for molecular and diagnostic pathology. *Pathol Res Pract* 198:317-325.

21. Jaiswal PK, Bentley G, Carrington RW, et al. 2012. The adverse effect of elevated body mass index on outcome after autologous chondrocyte implantation. *J Bone Joint Surg Br* 94:1377-1381.
22. Matsuoka M, Onodera T, Sasazawa F, et al. 2015. An Articular Cartilage Repair Model in Common C57Bl/6 Mice. *Tissue Eng Part C Methods*.
23. Rai MF, Sandell LJ. 2014. Regeneration of articular cartilage in healer and non-healer mice. *Matrix Biol* 39:50-55.
24. Fitzgerald J, Rich C, Burkhardt D, et al. 2008. Evidence for articular cartilage regeneration in MRL/MpJ mice. *Osteoarthritis Cartilage* 16:1319-1326.
25. Mak J, Leonard C, Foniok T, et al. 2015. Evaluating endogenous repair of focal cartilage defects in C57BL/6 and MRL/MpJ mice using 9.4T magnetic resonance imaging: A pilot study. *Magn Reson Imaging* 33:690-694.
26. Mull AJ, Berhanu TK, Roberts NW, et al. 2014. The Murphy Roths Large (MRL) mouse strain is naturally resistant to high fat diet-induced hyperglycemia. *Metabolism* 63:1577-1586.
27. Apovian CM, Bigornia S, Mott M, et al. 2008. Adipose macrophage infiltration is associated with insulin resistance and vascular endothelial dysfunction in obese subjects. *Arterioscler Thromb Vasc Biol* 28:1654-1659.
28. van Beek L, Lips MA, Visser A, et al. 2014. Increased systemic and adipose tissue inflammation differentiates obese women with T2DM from obese women with normal glucose tolerance. *Metabolism* 63:492-501.
29. Gierman LM, van der Ham F, Koudijs A, et al. 2012. Metabolic stress-induced inflammation plays a major role in the development of osteoarthritis in mice. *Arthritis Rheum* 64:1172-1181.
30. Wei W, Clockaerts S, Bastiaansen-Jenniskens YM, et al. 2014. Statins and fibrates do not affect development of spontaneous cartilage damage in STR/Ort mice. *Osteoarthritis Cartilage* 22:293-301.
31. Howard JS, Mattacola CG, Romine SE, et al. 2010. Continuous Passive Motion, Early Weight Bearing, and Active Motion following Knee Articular Cartilage Repair: Evidence for Clinical Practice. *Cartilage* 1:276-286.
32. Laplante M, Sabatini DM. 2009. mTOR signaling at a glance. *J Cell Sci* 122:3589-3594.
33. Zhang Y, Vasheghani F, Li YH, et al. 2015. Cartilage-specific deletion of mTOR upregulates autophagy and protects mice from osteoarthritis. *Ann Rheum Dis* 74:1432-1440.
34. Bush JR, Berube NG, Beier F. 2015. A new prescription for growth? Statins, cholesterol and cartilage homeostasis. *Osteoarthritis Cartilage* 23:503-506.
35. Zhang H, Lin CY. 2008. Simvastatin stimulates chondrogenic phenotype of intervertebral disc cells partially through BMP-2 pathway. *Spine (Phila Pa 1976)* 33:E525-531.
36. Peister A, Mellad JA, Larson BL, et al. 2004. Adult stem cells from bone marrow (MSCs) isolated from different strains of inbred mice vary in surface epitopes, rates of proliferation, and differentiation potential. *Blood* 103:1662-1668.

EPILOGUE



CHAPTER 8

Summary and general discussion

SUMMARY AND GENERAL DISCUSSION

The most characteristic changes in obesity are an increase in adipose tissue mass and adipose tissue inflammation. This in turn leads to increased loading of the joints and systemic metabolic and inflammatory changes. Because adipose tissue is a major contributor to the inflammation in obesity, we have focused on the effect of adipose tissue on different tissue in the knee joint and cartilage repair.

LOCAL EFFECTS OF ADIPOSE TISSUE

The infrapatellar fat pad, an adipose tissue not changed by obesity

The infrapatellar fat pad (IPFP) is an intra-articular adipose tissue in direct contact with the synovium membrane and can therefore influence the knee joint environment. It can play an role in biomechanics of the knee, act as a shock absorber and is a reservoir of inflammatory and regenerative cells¹⁻³. Adipose tissue in general functions as a reservoir for excess nutrients and increases in size in obesity. However, MRI studies suggest that, unlike most other adipose tissues in the body, IPFP size is not correlated to body mass index (BMI)^{4,6}. Furthermore, unlike in subcutaneous and visceral adipose tissue, the adipocyte size in osteoarthritic (OA) IPFP was not correlated to BMI (**Chapter 2**). Besides adipocyte hypertrophy, an increased infiltration of pro-inflammatory macrophages and formation of crown like structures in adipose tissue are generally considered to be characteristics for obesity⁷. However, we could not detect a difference in macrophage infiltration in IPFP between obese and non-obese donors in our previous work⁸ nor in **Chapter 4**. An in-vivo study in high fat diet fed C57BL/6 mice has confirmed our finding that adipocyte size and infiltration of macrophages are not changed by weight gain⁹.

Obesity increases secretion of pro-inflammatory factors such as TNF α , IL1 β , MCP-1, IL6 and leptin by adipose tissue¹⁰. However, we have previously shown by multiplex ELISA analysis that secretion of cytokines by OA IPFP is not associated to BMI¹¹. Finally, all the effects the IPFP had on cartilage, synovial fibroblasts and MSCs were not correlated to BMI (**Chapter 3 and 4**)⁸. This all suggests that IPFP, unlike subcutaneous and visceral adipose tissue, is not influenced by obesity.

The IPFP and inflammation

Although the IPFP seems not to be influenced by obesity, it could still become inflamed after joint trauma and surgery¹²⁻¹⁴. Inflammatory cytokines such as IL1 β can increase the secretion of inflammatory factors by IPFP¹¹. With more inflammatory stimuli, there is an increased secretion of inflammatory factors by the IPFP.

Because the synovium does not have a basal membrane, the only barrier for molecules between the synovial fluid and the IPFP is the extracellular matrix (ECM) of the synovial interstitium. In this case, the smaller the molecule, the easier it can freely diffuse through the synovial interstitium¹⁵. We investigated in **Chapter 4** the effect of IPFP secreted factors on cartilage repair, and found that they could inhibit MSC-based cartilage repair. Next to directly influencing the repair process, factors secreted by IPFP also influence the synovium membrane by stimulating pro-fibrotic processes (**Chapter 3**) and pro-catabolic processes in synovial fibroblasts¹⁶ (**Chapter 5**). In turn, this can lead to an increase in inflammatory factors in the synovial fluid and further deterioration of the joint environment for repair. Studies have shown an increased amount of pro-inflammatory cytokines such as IL1 α / β , IL6, IL8, and TNF α , in synovial fluids of patients with focal cartilage defects^{17; 18}, ACL rupture¹⁹⁻²¹ or OA²² knees compared to healthy knees. Pro-inflammatory cytokines such as IL1 α / β , IL6, IL17, IFN γ , TNF α , MCP1 can all inhibit MSC chondrogenesis²³⁻²⁶ and increase catabolic processes in the synovium and cartilage²⁷. Reduction of the secretion of these cytokines by the IPFP or inhibiting the effects of these cytokines could be promising strategies to improve the joint environment and cartilage repair. One should be careful however with inhibition of inflammation. Studies in MRL/MpJ mice, who possess super healing capacities, have shown that inflammation is necessary for successful wound healing^{28; 29}. Finding the right balance between sufficient inflammation to initiate wound healing and reduce chronic inflammation to inhibit catabolic processes is necessary for successful cartilage repair.

The IPFP consists mainly of adipocytes, stem cells and inflammatory cells such as macrophages. In **Chapter 4** we have shown that pro-inflammatory macrophages in IPFP contribute to the anti-chondrogenic effect of IPFP. Macrophages play an important role in inflammation and tissue repair. Pro-inflammatory macrophages secrete TNF α , IL1 β and IL6³⁰ and could therefore inhibit cartilage repair in vitro, induce catabolic processes in cartilage³¹ and pro-fibrotic processes in synovial fibroblasts (**Addendum figure 1**). An animal study reports that ablation of all synovial macrophages could inhibit development of OA³². Anti-inflammatory macrophages however, do not inhibit cartilage repair (**Chapter 4**)³³ and might be even beneficial to cartilage repair in vitro³⁴. Furthermore, Axolotls, which are known to be able to regenerate limbs, cannot regenerate without the presence of macrophages³⁵. The right balance between pro- and anti-inflammatory macrophages seems to be crucial for successful cartilage repair. In **Chapter 5** we used different medications to modulate the macrophages inside the IPFP towards a more anti-inflammatory phenotype. Of the medications we tested, only triamcinolone acetonide (TAA) was

able to reduce inflammation in IPFP and modulate the macrophages towards a anti-inflammatory phenotype. The anti-chondrogenic and pro-catabolic effects of the IPFP were also reduced by TAA. This suggests that modulation of macrophage phenotype by medication might improve the joint environment to reduce joint disease and be better suitable for cartilage repair.

Although the adipocyte size, macrophage phenotype in and the secretion of inflammatory cytokines by IPFP are not influenced by obesity, the IPFP remains a large source of inflammatory factors that affects the joint environment. Next to inflammatory cytokines, the adipocytes in IPFP secrete many adipokines such as leptin³⁶, adiponectin³⁶, resistin and visfatin¹¹. Leptin, resistin and visfatin stimulates catabolic processes in cartilage¹, synovium¹ and meniscus³⁷. The role of adiponectin is not yet fully understood. Adiponectin increases ATDC5-cell proliferation and chondrogenesis³⁸, however it is also associated with cartilage damage in OA and could increase MMP13 activity and PGE₂ release in OA chondrocytes³⁹. However blocking adiponectin and leptin did not inhibit the pro-catabolic effects of IPFP on OA chondrocytes and synovial fibroblasts³⁶. The effect of these adipokines on MSC chondrogenesis is still unknown, but reduction of catabolic processes in general would eventually benefit the joint environment. Glucocorticoids modulate adipokines secretion by adipose tissue⁴⁰⁻⁴². Therefore, the reduction of catabolic processes in **Chapter 5** by treatment with TAA could also have taken place via modulation of adipokine secretion by the IPFP, next to modulation of macrophages and their secretion profile.

The IPFP and adipocytes also release prostaglandins. Prostaglandins are a group of lipids that play an important role in inflammation⁴³, cartilage metabolism^{44,45} and pathogenesis of OA^{46,47}. In **Chapter 3** we describe that prostaglandin F_{2α} (PGF_{2α}) secreted by IPFP is involved in pro-fibrotic processes in synovial fibroblasts. However, PGF_{2α} does not inhibit MSC chondrogenesis (**Addendum figure 2**), but even enhances chondrogenesis in ATDC5 cells⁴⁵ and matrix deposition by articular chondrocytes⁴⁴. Next to PGF_{2α}, the IPFP also secretes prostaglandin E₂ (PGE₂)^{48,49}, which stimulates pro-catabolic processes in synovial fibroblasts⁴⁸. Inhibition of prostaglandin secretion is possible through inhibition of cyclooxygenase (COX) activity. Non-specific COX inhibitors such as non-steroid anti-inflammatory drugs (NSAIDs) and specific COX-2 inhibitors such as celecoxib are already clinically used to reduce inflammation and the symptoms of OA. Although COX inhibition could be beneficial to reduce pro-fibrotic and catabolic processes⁴⁷, non-specific COX-inhibition also inhibits MSC chondrogenesis⁵⁰. On the other hand, a specific COX-2 inhibitor is less detrimental to chondrogenesis⁵⁰⁻⁵². Therefore, specific COX-2

inhibitors such as celecoxib are possible candidates to improve the joint environment for cartilage repair. Surprisingly, celecoxib did not reduce IPFP inflammatory genes expression in **Chapter 5** and because reduction of general IPFP inflammation is important to improve the joint environment, we did not further investigate the effects of celecoxib on cartilage repair. In **Chapter 5** we demonstrated a reduction in anti-chondrogenic and pro-catabolic effects of IPFP after treatment with TAA. TAA is an often used glucocorticoid and glucocorticoids are known to inhibit prostaglandin synthesis⁵³. However, it also inhibits other pro-inflammatory pathways and therefore targeting prostaglandin synthesis alone might be insufficient to improve the joint environment for cartilage repair.

Next to prostaglandins, there are also other lipids in the synovial fluid of the knee joint^{49;54}. One group of lipids are the fatty acids and these fatty acids are being extensively studied. Fatty acids can stimulate or inhibit inflammatory processes⁵⁵ and influence cartilage loss in OA cartilage⁵⁶. An increased intake of omega-3 fatty acids could decrease chronic inflammation⁵⁷ and dietary fatty content could regulate wound healing in mice⁵⁸. It is therefore interesting to investigate whether changing diet is a possible strategy to modulate IPFP inflammation and thereby improve cartilage repair procedures. Furthermore, future research could be focused on using medications to modify the levels of specific types of fatty acids and in that way influence cartilage repair. In **Chapter 5** we used statins and fibrates, two often used serum lipid lowering drugs, to reduce IPFP inflammation. However, we did not see an effect on IPFP inflammatory genes expression. These medications are known to reduce systemic inflammation so they could still be useful in improving the general joint health during cartilage repair procedures, although more investigation is necessary.

Removal of the IPFP

Instead of modulation of the IPFP, it is also possible to surgically remove the IPFP². During total knee arthroplasty, the IPFP is often removed to improve visibility during the surgical procedure^{59;60}. However the removal of the IPFP during total knee arthroplasty is under debate⁶¹ because it is associated with shortened patellar tendon and anterior knee pain. Even subtotal removal of the IPFP with arthroscopy could lead to patellar tendon shortening^{60;62-64}. This supports the theory that the IPFP has a mechanical function that is necessary for proper joint movement.

Besides adipocytes and macrophages, there are also MSCs in the IPFP⁶⁵⁻⁶⁷. These MSCs have been shown to have chondrogenic^{66;67} as well as immunomodulatory⁶⁸ capacities and some authors have proposed to use these MSCs in MSC-based

cartilage repair procedures^{66;69}. It might also be possible that MSCs from the IPFP migrate to a cartilage defect and contribute to repair, although currently there is no study that have shown this. MSCs from the bone marrow⁷⁰ and synovial membrane⁷¹ could migrate towards a cartilage defect. Peripheral mononucleated cells migrate from the blood circulation to a cartilage defect in rats⁷², so future research might show that MSCs from IPFP could also do this.

Furthermore, we have previously shown that OA IPFP conditioned medium inhibits catabolic mediators in bovine cartilage⁸. This means that the effect of IPFP on the separate joint structures could be different. Hence, complete removal of the IPFP could change the joint environment too much and remove the beneficial cells in the IPFP that might contribute to successful cartilage repair in the knee.

Other intra-articular adipose tissues

Most synovial joints have adipose tissue filling the synovial folds around the articular margin. These fat depots possibly act as cushions during joint movement⁷³. Although the IPFP is the largest intra-articular adipose tissue, it is not the only one in the knee. In the knee there are also the supra-patellar fat pad, located beneath the quadriceps tendon^{74;75}, and the pre-femoral fat pad, located at the anterior side of the femur. Signal alterations on MRI of these fat pads are associated to synovitis, anterior knee pain and structural abnormalities^{74;76;77}. Due to their proximity to the IPFP and because they are in contact with the same synovial fluid, it might be expected that the same inflammatory signals that would influence the IPFP would also influence these fat pad depots.

Besides the knee, the ankle and the hip also have an intra-articular adipose tissue. In the ankle it is called the Kager's fat pad and is located posterior to the ankle joint, anterior to the Achilles tendon⁷⁸. The Kager's fat pad is also known as the pre-Achilles fat pad. Trauma to the calcaneus or Achilles tendinopathy can influence the Kager's fat pad^{78;79}. The intra-articular adipose tissue in the hip has only been recently described⁸⁰ and is similar to the IPFP in tissular phenotype⁸¹. Not much is known about this adipose tissue, but it can become impinged and cause pain during hip movement⁸⁰.

With more understanding of the role of these other intra-articular adipose tissues, we might improve our understanding of the role of the IPFP in the knee joint. Furthermore, these other intra-articular adipose tissue might also be targeted to modify the joint environment.

SYSTEMIC EFFECTS OF ADIPOSE TISSUE

Besides the local effects of adipose tissue on joint disease and repair, the systemic effects has also been a focus of investigation. Especially the systemic changes that occur in obesity is being extensively studied. Obesity increases the chance of developing the metabolic syndrome, which is characterized by low grade systemic inflammation, dyslipidemia, hyperinsulinemia and hyperglycemia. Metabolic syndrome has been shown to be a risk factor for the development of OA^{82, 83}. Obesity and the resulting metabolic syndrome are caused by an interplay between behavioral, environmental and genetic factors^{84, 85}. Although our work suggests that the IPFP is possibly not influenced by obesity, subcutaneous and visceral adipose tissues become inflamed due to obesity⁸⁶. In adipose tissue inflammation, there is more infiltration of pro-inflammatory macrophages, formation of crown like structures and there is an increase in secretion of inflammatory factors such as TNF α , IL1 β , MCP-1, IL6 and leptin⁸⁶. To investigate the effect of metabolic and inflammatory systemic changes on joint disease and cartilage repair, we performed two in-vivo studies with mice.

Obesity related metabolic and inflammatory changes on cartilage damage

In **Chapter 6** we used the STR/Ort strain of mice. These mice develop metabolic and inflammatory changes spontaneously on a normal diet (**Chapter 6**,⁸⁷). This is not caused by overeating as compared to the OB/OB strain of mice, which due to their leptin deficiency, does not stop eating⁸⁸. Next to developing spontaneous metabolic syndrome⁸⁹, male STR/Ort mice are also known to develop spontaneous cartilage damage⁹⁰. This mouse model therefore seemed to us very well suited to investigate whether development of spontaneous metabolic syndrome and cartilage damage are linked and whether cartilage damage could be prevented. In **Chapter 6** we fed male STR/Ort mice chow mixed with simvastatin and fenofibrate. These two lipid lowering medications are commonly used to treat dyslipidemia and to reduce cardiovascular morbidity and mortality^{91,92}. Statin use has been associated with decreased incidence and progression of knee OA⁹³. Furthermore, statins and fibrates also reduce systemic inflammation^{94,95}. In **Chapter 5** we have shown that statins and fibrates did not reduce IPFP inflammation, suggesting that these medications might only have systemic effects. In our in-vivo study, The STR/Ort mice developed dyslipidaemia and simvastatin and fenofibrate did not have an effect on dyslipidaemia in these mice. Fenofibrate reduced weight, systemic inflammation and volume of subchondral bone, whereas simvastatin did not have an effect. However, in contrast to what we expected, cartilage damage was not reduced by these two medications. Our results suggest that development of car-

tilage damage in STR/Ort mice is not primarily linked to metabolic inflammation, but is multi-factorial. This shows that a combination of metabolic inflammatory changes and genetic predisposition are the cause of cartilage damage in these mice. This also suggest that being obese does not always lead to cartilage damage.

Obesity and cartilage repair

When cartilage damage have occurred in obese patients, we need to repair it to prevent the development of OA. The clinical results of cartilage repair in obese patients is worse, but there is no information on the structural outcomes. In **Chapter 7** we investigated whether a high fat diet (HFD) induced obesity reduces cartilage repair in DBA/1 mice. Surprisingly, the HFD did not negatively influence cartilage repair, but even accelerated it. This was in contrast to common knowledge and what we hypothesized. Furthermore, although these mice are known to be resistant to OA development after cartilage damage, they did not even develop OA after cartilage damage in combination with a HFD. The DBA/1 mice on a HFD gained weight, but did not have serum inflammatory and metabolic changes. Furthermore, the subcutaneous adipocytes of these mice on a HFD became hypertrophic, but there was no increased infiltration of macrophages nor formation of crown like structures. This is in stark contrast to the STR/Ort mice we used in **Chapter 6**, which developed metabolic and inflammatory changes spontaneously. This suggests that resistance to HFD induced inflammatory and metabolic changes is associated with accelerated cartilage repair and reduced OA susceptibility. In humans, some individuals are prone to development of metabolic syndrome⁸⁴, but some also gain weight and become obese, but do not develop the accompanying metabolic and inflammatory changes. This group of obese individuals, also known as the metabolic healthy obese, are often characterized by less serum inflammation, less visceral fat, less macrophage infiltration in adipose tissue and less adipocyte hypertrophy^{96;97}. It remains inconclusive whether the risk of cardiovascular heart disease is different in this group of individuals⁹⁷ compared to obese individuals with metabolic changes. Furthermore, it is unknown whether these individuals are protected from joint disease or have improved repair capabilities. Future research investigating whether these individuals are protected against joint disease or have improved repair might provide us with new treatment targets.

The results of our two in-vivo studies indicate that the link between obesity related metabolic and inflammatory changes, degenerative joint disease and cartilage repair is complex. Furthermore, there is heterogeneity in individuals who are obese. A study by Green et al has shown that there are multiple types of obese individuals, who all have their specific causes for obesity and related diseases⁹⁸.

The authors have concluded that treatment strategies for obesity should not target obese individuals as a whole, but subgroup specific strategies should be used. To better understand how obesity influences the joint, it is therefore important to take into account this heterogeneity of obesity. Repetition of our in-vivo studies using different animal models should take this heterogeneity into account.

FUTURE PERSPECTIVES

Obesity, adipose tissue and the joint environment

Adipose tissue is not only a storage site for excess energy, but is also an endocrine organ, which secretes large amounts of immunological, endocrine and hormonal factors. Adipose tissue inflammation plays an important role in the pathophysiology of metabolic dysregulation in obesity. Much is known about the changes that occur in subcutaneous and visceral adipose tissue in obesity. Less is known, however, about obesity related changes in intra-articular adipose tissue. Obesity is a well-known risk factor for joint diseases and has been extensively studied in animal and clinical studies. Due to the intra-articular location of IPFP, it has long been thought that the IPFP would play an important role in obesity associated joint inflammation. However, we have shown that the IPFP might not be influenced by obesity and that obesity causes degenerative joint diseases via other pathways and not via IPFP inflammation. This could be through increased systemic inflammation or metabolic dysregulation due to inflammation of the bigger subcutaneous and visceral adipose tissue depots.

However, the effects of obesity could vary between individuals. We have now shown in animal studies that obesity is not always negative or the relationship between the changes caused by obesity on degenerative joint disease is not always completely clear. The obesity epidemic will only increase in the future and research will continue in this field. New targets for strategies to improve the joint environment in obesity might be found in research focusing on subgroups of individuals who are less susceptible to developing obesity related changes. It would be interesting to investigate whether these individuals are also protected against joint diseases.

Modulation of the infrapatellar fat pad to improve the joint environment for cartilage repair

Irrespectively to the effects of adipose tissue related systemic changes have on the local joint environment, the IPFP secretes a large amount of different adipokines and fatty acids. These individual factors might have anabolic or catabolic effects on

different joint structures. With in-vitro experiments using IPFP conditioned medium, we have shown what the effects are of IPFP secreted factors on the joint. Furthermore, we have shown that we can modulate in-vitro the secretion of factors by the IPFP and the resident macrophages with a commonly used glucocorticoid. The next step could be an in-vivo animal study to test the hypothesis that using TAA the IPFP can be modulated to be beneficial for the joint environment. Most experimental studies on the effect of inflammatory modulation on joint disease are first performed in rodents. However, due to the small size of the rodent knee, specific targeting the IPFP is difficult, although not impossible. Future experiments using canine or ovine models could be considered to investigate whether IPFP modulation would be feasible to improve the joint environment for cartilage repair. It would also be possible to directly perform a human study, because TAA is currently already injected intra-articularly as an anti-inflammatory treatment. The next step would only be injection of a dosage of TAA in the IPFP following microfracture surgery.

Currently, the effect of different intra-articular strategies using pharmacological drugs and immuno modulator cells is being studied for use to improve the joint environment for cartilage repair or directly influence cartilage repair itself⁹⁹. Next to the effect on cartilage repair, the effect of these intra-articular strategies on synovium is also important. The synovium can become inflamed and is a source of catabolic and anti-chondrogenic factors. On the other hand, with the experiments performed in this thesis, we have shown that the IPFP is an important tissue in the joint environment as well. The IPFP can stimulate catabolic processes in the synovium, although this could also be vice-versa, where synovium inflammation could stimulate catabolic processes in the IPFP. Nevertheless, it is possible that any future intra-articular therapy administered could influence the IPFP and via the IPFP influence the synovium. Therefore, IPFP changes should be carefully monitored during experimental treatments and reduction of inflammation in the IPFP could be considered as one of the secondary outcomes.

Concluding remarks

In conclusion, this thesis shows that the IPFP is not an ordinary adipose tissue and that it secretes specific factors that locally influence the knee joint and cartilage repair. In the future, it is possible to use medication to specifically modulate the IPFP to improve the joint environment for cartilage repair. Furthermore, this thesis provides evidence that there is variability in how obesity related systemic effects can affect degenerative joint disease and cartilage repair. Future studies on the relationship between obesity, adipose tissue and cartilage repair could focus on this variability to uncover novel therapeutic targets.

REFERENCES

1. Clockaerts S, Bastiaansen-Jenniskens YM, Runhaar J, et al. 2010. The infrapatellar fat pad should be considered as an active osteoarthritic joint tissue: a narrative review. *Osteoarthritis Cartilage* 18:876-882.
2. Dragoo JL, Johnson C, McConnell J. 2012. Evaluation and treatment of disorders of the infrapatellar fat pad. *Sports Med* 42:51-67.
3. Fontanella CG, Carniel EL, Frigo A, et al. 2016. Investigation of biomechanical response of Hoffa's fat pad and comparative characterization. *J Mech Behav Biomed Mater* 67:1-9.
4. Cai J, Xu J, Wang K, et al. 2015. Association Between Infrapatellar Fat Pad Volume and Knee Structural Changes in Patients with Knee Osteoarthritis. *J Rheumatol* 42:1878-1884.
5. Chuckpaiwong B, Charles HC, Kraus VB, et al. 2010. Age-associated increases in the size of the infrapatellar fat pad in knee osteoarthritis as measured by 3T MRI. *J Orthop Res* 28:1149-1154.
6. Duran S, Aksahin E, Kocadal O, et al. 2015. Effects of body mass index, infrapatellar fat pad volume and age on patellar cartilage defect. *Acta Orthop Belg* 81:41-46.
7. Apovian CM, Bigornia S, Mott M, et al. 2008. Adipose macrophage infiltration is associated with insulin resistance and vascular endothelial dysfunction in obese subjects. *Arterioscler Thromb Vasc Biol* 28:1654-1659.
8. Bastiaansen-Jenniskens YM, Clockaerts S, Feijt C, et al. 2012. Infrapatellar fat pad of patients with end-stage osteoarthritis inhibits catabolic mediators in cartilage. *Ann Rheum Dis* 71:288-294.
9. Chang W DC, Kent C, Kovats S, Garteiser P, Doblus S, Towner R, Griffin TM. 2011. Infrapatellar fat pad hypertrophy without inflammation in a diet-induced mouse model of obesity and osteoarthritis. *Osteoarthritis Cartilage* 19:S53-S236.
10. Grant RW, Dixit VD. 2015. Adipose tissue as an immunological organ. *Obesity (Silver Spring)* 23:512-518.
11. Clockaerts S, Bastiaansen-Jenniskens YM, Feijt C, et al. 2012. Cytokine production by infrapatellar fat pad can be stimulated by interleukin 1beta and inhibited by peroxisome proliferator activated receptor alpha agonist. *Ann Rheum Dis* 71:1012-1018.
12. Abreu MR, Chung CB, Trudell D, et al. 2008. Hoffa's fat pad injuries and their relationship with anterior cruciate ligament tears: new observations based on MR imaging in patients and MR imaging and anatomic correlation in cadavers. *Skeletal Radiol* 37:301-306.
13. Gandhi R, Takahashi M, Virtanen C, et al. 2011. Microarray analysis of the infrapatellar fat pad in knee osteoarthritis: relationship with joint inflammation. *J Rheumatol* 38:1966-1972.
14. Solbak NM, Heard BJ, Achari Y, et al. 2015. Alterations in Hoffa's fat pad induced by an inflammatory response following idealized anterior cruciate ligament surgery. *Inflamm Res* 64:615-626.
15. Evans CH, Kraus VB, Setton LA. 2014. Progress in intra-articular therapy. *Nat Rev Rheumatol* 10:11-22.
16. Eymard F, Pigenet A, Citadelle D, et al. 2017. Knee and hip intra-articular adipose tissues (IAATs) compared with autologous subcutaneous adipose tissue: a specific phenotype for a central player in osteoarthritis. *Ann Rheum Dis*.
17. Tsuchida AI, Beekhuizen M, Rutgers M, et al. 2012. Interleukin-6 is elevated in synovial fluid of patients with focal cartilage defects and stimulates cartilage matrix production in an in vitro regeneration model. *Arthritis Res Ther* 14:R262.
18. Tsuchida AI, Beekhuizen M, Hart MC, et al. 2014. Cytokine profiles in the joint depend on pathology, but are different between synovial fluid, cartilage tissue and cultured chondrocytes. *Arthritis Res Ther* 16:441.

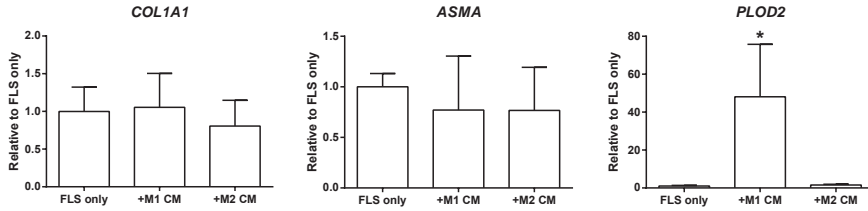
19. Bigoni M, Sacerdote P, Turati M, et al. 2013. Acute and late changes in intraarticular cytokine levels following anterior cruciate ligament injury. *J Orthop Res* 31:315-321.
20. Irie K, Uchiyama E, Iwaso H. 2003. Intraarticular inflammatory cytokines in acute anterior cruciate ligament injured knee. *Knee* 10:93-96.
21. Marks PH, Donaldson ML. 2005. Inflammatory cytokine profiles associated with chondral damage in the anterior cruciate ligament-deficient knee. *Arthroscopy* 21:1342-1347.
22. Beekhuizen M, Gierman LM, van Spil WE, et al. 2013. An explorative study comparing levels of soluble mediators in control and osteoarthritic synovial fluid. *Osteoarthritis Cartilage* 21:918-922.
23. Harris Q, Seto J, O'Brien K, et al. 2013. Monocyte chemotactic protein-1 inhibits chondrogenesis of synovial mesenchymal progenitor cells: an in vitro study. *Stem Cells* 31:2253-2265.
24. Jagielski M, Wolf J, Marzahn U, et al. 2014. The influence of IL-10 and TNFalpha on chondrogenesis of human mesenchymal stromal cells in three-dimensional cultures. *Int J Mol Sci* 15:15821-15844.
25. Kondo M, Yamaoka K, Tanaka Y. 2014. Acquiring chondrocyte phenotype from human mesenchymal stem cells under inflammatory conditions. *Int J Mol Sci* 15:21270-21285.
26. Wei H, Shen G, Deng X, et al. 2013. The role of IL-6 in bone marrow (BM)-derived mesenchymal stem cells (MSCs) proliferation and chondrogenesis. *Cell Tissue Bank* 14:699-706.
27. Lieberthal J, Sambamurthy N, Scanzello CR. 2015. Inflammation in joint injury and post-traumatic osteoarthritis. *Osteoarthritis Cartilage* 23:1825-1834.
28. Canhamero T, Garcia LV, De Franco M. 2014. Acute Inflammation Loci Are Involved in Wound Healing in the Mouse Ear Punch Model. *Adv Wound Care (New Rochelle)* 3:582-591.
29. Gourevitch D, Kossenkova AV, Zhang Y, et al. 2014. Inflammation and Its Correlates in Regenerative Wound Healing: An Alternate Perspective. *Adv Wound Care (New Rochelle)* 3:592-603.
30. Mosser DM, Edwards JP. 2008. Exploring the full spectrum of macrophage activation. *Nat Rev Immunol* 8:958-969.
31. Utomo L, Bastiaansen-Jenniskens YM, Verhaar JA, et al. 2016. Cartilage inflammation and degeneration is enhanced by pro-inflammatory (M1) macrophages in vitro, but not inhibited directly by anti-inflammatory (M2) macrophages. *Osteoarthritis Cartilage* 24:2162-2170.
32. Blom AB, van Lent PL, Libregts S, et al. 2007. Crucial role of macrophages in matrix metalloproteinase-mediated cartilage destruction during experimental osteoarthritis: involvement of matrix metalloproteinase 3. *Arthritis Rheum* 56:147-157.
33. Fahy N, de Vries-van Melle ML, Lehmann J, et al. 2014. Human osteoarthritic synovium impacts chondrogenic differentiation of mesenchymal stem cells via macrophage polarisation state. *Osteoarthritis Cartilage* 22:1167-1175.
34. Sesia SB, Duhr R, Medeiros da Cunha C, et al. 2015. Anti-inflammatory/tissue repair macrophages enhance the cartilage-forming capacity of human bone marrow-derived mesenchymal stromal cells. *J Cell Physiol* 230:1258-1269.
35. Godwin JW, Pinto AR, Rosenthal NA. 2013. Macrophages are required for adult salamander limb regeneration. *Proc Natl Acad Sci U S A* 110:9415-9420.
36. Gross JB, Guillaume C, Gegout-Pottier P, et al. 2016. The infrapatellar fat pad induces inflammatory and degradative effects in articular cells but not through leptin or adiponectin. *Clin Exp Rheumatol*.
37. Nishimuta JF, Levenston ME. 2015. Meniscus is more susceptible than cartilage to catabolic and anti-anabolic effects of adipokines. *Osteoarthritis Cartilage* 23:1551-1562.
38. Challa TD, Rais Y, Ornan EM. 2010. Effect of adiponectin on ATDC5 proliferation, differentiation and signaling pathways. *Mol Cell Endocrinol* 323:282-291.
39. Francin PJ, Abot A, Guillaume C, et al. 2014. Association between adiponectin and cartilage degradation in human osteoarthritis. *Osteoarthritis Cartilage* 22:519-526.

40. Fain JN, Madan AK, Hiler ML, et al. 2004. Comparison of the release of adipokines by adipose tissue, adipose tissue matrix, and adipocytes from visceral and subcutaneous abdominal adipose tissues of obese humans. *Endocrinology* 145:2273-2282.
41. Fardet L, Antuna-Puente B, Vazier C, et al. 2013. Adipokine profile in glucocorticoid-treated patients: baseline plasma leptin level predicts occurrence of lipodystrophy. *Clin Endocrinol (Oxf)* 78:43-51.
42. Heard BJ, Solbak NM, Chung M, et al. 2016. The infrapatellar fat pad is affected by injury induced inflammation in the rabbit knee: use of dexamethasone to mitigate damage. *Inflamm Res* 65:459-470.
43. Ricciotti E, FitzGerald GA. 2011. Prostaglandins and inflammation. *Arterioscler Thromb Vasc Biol* 31:986-1000.
44. Jakob M, Demartean O, Suetterlin R, et al. 2004. Chondrogenesis of expanded adult human articular chondrocytes is enhanced by specific prostaglandins. *Rheumatology (Oxford)* 43:852-857.
45. Kim J, Shim M. 2015. Prostaglandin F2alpha receptor (FP) signaling regulates Bmp signaling and promotes chondrocyte differentiation. *Biochim Biophys Acta* 1853:500-512.
46. Attur M, Al-Mussawir HE, Patel J, et al. 2008. Prostaglandin E2 exerts catabolic effects in osteoarthritis cartilage: evidence for signaling via the EP4 receptor. *J Immunol* 181:5082-5088.
47. Zweers MC, de Boer TN, van Roon J, et al. 2011. Celecoxib: considerations regarding its potential disease-modifying properties in osteoarthritis. *Arthritis Res Ther* 13:239.
48. Eymard F, Pigenet A, Citadelle D, et al. 2014. Induction of an inflammatory and prodegradative phenotype in autologous fibroblast-like synoviocytes by the infrapatellar fat pad from patients with knee osteoarthritis. *Arthritis Rheumatol* 66:2165-2174.
49. Gierman LM, Wopereis S, van El B, et al. 2013. Metabolic profiling reveals differences in concentrations of oxylipins and fatty acids secreted by the infrapatellar fat pad of donors with end-stage osteoarthritis and normal donors. *Arthritis Rheum* 65:2606-2614.
50. Pountos I, Giannoudis PV, Jones E, et al. 2011. NSAIDs inhibit in vitro MSC chondrogenesis but not osteogenesis: implications for mechanism of bone formation inhibition in man. *J Cell Mol Med* 15:525-534.
51. Welting TJ, Caron MM, Emans PJ, et al. 2011. Inhibition of cyclooxygenase-2 impacts chondrocyte hypertrophic differentiation during endochondral ossification. *Eur Cell Mater* 22:420-436; discussion 436-427.
52. Caron MM, Emans PJ, Sanen K, et al. 2016. The Role of Prostaglandins and COX-Enzymes in Chondrogenic Differentiation of ATDC5 Progenitor Cells. *PLoS One* 11:e0153162.
53. Goppelt-Strube M, Wolter D, Resch K. 1989. Glucocorticoids inhibit prostaglandin synthesis not only at the level of phospholipase A2 but also at the level of cyclo-oxygenase/PGE isomerase. *Br J Pharmacol* 98:1287-1295.
54. Kim IC, Cohen AS. 1966. Synovial fluid fatty acid composition in patients with rheumatoid arthritis, gout and degenerative joint disease. *Proc Soc Exp Biol Med* 123:77-80.
55. Soto-Vaca A, Losso JN, McDonough K, et al. 2013. Differential effect of 14 free fatty acids in the expression of inflammation markers on human arterial coronary cells. *J Agric Food Chem* 61:10074-10079.
56. Bastiaansen-Jenniskens YM, Siawash M, van de Lest CH, et al. 2013. Monounsaturated and Saturated, but Not n-6 Polyunsaturated Fatty Acids Decrease Cartilage Destruction under Inflammatory Conditions: A Preliminary Study. *Cartilage* 4:321-328.
57. Simopoulos AP. 2002. Omega-3 fatty acids in inflammation and autoimmune diseases. *J Am Coll Nutr* 21:495-505.
58. Wu CL, Jain D, McNeill JN, et al. 2015. Dietary fatty acid content regulates wound repair and the pathogenesis of osteoarthritis following joint injury. *Ann Rheum Dis* 74:2076-2083.

59. Van Beeck A, Clockaerts S, Somville J, et al. 2013. Does infrapatellar fat pad resection in total knee arthroplasty impair clinical outcome? A systematic review. *Knee* 20:226-231.
60. White L, Holyoak R, Sant J, et al. 2016. The effect of infrapatellar fat pad resection on outcomes post-total knee arthroplasty: a systematic review. *Arch Orthop Trauma Surg* 136:701-708.
61. Bos PK. 2014. CORR Insights (R): The effect of infrapatellar fat pad excision on complications after minimally invasive TKA: a randomized controlled trial. *Clin Orthop Relat Res* 472:702-703.
62. Pinsornsak P, Naratrikun K, Chumchuen S. 2014. The effect of infrapatellar fat pad excision on complications after minimally invasive TKA: a randomized controlled trial. *Clin Orthop Relat Res* 472:695-701.
63. Takatoku K, Sekiya H, Hayashi M, et al. 2005. Influence of fat pad removal on patellar tendon length during growth. *Knee Surg Sports Traumatol Arthrosc* 13:706-713.
64. Ye C, Zhang W, Wu W, et al. 2016. Influence of the Infrapatellar Fat Pad Resection during Total Knee Arthroplasty: A Systematic Review and Meta-Analysis. *PLoS One* 11:e0163515.
65. Garcia J, Wright K, Roberts S, et al. 2016. Characterisation of synovial fluid and infrapatellar fat pad derived mesenchymal stromal cells: The influence of tissue source and inflammatory stimulus. *Sci Rep* 6:24295.
66. Neri S, Guidotti S, Lilli NL, et al. 2016. Infrapatellar fat pad-derived mesenchymal stromal cells from osteoarthritis patients: In vitro genetic stability and replicative senescence. *J Orthop Res*.
67. Wickham MQ, Erickson GR, Gimble JM, et al. 2003. Multipotent stromal cells derived from the infrapatellar fat pad of the knee. *Clin Orthop Relat Res*:196-212.
68. Maumus M, Manferdini C, Toupet K, et al. 2013. Adipose mesenchymal stem cells protect chondrocytes from degeneration associated with osteoarthritis. *Stem Cell Res* 11:834-844.
69. Tangchitphaisut P, Srikaew N, Numhom S, et al. 2016. Infrapatellar Fat Pad: An Alternative Source of Adipose-Derived Mesenchymal Stem Cells. *Arthritis* 2016:4019873.
70. Shapiro F, Koide S, Glimcher MJ. 1993. Cell origin and differentiation in the repair of full-thickness defects of articular cartilage. *J Bone Joint Surg Am* 75:532-553.
71. Hunziker EB, Rosenberg LC. 1996. Repair of partial-thickness defects in articular cartilage: cell recruitment from the synovial membrane. *J Bone Joint Surg Am* 78:721-733.
72. Okano T, Wakitani S, Okabe T, et al. 2014. Nucleated cells circulating in the peripheral blood contribute to the repair of osteochondral defects only in the early phase of healing. *J Tissue Eng Regen Med* 8:414-420.
73. Fontanella CG, Carniel EL, Frigo A, et al. 2017. Investigation of biomechanical response of Hoffa's fat pad and comparative characterization. *J Mech Behav Biomed Mater* 67:1-9.
74. Schweitzer ME, Falk A, Pathria M, et al. 1993. MR imaging of the knee: can changes in the intracapsular fat pads be used as a sign of synovial proliferation in the presence of an effusion? *AJR Am J Roentgenol* 160:823-826.
75. Staeubli HU, Bollmann C, Kreutz R, et al. 1999. Quantification of intact quadriceps tendon, quadriceps tendon insertion, and suprapatellar fat pad: MR arthrography, anatomy, and cryosections in the sagittal plane. *AJR Am J Roentgenol* 173:691-698.
76. Tsavalas N, Karantanas AH. 2013. Suprapatellar fat-pad mass effect: MRI findings and correlation with anterior knee pain. *AJR Am J Roentgenol* 200:W291-296.
77. Wang J, Han W, Wang X, et al. 2014. Mass effect and signal intensity alteration in the suprapatellar fat pad: associations with knee symptoms and structure. *Osteoarthritis Cartilage* 22:1619-1626.
78. Ly JQ, Bui-Mansfield LT. 2004. Anatomy of and abnormalities associated with Kager's fat Pad. *AJR Am J Roentgenol* 182:147-154.
79. Pingel J, Petersen MC, Fredberg U, et al. 2015. Inflammatory and Metabolic Alterations of Kager's Fat Pad in Chronic Achilles Tendinopathy. *PLoS One* 10:e0127811.

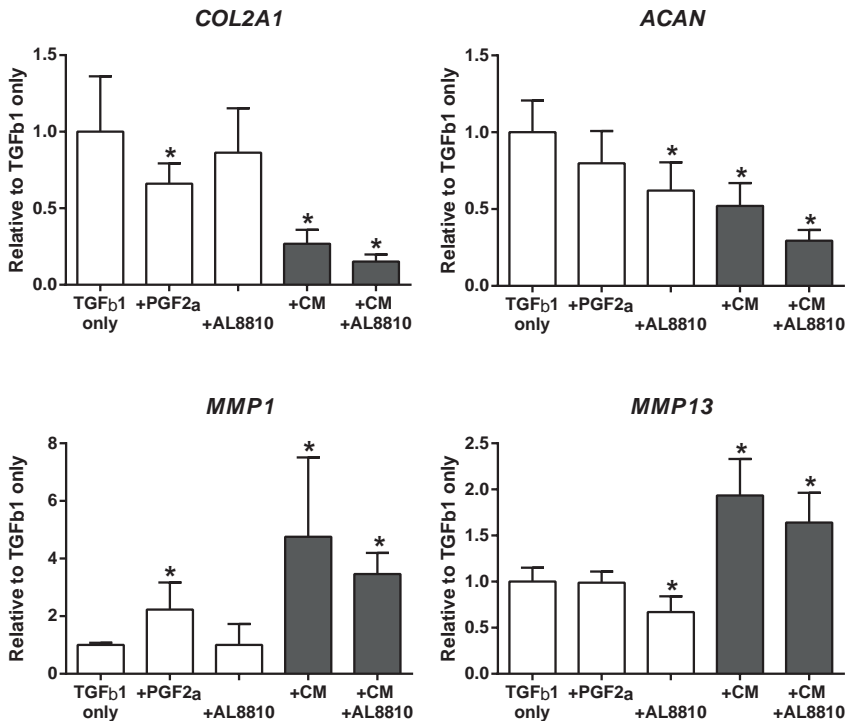
80. Jayasekera N, Aprato A, Villar RN. 2014. Fat pad entrapment at the hip: a new diagnosis. *PLoS One* 9:e83503.
81. Eymard F, Pigenet A, Citadelle D, et al. 2016. Knee and hip intra-articular adipose tissues share a common phenotype in osteoarthritis. *Osteoarthritis Cartilage* 24 (2016) S63-S534.
82. Berenbaum F, Griffin TM, Liu-Bryan R. 2017. Review: Metabolic Regulation of Inflammation in Osteoarthritis. *Arthritis Rheumatol* 69:9-21.
83. Zhuo Q, Yang W, Chen J, et al. 2012. Metabolic syndrome meets osteoarthritis. *Nat Rev Rheumatol* 8:729-737.
84. Albuquerque D, Stice E, Rodriguez-Lopez R, et al. 2015. Current review of genetics of human obesity: from molecular mechanisms to an evolutionary perspective. *Mol Genet Genomics* 290:1191-1221.
85. Bouchard C. 2007. The biological predisposition to obesity: beyond the thrifty genotype scenario. *Int J Obes (Lond)* 31:1337-1339.
86. Abranches MV, Oliveira FC, Conceicao LL, et al. 2015. Obesity and diabetes: the link between adipose tissue dysfunction and glucose homeostasis. *Nutr Res Rev* 28:121-132.
87. Uchida K, Satoh M, Inoue G, et al. 2015. CD11c(+) macrophages and levels of TNF-alpha and MMP-3 are increased in synovial and adipose tissues of osteoarthritic mice with hyperlipidaemia. *Clin Exp Immunol* 180:551-559.
88. Pelleymounter MA, Cullen MJ, Baker MB, et al. 1995. Effects of the obese gene product on body weight regulation in ob/ob mice. *Science* 269:540-543.
89. Uchida K, Urabe K, Naruse K, et al. 2009. Hyperlipidemia and hyperinsulinemia in the spontaneous osteoarthritis mouse model, STR/Ort. *Exp Anim* 58:181-187.
90. Mason RM, Chambers MG, Flannelly J, et al. 2001. The STR/ort mouse and its use as a model of osteoarthritis. *Osteoarthritis Cartilage* 9:85-91.
91. Fulcher J, O'Connell R, Voysey M, et al. 2015. Efficacy and safety of LDL-lowering therapy among men and women: meta-analysis of individual data from 174,000 participants in 27 randomised trials. *Lancet* 385:1397-1405.
92. Keene D, Price C, Shun-Shin MJ, et al. 2014. Effect on cardiovascular risk of high density lipoprotein targeted drug treatments niacin, fibrates, and CETP inhibitors: meta-analysis of randomised controlled trials including 117,411 patients. *BMJ* 349:g4379.
93. Clockaerts S, Van Osch GJ, Bastiaansen-Jenniskens YM, et al. 2012. Statin use is associated with reduced incidence and progression of knee osteoarthritis in the Rotterdam study. *Ann Rheum Dis* 71:642-647.
94. Izadpanah R, Schachtele DJ, Pfnur AB, et al. 2015. The impact of statins on biological characteristics of stem cells provides a novel explanation for their pleiotropic beneficial and adverse clinical effects. *Am J Physiol Cell Physiol* 309:C522-531.
95. Zhang O, Zhang J. 2015. Atorvastatin promotes human monocyte differentiation toward alternative M2 macrophages through p38 mitogen-activated protein kinase-dependent peroxisome proliferator-activated receptor gamma activation. *Int Immunopharmacol* 26:58-64.
96. Denis GV, Obin MS. 2013. 'Metabolically healthy obesity': origins and implications. *Mol Aspects Med* 34:59-70.
97. Navarro E, Funtikova AN, Fito M, et al. 2015. Can metabolically healthy obesity be explained by diet, genetics, and inflammation? *Mol Nutr Food Res* 59:75-93.
98. Green MA, Strong M, Razak F, et al. 2016. Who are the obese? A cluster analysis exploring subgroups of the obese. *J Public Health (Oxf)* 38:258-264.
99. Zhang Y, Pizzute T, Pei M. 2014. Anti-inflammatory strategies in cartilage repair. *Tissue Eng Part B Rev* 20:655-668.

ADDENDUM FIGURES



Addendum figure 1 Pro-inflammatory M1 macrophages secrete pro-fibrotic factors.

Human peripheral blood monocytes (pBMC) were stimulated to M1 or M2 phenotype and conditioned medium (CM) was made. Synovial fibroblasts (FLS) were treated with M1 or M2 macrophage CM for 4 days. Relative expression of COL1A1, ASMA and PLOD2 in FLS treated with 25% CM. Gene expression was normalized to the FLS only condition per donor. CM from 3 pBMC donors were used to treat 3 FLS donors, with each condition performed in triplicate (n=9). Values represent mean±SD. * $p < 0.05$ versus FLS only.



Addendum figure 2 Effect of PGF2 α on MSC chondrogenesis.

Chondrogenic stimulated MSC alginate beads were treated with PGF2 α , AL8810 inhibitor or CM from IPFP. Relative expression of COL2A1, ACAN, MMP1 and MMP13 in chondrogenic stimulated MSC alginate beads after treatment. Two pools of CM from 3 different IPFP donors each pool were used to treat 2 MSC donors, with each condition performed in triplicate (n=6). Values represent mean±SD. * $p < 0.05$ versus non-treated controls.

NEDERLANDSE SAMENVATTING

De knie heeft gewrichtsvlakken die bedekt worden door kraakbeen. Kraakbeen is een bindweefsel met een elastische karakter, het zorgt ervoor dat de gewrichtsvlakken soepel over elkaar heen kunnen glijden en het geeft schokdemping. Kraakbeen kan beschadigd raken en indien de kraakbeenschade niet hersteld wordt, kan dit uiteindelijk leiden tot artrose. De symptomen van artrose zijn onder andere pijn en verminderde bewegelijkheid. Bij artrose is niet alleen het kraakbeen aangetast maar de gehele knie, inclusief het bot, ligamenten en het synovium. Artrose is niet te genezen; alleen de symptomen zijn te behandelen. In het eindstadium van artrose kan het gehele kniegewricht vervangen worden door een prothese.

Kraakbeen herstelt uit zichzelf nauwelijks. Dit komt doordat het geen zenuwen en geen bloedvaten bevat. Daarnaast bestaat het kraakbeen vooral uit tussencelstof en maar voor een klein gedeelte uit kraakbeencellen. Indien er sprake is van een kraakbeendefect, is er momenteel een aantal methodes om het defect te herstellen. De meest gangbare is de microfracture procedure. Tijdens deze procedure worden er gaten gemaakt in het bot onder het kraakbeen. Hiermee worden de mesenchymale stamcellen in het beenmerg gestimuleerd om het kraakbeendefect op te vullen met littekenweefsel.

De resultaten van deze operaties kunnen door ontsteking negatief beïnvloed worden. In een ontstoken knie zijn er veel ontstekingsfactoren die ervoor zorgen dat stamcellen niet goed veranderen naar kraakbeencellen en daarom niet goed nieuw kraakbeen kunnen produceren. De resultaten van de kraakbeenoperaties kunnen ook negatief beïnvloed worden door obesitas. Bij obesitas zijn de vetcellen vergroot. Daarnaast is er meer infiltratie van ontstekingscellen, waaronder macrofagen. Macrofagen zijn witte bloedcellen die een belangrijk rol spelen in ons afweersysteem. Er zijn in het lichaam pro-inflammatoire macrofagen en weefselherstellende/anti-inflammatoire macrofagen. Het vetweefsel is bij obesitas ontstoken door onder andere een verhoogde infiltratie van pro-inflammatoire macrofagen en scheidt dan ook meer ontstekingsfactoren uit. Het meeste vet in het lichaam bevindt zich onder de huid. De ontstekingsfactoren bereiken de knie systemisch via de bloedbaan. Echter in de knie zelf bevindt zich ook vetweefsel. Het grootste vetweefsel in de knie is het infrapatellair vet weefsel, ofwel Hoffa's vetweefsel. Het Hoffa's vetweefsel ligt direct tegen het synovium aan. Het heeft als functie schokdemping en het helpen verspreiden van synoviale vloeistof. Het Hoffa's vetweefsel kan ontstoken raken en daarbij stoffen uitscheiden die het kraakbeen beïnvloeden.

In **Hoofdstuk 2** beschreven wij of het Hoffa's vetweefsel ook daadwerkelijk veranderd is door obesitas. Wij hebben daarbij stukjes Hoffa's vetweefsel gebruikt van patiënten die een totale knieprothese kregen en stukjes onderhuids vetweefsel van patiënten die een totale heupprothese kregen. Wij analyseerden de grootte van de vetcellen met histologie. Obesitas leidt tot vergroting van de onderhuidse vetcellen en dit is een aanwijzing voor vetweefsel ontsteking. Wij konden geen verschil in grootte vinden tussen vetcellen van het Hoffa's vetweefsel van patiënten met een body mass index (BMI) van $<25\text{kg/m}^2$ en $>30\text{kg/m}^2$. Wij concluderen hieruit dat de vetcellen in het Hoffa's vetweefsel waarschijnlijk niet door obesitas beïnvloed worden. Dit suggereert verder dat het Hoffa's vetweefsel niet hetzelfde is als onderhuids vetweefsel.

Obesitas is een risicofactor voor artrose. Een van de kenmerken van artrose is stijfheid van het gewricht. Dit wordt deels veroorzaakt door fibrosering, ofwel verlittekening van het synovium. Dit proces ontstaat doordat fibroblasten in het synovium meer fibrotisch weefsel gaat produceren. De fibroblasten produceren meer fibrotisch weefsel door aanwezigheid van ontstekingsfactoren of een overdaad aan groeifactoren. Het Hoffa's vetweefsel ligt in de knie direct tegen het synovium aan. Het synovium wordt dus mogelijk continue beïnvloed door het Hoffa's vetweefsel. In **Hoofdstuk 3** hebben wij beschreven dat factoren die het Hoffa's vetweefsel uitscheidt synoviale fibrose kan veroorzaken. Dit hebben wij onderzocht door eerst de factoren die het Hoffa's vetweefsel uitscheidt op te vangen in kweekmedium. Daarna hebben wij fibroblasten uit het synovium geïsoleerd en deze gekweekt met het kweekmedium. Wij zagen hierbij dat de fibroblasten meer fibrotische eigenschappen ontwikkelden. We merkten ook op dat er geen verschil was in effect tussen kweekmedium gemaakt van Hoffa's vetweefsel van obese en van niet-obese donoren. Verder ontdekten we dat prostaglandine F_{2a} (PGF_{2a}) uitgescheiden door het Hoffa's vetweefsel mede verantwoordelijk is voor deze reactie. Dit betekent dus dat een prostaglandine remmer, zoals celecoxib, mogelijk gebruikt zou kunnen worden om ontstaan van synoviale fibrose te remmen.

We weten nu dat het Hoffa's vetweefsel stoffen uitscheidt dat het kraakbeen en synovium beïnvloeden. In de kliniek zijn de resultaten van kraakbeenhersteloperaties niet optimaal, want er ontstaat een soort litteken kraakbeen. In **Hoofdstuk 4** hebben wij experimenten uitgevoerd om te kijken of het Hoffa's vetweefsel ook stoffen uitscheidt die de kraakbeenvormende capaciteit van stamcellen remmen. Wij gebruikten hetzelfde soort kweekmedium welke we eerder gebruikt hebben voor de synoviale fibrose experimenten in **Hoofdstuk 3**. Wij zagen dat dit kweek-

medium kraakbeenvormende capaciteit van stamcellen remde. Verder vonden wij geen verschil in het remmende effect van Hoffa's vetweefsel tussen obese en niet-obese donoren, noch tussen artrotische en post-traumatische donoren. Dit effect was wel Hoffa's vetweefsel specifiek, want subcutane vetweefsel had geen effect op de stamcellen. Tenslotte toonden we aan dat pro-inflammatoire macrofagen in het Hoffa's vetweefsel bijdragen aan het kraakbeenvorming remmende effect van het Hoffa's vetweefsel. Dit betekent dus dat als we de negatieve effecten van het Hoffa's vetweefsel willen verminderen, dat we een medicijn moeten gebruiken dat de pro-inflammatoire macrofagen in het Hoffa's vetweefsel beïnvloedt.

In **Hoofdstuk 5** probeerden we vervolgens met medicijnen ontsteking in het Hoffa's vetweefsel te remmen. We gebruikten celecoxib en triamcinolone acetonide, twee vaak gebruikte ontstekingsremmers, en pravastatine en fenofibraat, twee vaak gebruikte cholesterol- en triglyceridegehalte verlagers met ontstekingsremmende effecten. We kweekten stukjes Hoffa's vetweefsel met de verschillende medicijnen. We vonden dat alleen triamcinolone acetonide ontsteking in het Hoffa's vetweefsel kon verlagen. Daarnaast remde het ook specifiek de pro-inflammatoire macrofagen. Hierdoor werd het Hoffa's vetweefsel minder negatief voor kraakbeenvormende capaciteit van de stamcellen. Verder zagen wij ook het effect van Hoffa's vetweefsel op synoviale fibroblasten veranderde. Er traden namelijk kraakbeenafbraak processen op synoviale fibroblasten. Het lijkt er dus op dat triamcinolone acetonide gebruikt kan worden om specifiek het Hoffa's vetweefsel te moduleren naar een meer voor kraakbeenherstel geschikte staat.

Het meeste vetweefsel in het lichaam bevindt zich onder de huid. Bij obesitas is dit onderhuidse vetweefsel ontstoken en de ontstekingsfactoren worden systemisch uitgescheiden en bereiken dan via de bloedbaan de knie. Hierdoor kan kraakbeenschade en uiteindelijk artrose ontstaan. Daarnaast is dit ontstoken milieu mogelijk minder geschikt voor kraakbeenhersteloperaties. Naast ontsteking speelt ook metabole ontregeling een rol bij obesitas en het ontstaan van artrose. Om de complexe verschillende veranderingen in obesitas te onderzoeken, is het noodzakelijk dierproeven uit te voeren. In **Hoofdstuk 6** gebruikten wij de STR/Ort muizenstam, die spontaan obesitas en metabole- en inflammatoire veranderingen ontwikkelt. Deze muizen kregen gedurende een half jaar dagelijks simvastatine of fenofibraat of een combinatie hiervan. Dit zijn twee vaak gebruikte cholesterol- en triglyceridegehalte verlagers met ontstekingsremmende effecten. Na een half jaar konden we geen effect op kraakbeenschade vinden. Fenofibraat voorkwam wel obesitas, verlaagde systemische ontsteking en botsclerose, maar kon kraakbeenschade niet voorkomen. Tenslotte waren metabole inflammatoire veranderingen

in de muizen niet geassocieerd met het ontstaan van kraakbeenschade. Wij concludeerden uit deze muizenstudie dat obesitas en obesitas gerelateerde metabole en inflammatoire veranderingen niet direct de oorzaak zijn van kraakbeenschade in deze muizen. Voor de patiënt suggereert dit dat obesitas niet altijd leidt tot kraakbeenschade.

Als een obese patiënt eenmaal wel kraakbeenschade heeft, is het noodzakelijk een kraakbeenhersteloperatie uit te voeren om de progressie tot artrose te voorkomen. Op dit moment worden obese patiënten in principe niet geopereerd omdat de klinische resultaten minder zijn bij deze patiënten. Echter is het nog niet duidelijk of daadwerkelijk de kwaliteit van herstelde kraakbeen beïnvloed wordt door obesitas en hoe dit gebeurt. Wij hebben geprobeerd deze vraag te beantwoorden in **Hoofdstuk 7**. In dit hoofdstuk gebruikten wij DBA/1 muizen, waarvan bekend is dat ze kraakbeenschade kunnen herstellen. Wij hebben deze muizen een hoog vet dieet gevoerd waar 60% van de energie uit vet komt. Daarnaast maakten we een kraakbeendefect in hun knie. Deze muizen werden dikker, maar tegen de verwachting in, herstelde de groep die een hoog vet dieet kregen beter dan de muizen die een controle dieet kregen. Daarnaast ontwikkelde de groep die een hoog vet dieet kregen ook geen artrose en hadden de muizen geen metabole of inflammatoire veranderingen op de lange termijn. Wij concludeerden naar aanleiding van deze resultaten dat resistentie tegen hoog vet dieet geïnduceerde metabole en inflammatoire veranderingen mogelijk gelinkt is aan beter kraakbeenherstel. Wij weten niet precies welke mechanismes hierin een rol spelen, daarvoor is meer onderzoek nodig.

Concluderend heb ik met het onderzoek beschreven in dit proefschrift aangetoond dat het Hoffa's vetweefsel niet hetzelfde is als onderhuidse vetweefsel. Het Hoffa's vetweefsel van patiënten met artrose of knieschade scheidt factoren uit die het kniegewricht en kraakbeenherstel kunnen beïnvloeden. In de toekomst is het mogelijk met medicijnen het Hoffa's vetweefsel te moduleren om zo de gewrichtsomgeving te optimaliseren voor kraakbeenherstel. Verder hebben wij aanwijzingen gevonden dat obesitas niet altijd leidt tot artrose en niet per definitie negatief is voor kraakbeenherstel. Om beter te begrijpen waarom dit verschillend is tussen obese patiënten zijn er meer onderzoeken nodig. Wellicht kunnen wij in de toekomst hierdoor ook nieuwe therapieën vinden om artrose te verminderen en kraakbeenherstel te verbeteren.

中文简介

盖软骨作为减震器，可以使膝盖平滑无痛的运动。软骨可能会受损，一旦受损就不能恢复，最终可能导致膝关节骨性关节炎。膝关节骨性关节炎不能治愈，但通过治疗可以缓解其症状。在骨性关节炎末期，需要施行关节置换手术更换整个关节。

软骨损伤可以通过软骨修复手术来治疗。但是，炎症会影响手术的效果。在肥胖人群的脂肪组织多于常人，大多数脂肪组织位于皮下，而且会发炎。在膝盖内部有不小的一片脂肪组织，称为髌下脂肪垫或霍法氏脂肪垫。本论文的研究表明，这种脂肪垫与皮下脂肪不同。霍法氏脂肪垫分泌因子可能对膝关节和软骨的修复具有负面影响。这可能是 $\text{PGF}_{2\alpha}$ 因子的分泌和促炎性巨噬细胞的存在引起的。添加曲安奈德可以部分抵消这种负面作用。这意味着将来可以使用药物来调节霍法氏脂肪垫，从而改善膝关节软骨修复的环境。

除了研究霍法氏脂肪垫引起的炎症之外，本论文还研究了额外关节脂肪组织炎症对关节疾病和软骨修复的影响。通过小鼠活体实验发现，肥胖和肥胖相关的代谢和炎症变化并不总是导致软骨损伤，也不总是对软骨修复具有负面作用。研究实验提供的证据表明，肥胖相关的全身效应对退行性关节疾病和软骨修复影响具有变化性。关于肥胖，脂肪组织和软骨修复之间的关系的未来研究可以侧重于这种变化性以揭示新的治疗靶点。

PHD PORTFOLIO

Name PhD Student:	Wu Wei
Erasmus MC Department:	Orthopedics
Research School:	Postgraduate School Molecular Medicine (Mol-Med)
PhD Time-span:	February 2012 – December 2015
Promoters:	Prof. dr. G.J.V.M. van Osch Prof. dr. J.A.N. Verhaar
Co-promotor:	Dr. Y.M. Bastiaansen-Jenniskens

PhD Training

	Year	Workload (ECTS)
In-depth courses		
Laboratory animal science (Erasmus MC Graduate School)	2012	4.0
Biostatistical methods I: Basic principles (NIHES)	2013	2.0
Biomedical English writing course (MolMed)	2013	2.0
Research integrity course (Erasmus MC Graduate School)	2014	0.3
Biomedical English Writing and Communication (Erasmus MC Graduate School)	2014	4.0
ICRS Focus Meeting – The Knee (ICRS)	2014	1.0
Podium presentations		
Statins and fibrates to prevent spontaneous osteoarthritis: an in vivo study in mice <i>NVMB Meeting, Lunteren</i>	2013	1.0
Pro-inflammatory macrophages in Hoffa's fat pad reduces chondrogenic potential of mesenchymal stem cells <i>NOV Jaarcongres, Rotterdam</i>	2014	1.0
The infrapatellar fat pad inhibits chondrogenesis of mesenchymal stem cells <i>Molecular Medicine Day, Rotterdam</i>	2014	1.0
Obesity does not negatively influence cartilage repair in mice <i>NOV Jaarcongres, Rotterdam</i>	2015	1.0

PhD Training

	Year	Workload (ECTS)
The infrapatellar fat pad from diseased joints inhibits chondrogenesis of mesenchymal stem cells <i>ICRS World conference, Chicago, USA</i>	2015	1.0
Award for excellence in cartilage research		
The infrapatellar fat pad of diseased joints inhibits chondrogenesis of mesenchymal stem cells <i>SEOHS 2015, Leiden</i>	2015	1.0
Best abstract nominee		
Anti-chondrogenic and pro-catabolic effect of the infrapatellar fat pad can be modulated by triamcinolone acetone <i>ICRS World conference, Sorrento, Italy</i>	2016	1.0
Poster presentations		
Statins and fibrates to prevent spontaneous osteoarthritis: an in vivo study in mice <i>Molecular Medicine Day, Rotterdam</i>	2013	1.0
Statins and fibrates do not affect development of spontaneous osteoarthritis in STR/Ort mice <i>OARSI World conference, Philadelphia, USA</i>	2013	1.0
PPAR α signalling reduces subchondral bone thickening and inflammation, but does not prevent cartilage damage in STR/Ort mice <i>OARSI World conference, Philadelphia, USA</i>	2013	1.0
The infrapatellar fat pad inhibits chondrogenesis of mesenchymal stem cells <i>Matrix Biology Europe Meeting, Rotterdam</i>	2014	1.0
High fat diet accelerates cartilage repair in DBA/1 mice <i>Molecular Medicine Day, Rotterdam</i>	2015	1.0
The infrapatellar fat pad from diseased joints inhibits chondrogenesis of mesenchymal stem cells <i>OARSI World conference, Seattle, USA</i>	2015	1.0

PhD Training

	Year	Workload (ECTS)
High fat diet accelerates cartilage repair in DBA/1 mice <i>OARSI World conference, Seattle, USA</i>	2015	1.0
High fat diet accelerates cartilage repair in DBA/1 mice <i>ICRS World conference, Chicago, USA</i>	2015	1.0

Teaching

Tutoraat first year medical students	2012	1.5
Supervising third year medical students attending the minor "Orthopedic Sports Traumatology"	2012- 2014	1.0
Supervising Master student Molecular Medicine	2014	5.0
Supervising medical student	2014	0.5
Supervising Junior Med School Students	2014	1.0

Winner best presentation**Other**

Anna Fonds grant	2012	0.2
Reviewer for international journals <i>Cartilage (2x)</i> <i>Osteoarthritis and cartilage (2x)</i> <i>Rheumatology</i> <i>Journal of Biomedical Materials Research Part A</i>	2013- 2015	
Visiting researcher AO Research Institute <i>Davos, Switzerland</i>	2015	4.0

Total		43.3
--------------	--	------

LIST OF PUBLICATIONS

1. **Wei W**, Capar S, Kops N, Verhaar JAN, Clockaerts S, Van Osch GJVM, Bastiaansen-Jenniskens YM. Anti-chondrogenic and pro-catabolic effect of infrapatellar fat pad and its residing macrophages can be modulated by triamcinolone acetone. Submitted. 2017.
2. **Wei W**, Bastiaansen-Jenniskens YM, Suijkerbuijk M, Kops N, Bos PK, Verhaar JAN, Zuurmond AM, Dell'Accio F, van Osch G. High fat diet accelerates cartilage repair in DBA/1 mice. *J Orthop Res*. 2017 Jun;35(6):1258-64.
3. De Jong A, Klein-Wieringa I, Andersen S, Kwekkeboom J, Herb-van Toorn L, De Lange-Brokaar B, Van Delft D, Garcia J, **Wei W**, Van der Heide H, Bastiaansen-Jenniskens Y, Van Osch G, Zuurmond A, Stojanovic-Susulic V, Nelissen R, Toes R, Kloppenburg M, Ioan-Facsinay A. Lack of high BMI-related features in adipocytes and inflammatory cells in the infrapatellar fat pad. *Accepted Arthritis Res Ther* 2017. 2017.
4. Rezaie W, **Wei W**, Cleffken BI, van der Vlies CH, Roukema GR. Internal Fixation Versus Hemiarthroplasty for Displaced Intra-Capsular Femoral Neck Fractures in ASA 3-5 Geriatric Patients. *Open Orthop J*. 2016;10:765-71.
5. **Wei W**, Rudjito E, Fahy N, Verhaar JA, Clockaerts S, Bastiaansen-Jenniskens YM, van Osch GJ. The infrapatellar fat pad from diseased joints inhibits chondrogenesis of mesenchymal stem cells. *Eur Cell Mater*. 2015 Dec 02;30:303-14.
6. Siebelt M, Korthagen N, **Wei W**, Groen H, Bastiaansen-Jenniskens Y, Muller C, Waarsing JH, de Jong M, Weinans H. Triamcinolone acetone activates an anti-inflammatory and folate receptor-positive macrophage that prevents osteophytosis in vivo. *Arthritis Res Ther*. 2015 Dec 05;17:352.
7. **Wei W**, Clockaerts S, Bastiaansen-Jenniskens YM, Gierman LM, Botter SM, Bierma-Zeinstra SM, Weinans H, Verhaar JA, Kloppenburg M, Zuurmond AM, van Osch GJ. Statins and fibrates do not affect development of spontaneous cartilage damage in STR/Ort mice. *Osteoarthritis Cartilage*. 2014 Feb;22(2):293-301.

8. Fahy N, de Vries-van Melle ML, Lehmann J, **Wei W**, Grotenhuis N, Farrell E, van der Kraan PM, Murphy JM, Bastiaansen-Jenniskens YM, van Osch GJ. Human osteoarthritic synovium impacts chondrogenic differentiation of mesenchymal stem cells via macrophage polarisation state. *Osteoarthritis Cartilage*. 2014 Aug;22(8):1167-75.
9. Bastiaansen-Jenniskens YM, **Wei W**, Feijt C, Waarsing JH, Verhaar JA, Zuurmond AM, Hanemaaijer R, Stoop R, van Osch GJ. Stimulation of fibrotic processes by the infrapatellar fat pad in cultured synoviocytes from patients with osteoarthritis: a possible role for prostaglandin f2alpha. *Arthritis Rheum*. 2013 Aug;65(8):2070-80.
10. **Wei W**, Akkersdijk GP. Spontaneous aneurysm of the superficial temporal artery. *Lancet*. 2011 Jul 09;378(9786):168.
11. Damen TH, **Wei W**, Mureau MA, Tjong-Joe-Wai R, Hofer SO, Essink-Bot ML, Hovius SE, Polinder S. Medium-term cost analysis of breast reconstructions in a single Dutch centre: a comparison of implants, implants preceded by tissue expansion, LD transpositions and DIEP flaps. *J Plast Reconstr Aesthet Surg*. 2011 Aug;64(8):1043-53.

ABOUT THE AUTHOR



Wu Wei (韦芜) was born on May 28th 1986 in Songzi, Hubei, China. In 1993 he moved to the Netherlands. After obtaining his VWO diploma (Christelijk Lyceum Delft, Delft), he started medical school at the Erasmus University Rotterdam in 2004. During medical school, he spent a year as full time board member of the Medical Student Association of Rotterdam (MFVR) and was active in various other committees of the study. He also worked as an Erasmus ambassador and at the Emergency Department as a student-assistant. Furthermore he participated for several years in the Erasmus Anatomy Research Project, which increased his enthusiasm for Orthopedics.

In 2012 he obtained the degree of Medical Doctor. Subsequently he started his PhD project entitled 'Adipose tissue and the knee: role of inflammation on joint degeneration and cartilage repair' at the department of orthopedics under the supervision of prof. dr. Gerjo J.V.M. van Osch, prof. dr. Jan A.N. Verhaar and dr. Yvonne M. Bastiaansen-Jenniskens.

From January 2016 till June 2017, Wu worked as a resident (VAIOS) at the Department of Surgery at the Reinier de Graaf Gasthuis in Delft (under the supervision of dr. Maarten van der Elst and dr. Mark R. de Vries). From July 2017 onwards he is a resident (AIOs) at the Department of Orthopedics in Erasmus MC University Medical Center in Rotterdam (supervision by dr. Pieter K. Bos)

Besides his work, Wu enjoys running, cycling, food and cooking.

DANKWOORD

Er wordt altijd gevraagd of je iets opnieuw had willen doen als je wederom voor dezelfde keuze staat. Mijn antwoord op de vraag of ik opnieuw voor een promotietraject zou hebben gekozen, is volmondig “JA!”. De vier jaren in het lab op de 16^e zijn voorbij gevlogen. Dit proefschrift was nooit tot stand gekomen zonder de steun van anderen. Hierbij wil ik in het bijzonder een aantal personen bedanken.

Allereerst mijn eerste promotor prof.dr. Van Osch. Beste Gerjo, al in het voorjaar van 2010 liep ik bij je naar binnen om te komen praten over mijn keuze onderzoek. Ik had nauwelijks een idee wat fundamenteel wetenschappelijk onderzoek inhield, noch wat er te doen was op het lab. Na een halfjaar intensieve begeleiding van jou en Yvonne, was ik heel blij dat je mij de kans bood om een promotietraject te starten. Je was altijd heel laagdrempelig te bereiken voor overleg, hoe druk je het ook had. Daarnaast was er nog iets waar je ook altijd tijd voor vrij maakte: jouw goudvissen. Tijdens je afwezigheid werden complete schema's opgesteld om te zorgen dat ze niet overvoerd werden. Ik vond het leuk dat je onze goudvis Sep (je noemde hem mini-Wu) wilde adopteren. Helaas heeft hij de finish van dit boek niet gehaald. Gerjo, ik ben blij en dankbaar jou als promotor te hebben.

Daarnaast mijn tweede promotor, prof.dr. Verhaar. Beste professor Verhaar, dank u dat u mij de kans gegeven hebt om promotie onderzoek te doen op de afdeling orthopedie. Met uw uitgebreide kennis uit de kliniek, had u altijd kritische vragen over mijn onderzoek. U heeft mij geleerd én uitgedaagd basaal wetenschappelijk onderzoek zo klinisch relevant mogelijk te maken. Ik kijk er naar uit om meer van u te leren in de kliniek.

Dr. Bastiaansen-Jenniskens, mijn co-promotor Yvonne. Door de zeer intensieve begeleiding heb ik veel van de fundamentele technische zaken van het lab van jou geleerd. Veel van jouw werk vormde de basis van dit boek. Zelfs via de WhatsApp konden wij het vaak hebben over verse data. Ook buiten het werk heb ik veel lol met je gehad met de door jou geliefde slechte House muziek. Na al het intensief samenwerken ben ik blij dat ik niet jouw voorkeur voor roze heb overgenomen en dat jij niet Aziaat bent geworden.

Beste prof. dr. Hazes, prof.dr. Bulstra en dr. Emans, leden van de kleine commissie. Hartelijk dank voor het kritisch lezen en beoordelen van dit proefschrift. Dear prof.dr. Dell'Accio, thank you for taking time to visit us from the UK. I thank you for teaching me the cartilage defect model and for your input and sharing your view

on cartilage repair. Prof. dr. Van Saase, prof.dr. Kleinrensink en dr. Van Lent, dank voor uw bereidheid om plaats te nemen in de grote commissie.

Dr. Clockaerts, beste Stefan, jouw werk vormde samen met dat van Yvonne de basis voor mijn proefschrift. Dank voor je voorwerk zodat ik direct kon instromen. Wie kon bedenken dat er nog zoveel onderzoek uitgevoerd zou worden over dat ene stukje vet in de knie? De filosofieersessies tijdens de ICRS congressen waren zeer inspirerend en hopelijk kunnen we in de toekomst nog iets samen opstarten.

Daarnaast wil ik de andere senior onderzoekers en stafleden van de afdeling orthopedie graag bedanken. Jullie waren altijd bereid kritisch naar mijn onderzoek te kijken en actief weefsel te verzamelen. De volgende personen wil ik hierbij speciaal benoemen. Beste dr. Bos, vanaf het begin hebben we vaak met Gerjo gebrainstormd over mijn promotie onderzoek. Dank voor je ideeën hierbij. Max, trouwe Ajacied, dank voor je kritische blik op mijn manier van presenteren. Erwin, statistiek blijft bijzonder. Ik waardeer heel erg je visie hierin.

Graag wil ik alle co-auteurs bedanken voor hun expertise en inzet, waarbij ik de volgende speciaal wil benoemen. Lobke Gierman en Anne-Marie Zuurmond, jullie waren mijn grote TNO-hulplijnen. Jullie expertise in high-fat-diet heeft onverwachte inzichten opgeleverd. Ik kijk nooit meer hetzelfde naar dikke muizen. Sander Botter, bedankt voor het delen van je expertise in micro-CT en subchondraal bot bij vroeg artrose. Dear Niamh, talking about research, macrophages and gingers came 'hand in hand' with you. Good to see you in Holland again! Resti, you were so organized and precise in your work. Your Master project made chapter 4 possible. Good luck in Sweden with finishing your own PhD. Mathijs, ik heb nooit begrepen waar je alle tijd vandaan haalde om alles tegelijk te doen, maar het is je allemaal gelukt. We spreken elkaar nog in de kliniek. Dear John, fellow Hoffa enthusiast! Maybe in the future we can really start a fan club? Thank you for your contribution! Serdar, thanks for culturing the Hoffa and performing the FACS analysis and good luck with finishing your own PhD!

Het 'analistentrio' Nicole, Wendy en Janneke. Jullie zijn de vaste krachten van het lab. Altijd ontspannend even bij te praten in jullie kantoor/kamer/hok. Janneke, bedankt voor de gezellige momenten in de ML2 tijdens het vele verversen. Wendy, jij hebt dit groentje veel begeleid tijdens het pipetteren. Aan het eind kon ik het best goed, al zeg ik het zelf. Nicole! Het is jammer dat je niet in het histologiehok kunt snijden, terwijl je aan het internetshoppen bent bij de Bijenkorf, zonder de

cake van de week te missen, voor de paraffinemachine. Dank voor het snijden van al die knietjes en uitvoeren van vele kleuringen.

Sandra, altijd vrolijk. Zonder jou was het qua formulieren niet goed gekomen bij mij. Ik ben dankbaar dat jij mij via de mail structuur hebt gegeven aan de afgelopen periode.

The foreign seniors of the lab. Roberto, I was there when you did your first marathon and one day you, Maarten and I will do another one together! Keep up the good work and don't forget to eat less when not running. Eric, thank you for your wisdom about FACS, bone, wine and cured ham. Kavitha, grateful for your advice in the last months of my time in the lab.

Aan alle collega promovendi op de 16^e: Callie, Johannes, Marloes, Nienke, Mieke, Johan, Jasper, Michiel, Anna, Panithi, Rintje, Marjan, Mairéad, Marianne, Lizette, Caoimhe, Shorouk, Simone, Sohrab en Laurie. Bedankt voor de samenwerking, koffie drinken, lab days, cake van de week, cursussen, borrels, inpakken van mijn bureau in aluminium folie, selfies, collages, congressen in Amerika en leerzame tijd. De klinische collega's ook bedankt voor de gezelligheid.

Collega's van de chirurgie in Delft, gedurende de vooropleiding ben ik een échte dokter geworden. Het was een warm bad om in te starten. Ik heb met plezier met jullie gewerkt, inclusief de voetenpoli en proctopok. Dank voor de zeer leerzame tijd en de skireis.

Team Whiskey, mijn studievrienden, waarvan een kleine delegatie uiteindelijk ook in de toren gepromoveerd is of gaat promoveren. Ik hoop dat we onze vriendschap zullen blijven voortzetten met regelmatig etentjes, reizen, festivals en fietsen. De SV-mannen en oud-CLD'ers van de KEB-groep: jullie vormden een belangrijke bron van afleiding tussen het schrijven en pipetteren door. Niek, denkende aan het oude Sintinel tijdperk, wil ik je hierbij speciaal danken voor de mooie omslag.

Chris en Maarten: de een kon zijn benen in zijn nek leggen, de ander had haar tot zijn schouders en ik had iets meer weke delen. Vroeger stonden we met veel bier bij Goldfish vooraan, tegenwoordig gewoon rustig met een wijntje aan tafel. Maarten, met jou ben ik in 2011 tegelijk met dat pipetteren begonnen, de start van een geweldige periode. Een muur was niet dik genoeg om ons te scheiden. ik ben blij dat we ook de volgende stap van onze carrière tot orthopedisch chirurg samen kunnen volgen. Bedankt dat je mijn paranimf wil zijn.

Mijn schoonzussen Lisa en Malou. Lisa, altijd aan het lachen en geïnteresseerd in wat ik aan het doen ben. Onze discussies zijn soms fel, maar dat maakt mij ook weer scherp. Jij en Joost hebben een prachtig dochter, Evi. Ik ben blij dat ik voor het eerst oom geworden ben! Malou, de kleine sportieveling. Je wordt onderschat door je lengte, maar zwemmend in het water, rennend op het land en rijdend op de fiets, ben je super snel. Misschien zelfs iets sneller dan Michiel? Dat promoveren gaat jou natuurlijk makkelijk lukken!

Lieve schoonvader Jos, op geneeskundig vlak ben je misschien een leek, maar desondanks vind ik dat je toch veel van het medische af weet. Misschien ook wel doordat we aan tafel alleen maar hierover kunnen praten. Om dit goed te maken zijn er wel twee in je geliefde stad gepromoveerd, echter de derde moet je helaas aan de concurrent over laten. Je bent een fijn en zacht persoon en altijd welkom bij ons. Lieve schoonmoeder José, je was altijd geïnteresseerd in wat ik deed en vroeg mij de oren van het lijf. Door je betrokkenheid voelde ik me al snel thuis bij jullie. Ik zal je blijven herinneren als een liefdevol persoon.

Mijn lieve ouders, omdat Chinees binnen ons gezin de voertaal is, zal ik verder gaan in het Chinees. 我亲爱的爸妈，谢谢你们让我成长在这么温暖又充满爱的家庭里。你们俩一直希望我能够生活幸福事业顺利。妈，你经常说作为一个中国父母，孩子是最重要的。一直到现在，无论我做什么你们都无条件地支持和帮助我。爸，我现在跟你一样也是博士了，能够引用你的论文并且由你来当我的paranimf，我十分高兴也非常很骄傲。除了你们，我也想用这个机会感谢我的全部家人和其他好友。谢谢你们一直以来对我的照顾与关心，以及对我完成博士论文的支持与鼓励。

Mijn allerliefste Myrthe. Jij bent de meest veerkrachtige en sterkste persoon die ik ken. Na alles wat de afgelopen jaren gebeurd is en hoe gestrest en chagrijnig ik ook was, jij bleef altijd super lief en geduldig. Als stel zijn wij soms een complete chaos, maar meestal voelen wij elkaar heel goed aan. Wat we ook samen doen, de tijd vliegt veel te snel voorbij. Ik ben heel gelukkig dat jij in mijn leven bent en ik weet dat wij er altijd voor elkaar zullen zijn. Ik hou van je.

